Aus der Klinik für Strahlentherapie und Radioonkologie,
Universitätsklinikum des Saarlandes, Homburg/Saar
Direktor: **Prof. Dr. med. Christian Rübe**

Employment statistics and positioning accuracy of three different image-guidance systems; CTV-PTV margin calculation for two different populations

Dissertation zur Erlangung des Grades eines Doktors der Medizin
der Medizinischen Fakultät
der UNIVERSITÄT DES SAARLANDES
2015

vorgelegt von

Monica Elisa Beyhs

geboren am 10.03.1983 in Düsseldorf, Deutschland

Dedicated to my parents

for their unconditional love and support

Index

Summary

Purpose of this study: To evaluate the impact kilovoltage imaging, a new imaging technology at our department, has had on the treatment of our patients and to determine the preferred imaging modality and treatment machine for different situations. Additionally, based on a retrospective evaluation of the alignment data for two different patient populations, set-up errors for individual patients and for the two populations, as well as adequate treatment margins are calculated.

Methods and materials: Three different linacs, the Siemens Arstiste ART1 and ART 2 and the Siemens Oncor ONC2, each offering different imaging modalities for IGRT, were used. The ART1 is equipped with the best imaging technique, kilovoltage imaging. The data from 89 patients, 36 prostate cancer and 53 head-and-neck cancer patients, receiving IGRT between January 2013 and December 2013, was analyzed. A total of 3061 radiation fractions and 1260 set-up images were retrospectively evaluated. Set-up errors were calculated for three dimensions (superior-inferior (S-I), left-right (L-R) and anterior-posterior (A-P)) based on the alignment data from the couch shifts performed, in order to account for set-up variation detected in the verification imaging prior to treatment delivery. CTV-PTV margins were calculated applying the set-up errors to common margin recipes: $2\sum+0.7\sigma$ (Stroom et al., 1999) and $2.5\sum+0.7\sigma$ (van Herk et al., 2000).

Results: Linac employment statistics: The preferred treatment machine for head-and-neck cancer treatment was the linac ART2 (56%) followed by the ART1 (31%) and the ONC2 (13%). Prostate cancer patients were treated mostly at the ART1 (44%) and the ONC2 (37%). The ART2 was used the least (19%). Planar imaging was used more frequently than CBCT imaging. The frequency of CBCT imaging was higher for prostate cancer patients in comparison to head-and-neck cancer patients. At the ART1 the best imaging modality, kV imaging, was not always used. Especially when treating head-and-neck cancer IBL planar images were often preferred. Set-up errors and margins: Systematic set-up errors (μ) for the individual head-and-neck cancer patients range mainly from -0.15 to 0.2 cm (S-I), -0.1 to 0.3 cm (L-R) and -0.1 cm to 0.1 cm (A-P) and for the individual prostate cancer patients from

-0.4 to 0.25 cm (S-I), -0.3 to 0.1 cm (L-R) and -0.3 to 0.2 cm (A-P). Random errors (r) for individual head-and-neck cancer patients range from 0.06 to 0.43 cm (S-I), 0.07 to 0.48 cm (L-R) and 0.09 to 0.40 cm (A-P) and for individual prostate cancer patients from 0.15 to 0.72 cm (S-I), 0.21 to 0.83 cm (L-R) and 0.11 to 0.51 cm (A-P). The population systematic set-up error (M) for both populations is approximately zero; in all three directions values are smaller than 1 mm. The variation of the population systematic error ($\sum$) is larger for prostate cancer patients with values of 0.16 cm (S-I), 0.18 cm (L-R), and 0.17 cm (A-P) in comparison to 0.10 cm in all three directions for head-and-neck cancer patients. The population random error (σ) for head-and-neck cancer patients is 0.19 cm (L-R and A-P) and 0.22 cm (S-I) and for prostate cancer patients 0.37 cm (S-I), 0.49 cm (L-R) and 0.35 cm (A-P). No clear differences are found in the calculation of set-up errors when using the data from the different imaging modalities separately. The calculated margins for head-and-neck cancer patients are 0.35 cm (S-I) and 0.33 cm (L-R and A-P) according to Stroom et al. (1999) or 0.4 cm (S-I) and 0.38 cm (L-R and A-P) according to van Herk et al. (2000) and for prostate cancer patients 0.57 cm (S-I), 0.70 cm (L-R) and 0.58 cm (A-P) according to Stroom et al. (1999) and 0.66 cm (S-I) 0.79 cm (L-R) and 0.67 cm (A-P) according to van Herk et al. (2000).

Conclusion: The study shows that at our department anatomic differences are taken into account when choosing the different linacs and imaging techniques. Generally, for IGRT better imaging is used for patients with larger set-up errors. However, the study has also revealed that especially at the linac ART1 there is still room for improvement. As shown, prostate cancer patients are subject to much greater geometric variability in comparison to head-and-neck cancer patients. The random population set-up errors (σ) are larger for prostate cancer in comparison to head-and-neck cancer patients. The study has demonstrated that there is practically no systematic set-up error (M) for either patient population. Therefore, the quality assurance measures in our clinic are shown to be successful. Additionally, this study has revealed that the choice of imaging modality used for IGRT does not have a clear effect on the calculation of set-up errors. According to the margin recipes presented by van Herk (2000) and Stroom et al. (1999) the CTV-PTV margins applied in our clinic for prostate and head-and-neck cancer patients are sufficient.

Zusammenfassung

Zielsetzung: Evaluierung der Auswirkungen einer neuen Kilovolt-Bildgebungstechnologie für IGRT in unserer Klinik und Ermittlung der bevorzugten Bildgebungsmethode und Bestrahlungsmaschine für verschiedene Situationen. Berechnung von systematischen und randomisierten Lage-Fehlern in der Positionierung von einzelnen Patienten und Patienten Populationen anhand einer retrospektiven Auswertung der Verschiebungsdaten der Bestrahlungs-Liege, sowie Berechnung der adäquaten CTV-PTV Expansion.

Methoden und Materialien: Drei verschiedene Bestrahlungs-linacs (Siemens Artiste ART1 und ART2, Siemens Oncor ONC2) mit unterschiedlichen Bildgebungstechnologien für IGRT wurden verwendet. Ausgestattet mit Kilovolt Energie für die Bildgebung liefert der Beschleuniger linac ART1 die beste Bildqualität. Die Daten von 89 Patienten, 36 Prostatakrebs und 53 HNO-Krebs Patienten, welche zwischen Januar und Dezember 2013 Bestrahlung erhielten, wurden analysiert. Insgesamt 3061 Bestrahlungsfraktionen und 1260 Bildgebungen wurden retrospektiv evaluiert. Anhand der Daten der einzelnen Verschiebungen der Bestrahlung-Liege nach Bildgebung wurden Lage-Fehler (set-up error) in drei Dimensionen berechnet (superior-inferior (S-I), links-rechts (L-R) und anterior-posterior (A-P)). Die Fehler wurden verwendet um „CTV-PTV-marigns" anhand herkömmlicher Formeln, $2\Sigma+0.7\sigma$ (Stroom et al., 1999) und $2.5\Sigma+0.7\sigma$ (van Herk et al., 2000), zu berechnen.

Ergebnisse: <u>Linac-Anwendungsstatistik:</u> Der bevorzugte Beschleuniger für HNO Patienten war der linac ART2 (56%), gefolgt von dem ART1 (31%) und dem ONC2 (13%). Prostata Patienten wurden meist am ART1 (44%) und am ONC2 bestrahlt; der ART2 wurde nur selten verwendet (19%). 2D Achsen Aufnahmen wurden häufiger als 3D CBCT Aufnahmen verwendet, jedoch erhielten im Vergleich Prostata Patienten deutlich häufiger CBCT Aufnahmen als HNO Patienten. Nicht immer wurde am ART1 die Energie für die beste Bildqualität, Kilovolt, für die Bildgebung verwendet. Insbesondere für HNO Patienten wurden häufig IBL Achsen Aufnahmen bevorzugt. <u>„Set-up" Fehler und „CTV-PTV Expansion":</u> Systematische Fehler (μ) für einzelne HNO-Patienten lagen zwischen -0.15 cm und 0.2 cm (S-I), -0.1 cm und 0.3 cm (L-R), sowie -0.1 cm und 0.1 cm (A-P), für einzelne Prostata Patienten zwischen -0.4 cm und 0.25 cm (S-I), -0.3 cm und 0.1 cm (L-R), sowie -0.3 cm und 0.2 cm (A-P).

Zufällige Fehler (r) für einzelne HNO-Patienten lagen zwischen 0.06 cm und 0.43 cm (S-I), 0.07 cm und 0.48 cm (L-R), sowie 0.09 cm und 0.40 cm (A-P) und für einzelne Prostata Patienten zwischen 0.15 cm und 0.72 cm (S-I), 0.21 cm und 0.83 cm (L-R), sowie 0.11 cm und 0.51 cm (A-P). Der systematische Fehler für die gesamte Population (M) für sowohl HNO, als auch Prostata Patienten beträgt nahezu Null, mit weniger als 1 mm in allen drei Dimensionen. Mit 0.16 cm (S-I), 0.18 cm (L-R), und 0.17 cm (A-P) ist die Variation des systematischen Fehlers für die gesamte Population (∑) größer für Prostata Patienten im Vergleich zu HNO-Patienten (0.10 cm in alle drei Richtungen). Der randomisierte Fehler für die gesamte Population (σ) für HNO-Patienten beträgt 0.19 cm (L-R und A-P) und 0.22 cm (S-I) und für Prostata Patienten 0.37 cm (S-I), 0.49 cm (L-R) und 0.35 cm (A-P). In der Berechnung der verschieden „set-up" Fehler unter gesonderter Anwendung der Daten der unterschiedlichen Bildgebungsmodalitäten konnten keine Unterschiede festgestellt werden. Die berechnete "CTV-PTV Expansion" für HNO Patienten liegen bei 0.35 cm (S-I) und 0.33 cm (L-R und A-P) nach Stroom et al. (1999) oder 0.4 cm (S-I) und 0.38 cm (L-R und A-P) nach van Herk (2004) und für Prostata Patienten bei 0.57 cm (S-I), 0.70 cm (L-R) und 0.58 cm (A-P) nach Stroom et al. (1999) oder 0.66 cm (S-I) 0.79 cm (L-R) und 0.67 cm (A-P) nach van Herk et al. (2000).

Schlussfolgerung: In unserer Klinik werden die anatomischen Unterschiede der verschiedenen Patienten-Populationen in der Auswahl des Bestrahlungsgerätes und der Auswahl der Bildgebungsmodalität berücksichtigt. Generell werden für Patienten mit größeren Lage-Fehlern bessere Bildgebungen verwendet, am linac ART1 ist diesbezüglich jedoch eine Verbesserung noch möglich. Im Vergleich zu HNO Patienten unterliegt das Zielvolumen bei Prostata Patienten einer viel größeren geometrischen Variabilität. Die randomisierten Populations-Fehler (σ) für Prostata Patienten sind größer im Vergleich zu HNO Patienten. Weiterhin hat diese Studie gezeigt, dass für beide Populationen praktisch kein systematischer Lage-Fehler (M) nachgewiesen werden kann, folglich sind die Qualitätssicherungsmethoden in unserer Klinik suffizient. Die Studie hat weiterhin gezeigt, dass die Wahl der Bildgebungsmodalität keinen Einfluss auf die Größe der Lage-Fehler hat. Nach den Berechnungsformeln von van Herk et al. (2000) und Stroom et al. (1999) ist die in unserer Klinik angewandten „CTV-PTV Expansion" angemessen.

1. Introduction

Radiation therapy is a key element in the treatment of cancer patients. It has the potential to control tumor progression and improve survival. It can also increase the quality of life of cancer patients, reducing pain or other symptoms. Radiation oncology is constantly undergoing changes due to rapid advances in technology and better understanding of human molecular biology. This has led to many improvements in achieving the main goal of radiation therapy: To eliminate or control malignant cells while sparing healthy tissue.

1.1 Conformal radiation therapy

Conformal irradiation techniques like three-dimensional conformal radiation therapy (3DCRT) and intensity-modulated radiation therapy (IMRT), made possible by improved CT based planning systems and advances in planning software and computer-controlled radiation delivery, have become standard methods in external beam radiation therapy. These conformal radiation techniques allow an extremely accurate application of external beam radiation, using specialized software during treatment planning to precisely conform the radiation dose distribution to the shape of the tumor volume. This allows sparing of the surrounding normal tissues and organs at risk (OAR's), therefore, limiting the toxicity delivered to healthy tissue (Koper et al., 1999; Nutting et al., 2000; Pirzkall et al., 2000; Dawson et al., 2006; Nutting et al., 2011).

Conformal radiation therapy is associated with sharp dose gradients between the edges of the target volume and the surrounding healthy tissue. This is due to the precise conformity of the dose delivered to the tumor and the fast drop off of the dose outside the tumor volume. In general, the consequences of geometrical errors are more severe due to the sharp dose gradients in conformal radiation therapy since even small geometric variations may lead to a geometric miss, increasing the chances of toxicity to the surrounding organs at risk (OAR's) and the risk of underdosage of the target volume (Chen et al., 2011). This further increases the importance of accurately delivering the radiation dose to the defined target

volume. Ideally, the position and anatomy of the patient during the daily treatments should be equivalent to the setting at the time of treatment planning. To compensate for inevitable geometrical uncertainties in the daily positioning of the patient a "safety" margin is added to the target volume for treatment (Dawson et al., 2006, Korreman et al., 2010).

1.2 Target volume

According to the International Commission on Radiation Units and Measurements (ICRU), different volumes are classified as followed: The macroscopic volume of the tumor is identified as the GTV, the gross tumor volume. It can be determined by clinical examination or different imaging technics. The GTV is further extended to regions which contain the suspected subclinical microscopic malignant tumor growth. This volume is defined as the CTV, the clinical target volume. It may consist of the GTV plus a margin or it may additionally include lymph nodes. To reach the goal of the radiation therapy, the CTV needs to be treated adequately. The CTV is an anatomical-clinical concept, it has to be defined before a choice of treatment modality and technique is made. The third volume defined by the ICRU Report 50 is the PTV, the planning target volume. The PTV is a geometrical concept defined in order to select the appropriate radiation technique (field sizes and beam arrangements). To determine the PTV a margin is added to the CTV. It includes all the possible geometrical variations and inaccuracies, such as organ motion, patient motion and set-up error. Defining the PTV is important to ensure that the prescribed radiation dose is actually delivered to the CTV. Additionally the OAR's, the organs at risk, are delineated. OAR's are considered as the organs in the radiation field that are especially sensitive to the radiation toxins and therefore need to be spared. In Figure 1 these volumes are shown in a schematic illustration. (ICRU-Report 50, 1993; ICRU-Report 62, 1999)

Figure 1: schematic illustration of the volumes for treatment planning defined by the ICRU
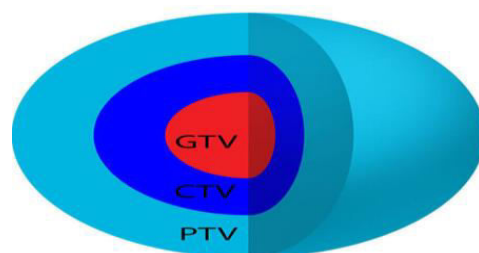
1.3 Image-guided Radiotherapy (IGRT)

Because the precise delivery of radiation is of such great importance when using conformal radiation techniques, the interest and importance of image guided radiation therapy (IGRT) is steadily increasing in the radiation oncology field. The term image-guided radiotherapy (IGRT), generally speaking, refers to any implementation of imaging techniques in radiation therapy in order to improve the quality of treatment. Since the advent of IGRT the available imaging techniques are constantly being further developed and improved. For target delineation during treatment planning the planning CT is often additionally fused with other imaging techniques, such as MRI and PET, for better tumor localization (Dawson et al., 2006). Imaging techniques, however, are not only used during treatment planning, but also during the delivery of the radiation treatment itself. During the actual delivery of the radiation treatment imaging techniques are usually used as a method of quality assurance to improve the geometrical accuracy of the delivered dose. The term IGRT, therefore, most often refers to the imaging obtained directly before the actual treatment delivery. Frequent set-up verification images are obtained over the course of the radiation treatment in order to localize the target volume and guide the administration of the radiation accordingly. Set-up errors and other geometrical errors are registered and corrected, either by altering the patient's posture or the position of the treatment couch, or by adapting the treatment plan to the geometrical changes occurring during the course of radiation treatment. This enables a more precise delivery of the intended radiation dose to the target volume (Mackie et al., 2003; Dawson et al., 2006; Verellen et al., 2008; Korremann et al., 2010). Because of its ability to identify, evaluate and reduce interfraction set-up errors (errors occurring within different radiation fractions) and detect intrafraction target motion (changes of the target volume within the same radiation fraction) image-guided radiotherapy (IGRT) is incorporated in more and more clinical trials (Ghilezan et al., 2004; Letourneau et al., 2005; Li et al., 2008).

The increased accuracy achieved through the implementation of conformal radiation techniques in cooperation with in-room imaging techniques has allowed a reduction of "safety" margins (Beltran et al., 2008). On the one hand, this has been shown to improve sparing of normal tissues and to minimize toxicity. A typical example of this is found in the

treatment of head-and-neck cancer where the reduced toxicity to the parotic glands has been proven to reduce the incidence of xerostomia (dry mouth syndrome), thereby improving the quality of life (Pow et al., 2006; Wang et al., 2009). On the other hand the reduction of margins has allowed dose escalations in many cases. For example, in radiation therapy for prostate cancer this has led to an improvement of biochemical control rates and a decrease in rectal and bladder complications (Peeters et al., 2006, Kupelian et al., 2006, Pollack 2006, e.g.).

1.4 Geometrical errors and their sources

In radiation therapy the term "error" is used to describe the geometrical variability and uncertainty encountered during radiation therapy. It does not refer to actually committed "errors". Geometrical errors in radiation therapy may be introduced during treatment planning or at the delivery stage of radiation treatment. In both instances, there are numerous sources for geometrical errors limiting the accuracy of radiation therapy.

Systematic errors are deviations which affect every radiation fraction in the same way. They are consistent over the course of treatment. They occur in the same direction and have a similar magnitude for each fraction throughout the treatment time, for each individual patient or for each patient population. They can be introduced during the acquisition of the planning CT during virtual simulation or during treatment planning and, therefore, are often referred to as "preparation" errors. **Random errors** are deviations that vary from fraction to fraction. Their magnitude and direction are different in each individually delivered treatment fraction.

During treatment planning the tumor in the planning CT is imaged in an arbitrary position which may not be representative for the average position of the tumor and therefore may lead to a systematic error. Also the motion of the patient's skin relative to the internal anatomy may lead to a systematic error (van Herk, 2004). The potentially largest source for systematic errors is the process of target delineation. The quality and resolution of the imaging technique used and the inter- and intra-observer variability in outlining the target, as well as the anatomic site of the tumor all have an impact on the magnitude of the

systematic error introduced during the delineation process. Other sources for systematic errors may be caused by errors in the calibration of the isocenter of treatment machines in respect to the isocenter of the planning CT scanner, by transfer errors created when transferring the data from the planning system to the treatment system or by other technical errors such as deviations of the room lasers. These errors, however, are usually minimal due to quality assurance methods (Korreman et al., 2010).

Errors in the delivery stage of the radiation treatment are often caused by set-up variability. Set-up errors are introduced through geometric variations of the patient's position and anatomy in relation to the conditions present during treatment planning. Factors that influence these set-up errors are, among others, positioning and immobilization methods, as well as the anatomic site treated. Immobilization methods aim at reducing this variability by increasing the reproducibility of the patient's positioning (van Herk, 2004; Korremann et al., 2010).

Motion of the patient during treatment delivery, changes in the position of the tumor within the body due to organ motion, weight loss, breathing, bladder and rectum filling and changes in size and shape of the target volume due to deformation of the tumor throughout the course of radiation therapy are all factors causing geometric variations and therefore introducing errors - both systematic and random (van Herk, 2004).

1.5 Set-up verification imaging

The purpose of verification imaging is to identify and correct this geometrical variability during treatment delivery. Set-up verification images can be obtained before, during or after radiotherapy, they may be two-dimensional or three-dimensional. The main goal of obtaining verification images prior to treatment delivery is to detect set-up errors directly before treatment and enable an immediate correction. Deviations in the positioning of the patient, leading to a geometric variation of the target volume relative to the position of the target volume defined during treatment planning, can be registered and corrected. Evaluation of these set-up verification images retrospectively, after the delivery of the treatment fraction, is referred to as "off-line" verification. Offline verification is a means of

eliminating systematic errors by evaluating and averaging the errors over several treatment fractions and shifting the patient's position accordingly. Offline verification also offers the opportunity to adapt the treatment plan in cases of gross errors due to changes in shape and position of the target volume - this is referred to as "adaptive planning" (Bel et al., 1996; de Boer 2002). In "on-line" verification the patient's set-up is evaluated and corrected directly prior to the delivery of the treatment fraction. Online verification with immediate correction via couch shifts is a means to correct not only systematic errors but also the random errors present in the respective treatment fraction (van Herk, 2004).

1.6 Different Imaging techniques

Electronic portal imaging and ultrasound image guidance have been some of the earliest imaging techniques used for IGRT. Since the interest in IGRT has steadily increased there is a constant development of new imaging techniques. Different in-room imaging techniques available are, among others, megavoltage imaging using the treatment beam line or, in some treatment machines, using an additionally added imaging beam line. Later, for reasons of better soft-tissue contrast and reduced extra imaging dose, kilovoltage x-ray imaging techniques were added. In the past years the development of imaging techniques has advanced from two-dimensional imaging techniques to volumetric three-dimensional imaging methods. These include megavoltage and kilovoltage cone beam CT systems and diagnostic CT scanners on rails (van Herk, 2007). With the rapid development in radiation oncology other advanced technologies for image-guided radiation therapy are also applied, for example electromagnetic localization, magnetic resonance imaging, fluoroscopy, tomosynthesis (Balter et al., 2007).

1.7 Margin calculation

As explained earlier the ICRU Report 50 and 62 recommend adding a „safety" margin to the CTV in order to account for geometrical uncertainties, thereby defining the PTV. Since inappropriate definition of the CTV-PTV margin may result in underdosing of the CTV and/or

overdosing of the OAR's, it is important to choose this margin correctly. According to the ICRU the margin should ensure that 99% of the CTV receives 95% of the prescribed dose. Several margin recipes combining uncertainties in order to calculate adequate CTV-PTV margins have been published (van Herk et al., 2000; Stroom et al., 1999)

The ICRU-62 Report states that a linear addition of margins for set-up error and organ motion, a method suggested by the Nordic Association of Clinical Physics (NACP), is not recommended because the CTV-PTV margin would become too large and too much surrounding healthy tissue would be damaged. Instead the ICRU-62 Report suggests to quadratically add standard deviations for systematic and random errors in order to determine an overall standard deviation for margin calculation. (Aaltonen et al., 1997; ICRU-62, 1999)

However, as shown in Figure 2, geometrical uncertainties, classified into systematic and random errors, have different impacts on the dose distribution delivered during irradiation. Systematic errors affect all fractions in the same direction, leading to a shift of the dose distribution in respect to the CTV, whereas random errors point into different directions in each fraction and therefore lead to a blurring of the dose distribution. This explains why systematic errors have a much higher impact on the dose distribution than random errors.

Figure 2: Schematic illustration showing the different effect of random and systematic errors
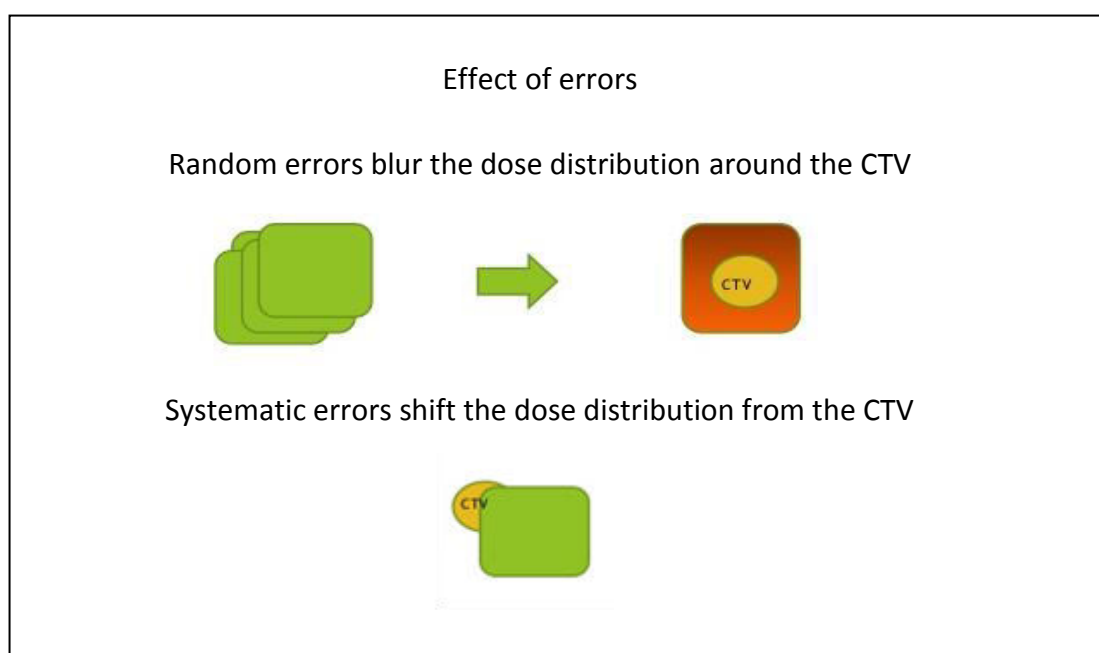
Stroom et al. (Stroom et al., 1999) and van Herk (van Herk et al., 2000), two different groups of researchers, have taken this into consideration and have presented us with margin recipes that account for the differences between systematic and random errors. Based on coverage probability Stroom et al. (1999) have presented the following margin to ensure that, on average, 99% of the target volume receives 95% of the prescribed dose or more:

$$M = 2\sum + 0.7\sigma$$

(M = CTV-PTV Margin, $\sum$ = variation of the systematic setup error of a population, σ = random set-up error of a population)

Van Herk et al. (2000) state, that the coverage probabilities do not account for very sharp tumor extensions. Based on dose population histograms van Herk et al. (2000) presented the following margin recipe which guarantees that 90% of patients in the population receive a minimum cumulative CTV dose of at least 95% of the prescribed dose:

$$M = 2.5\sum + 0.7\sigma$$

(M = CTV-PTV Margin, $\sum$ =variation of the systematic setup error of a population, σ = random set-up error of a population

As we can see the margin recipe by van Herk et al. (2000) leads to margins slightly larger than the recipe presented by Stroom et al. (1999).

1.8 Purpose of this study

In November 2012 a diagnostic x-ray imaging modality (kVision) was added to one of our three treatment machines offering a new imaging technique with kilovoltage imaging. The kVision system from Siemens was tested for clinical practice at our clinic and a few other radiotherapy departments in Germany and was later incorporated into the clinical routine at our clinic after the end of the testing phase. After working with this additional kilovoltage imaging modality for more than a year our goal was to evaluate the impact this new imaging technology has had on the treatment of our patients. In this study we compare and analyze the implementation of the different imaging modalities and treatment machines available at our institution. Is there a change or trend visible after incorporating kilovoltage imaging into our daily routine? The employment of the different treatment machines and imaging modalities was investigated for different treatment situations. We evaluated the preferred imaging modality for different treatment situations and the frequency of imaging per treatment for the different machines and situations. Furthermore, the set-up variability for the different patient populations included in this study were analyzed. Random and systematic set-up errors were calculated and the effect of the different imaging modalities on these errors was evaluated. After determining the systematic and random errors we calculated margins according to the margin recipes presented by Stroom et al. (1999) and van Herk et al. (2000) in order to estimate appropriate CTV-PTV margins for different patient populations.

This study concentrates on the data of two different patient populations. By selecting patients treated for head-and-neck cancer and patients treated for prostate cancer we chose two populations that have very different anatomic predispositions and are both very common tumors which are routinely treated with image-guided radiotherapy.

1.9 This study is organized as follows:

After this general **introduction** on conformal radiation therapy, with an explanation of the target volume, the concept of IGRT with set-up verification imaging, the definition of geometric errors and the idea of margin calculation in order to establish sufficient CTV-PTV margins, the Methods and Materials used in order to realize this study are presented.

In **Methods and Materials** the different treatment machines available in our clinic are introduced and their individual differences and qualities are discussed. Then the process of treatment planning, which entails the acquisition of a planning computed Tomography (CT), Target volume and CTV-PTV margin definition and the creation of the treatment plan as well as a description of the positioning standards used, is explained. Furthermore, additional details on systematic and random set-up errors as well as margin calculations are provided. Finally, in the last part of Methods and Materials, the two study populations included in this study are introduced.

In the **Results** chapter, first of all, the statistics assessed for the employment of the different linacs within both patient populations are displayed. Then, the employment of the two different radiation techniques used for radiation of prostate cancer patients, 3DCRT versus IMRT, is compared. Next, the analysis of the employment of the different imaging modalities used for both study populations over the course of time is presented. Afterwards, the data collected from the evaluation of the alignment data of the couch shifts for both population groups is shown and discussed. Also, the different systematic and random errors calculated for individual patients within the two populations and for the entire population are presented. Then, these values are applied to the margin recipes presented by Stroom et al. (1999) and van Herk et al. (2000) in order to establish adequate CTV-PTV margins for head-and-neck cancer and prostate cancer patients in our clinic. After presentation of each of these results a brief discussion and conclusion is offered before further discussing these results in the general **Discussion** chapter.

Finally, a general **conclusion** that can be drawn from the results of this study is provided.

2. Methods and Materials

2.1 Treatment machines

At our clinic there are three different linear accelerators (linacs) available for external beam radiation, two Siemens Artiste (denominated ART1 and ART2), and one Siemens Oncor (denominated ONC2). All three linacs allow the delivery of intensity-modulated radiation therapy (IMRT) using 6MV matched energies. Additionally, the ART 1 and ONC2 are able to deliver 18MV matched radiation therapy. All three treatment machines are capable of on-board image-guided radiotherapy (IGRT) with different imaging techniques. For verification imaging all three linacs are able to obtain two dimensional orthogonal planar images and volumetric three-dimensional cone beam computer tomography (CBCT) images. The energy available for these images however is different for each treatment machine. All three linear accelerators are capable of generating images using the treatment beam line (TBL) with the lowest photon energy (6MV) available for radiation treatment. These 6MV treatment beam line images are low in soft tissue contrast and deliver a relatively high imaging dose compared to the standard diagnostic x-ray images. For better imaging quality the ART2 linac and the ART1 linac are additionally equipped with a dedicated imaging beam line (IBL) which allows the acquisition of images with a reduced photon energy of nominally 1MV and a higher soft-tissue contrast. The imaging beam line (IBL) is used exclusively for imaging purposes. The most advanced imaging technique available in our clinic is provided by the ART1 linac. The ART1 linac has the capability of generating kilovoltage (kV) images delivered by an additionally added diagnostic X-ray tube, mounted opposite to the treatment head. These kilovoltage (kV) images offer an even better image contrast while further reducing the imaging dose in comparison to the IBL images. The type of image modality used for verification imaging of the individual fractions was at the discretion of the radiation therapist and depended on the treatment machine used for the particular radiation fraction and other organizational factors such as time- and patient-capacity. However a general protocol with guidelines for imaging type and frequency is provided for each individual patient by the radiation oncologist. Figure 3 shows the ART1 linac during IBL imaging (1) and during kV imaging with the diagnostic X-ray tube opposite to the treatment head (2). Figure 4 shows

examples of planar images created with the three different imaging energies, 6MV, IBL (1MV) and kV for both head-and-neck cancer and prostate cancer patients.

Figure 3: ART1 linac 1) during IBL imaging and 2) during KV imaging with the diagnostic X-ray tube opposite of the treatment head
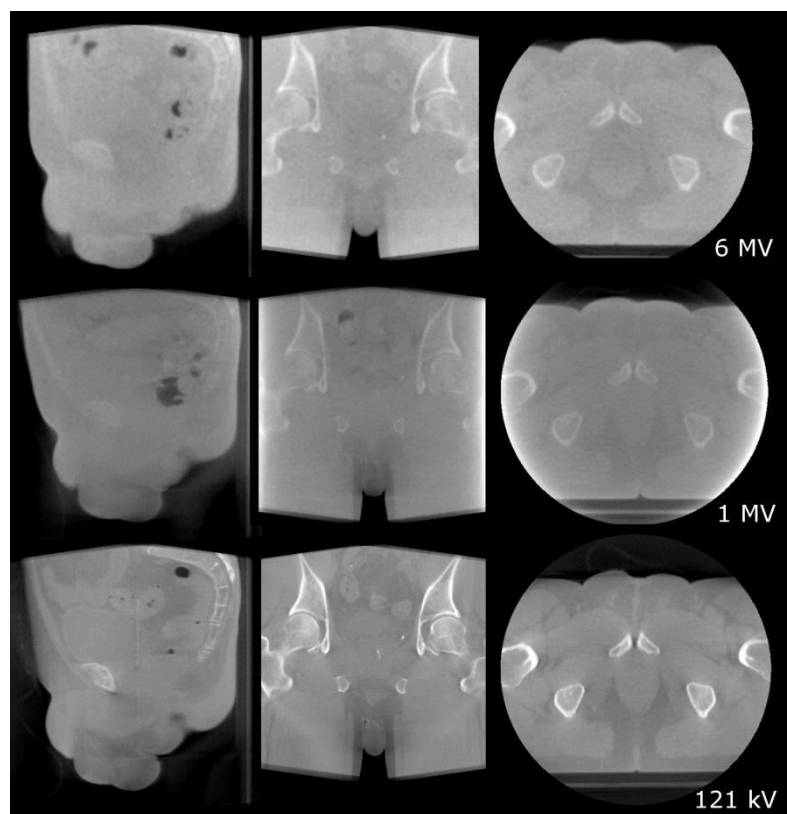
1)

2)

Figure 4: Comparison of three planar set-up verification images taken with different imaging energies. 6MV, 1MV = IBL and kV for the example of a (1) head-and-neck cancer patient and a (2) prostate cancer patient

1)

2)

2.2 Treatment planning

2.2.1   Planning Computed Tomography (CT)

Before commencing radiation treatment, all patients received a planning computerized tomography scan with a Philips BigBore 120kV CT-scanner. The patient was positioned on the CT couch by the radiation therapist in a comfortable and easily reproducible manner and immobilized. A thermoplastic mask, knee support or other equipment necessary for immobilization was fitted on the CT couch as required. With the help of room lasers, reference points were determined on the patient's skin or mask. These reference points were marked with marking pens. A series of CT slices of the region of interest were taken and verified on screen. The CT reconstruction was transferred online to the Philips Pinnacle v.9.0-9.4 treatment planning system (TPS).

2.2.2   Target volume and CTV-PTV margin definition

Target delineation was conducted by the radiation oncologist on the CT slices by manually contouring the target volume and the organs at risk in agreement with the recommendations of the International Commission on Radiation Units and Measurements (ICRU) Report 50 (ICRU-50). In order to account for geometrical variations PTV's were generated by adding a margin to the CTV. For prostate cancer patients a margin of 10 mm was added to the CTV. For head and neck cancer patients the PTV was directly delineated in the planning CT's without previously defining the CTV. However, generally a margin between 5 mm and 10 mm is implicitly assumed.

2.2.3   Creation of the treatment plan

After defining the target volume, the number of fractions and the desired treatment dose, the treatment plan is created by a physicist with the help of the Philips Pinnacle TPS. The physicist evaluates the treatment plan based on dose distribution and dose-volume histograms. Each final treatment plan is reviewed and verified by several radiation oncologists and physicians. After acceptance the plan is transferred to the treatment machines together with reference images and reference points determined during planning.

2.3 Patient positioning, Set-up and treatment

For radiation treatment all patients were positioned on the treatment couch in the same way they were positioned for the treatment planning CT. Patients with head-and-neck cancer were immobilized with a customized thermoplastic mask that is secured to the couch. All prostate cancer patients were instructed on proper bowel and rectum preparation, and were treated with an empty rectum and a full bladder to help improve OAR sparing and minimize daily anatomic variations. Knee support and other immobilization equipment were applied. The patient was then positioned according to the reference marks on skin and mask by aligning them to the room lasers in the correct position.

Verification images were obtained prior to irradiation at least once a week, depending on the frequency determined by the radiation oncologist in the treatment plan, and also depending on other factors, such as time constraints due to patient scheduling or other eventualities. The set-up verification images were compared to the reference images acquired from the planning CT scan. Two dimensional planar images were matched with digitally reconstructed radiographies (DRR's) created by the treatment planning system and volumetric CBCT images were matched with the planning CT scan directly. Special software was used to match the verification image to the reference data set in all three dimensions. An initial automated grey scale match was performed to assess the coincidence of the anatomy with the reference image, which was followed by manual registration and correction. The patient's position was then adjusted accordingly by executing translational shifts of the treatment couch (in anterior-posterior, superior-inferior or left-right direction) in order to ensure an optimal alignment of the target volume. Implementing a roll/pitch movement for adjustment of the couch is not possible.

2.4 Systematic and random set-up error

As explained earlier, the term "set-up error" or "set-up variation" describes the discrepancy between the intended and actual treatment position. It includes a systematic and random component. It is usually calculated as a shift of the treatment field position when comparing a verification image against its corresponding reference.

In order to calculate the systematic and random set-up errors for individual patients and for different groups of patients in this study, the alignment data obtained during treatment was evaluated according to the methodology introduced by van Herk (van Herk, 2004). The alignment data is collected from the individual couch shifts (in cm) realized in order to correctly align the target volume of the patient to the target volume defined in the reference images.

2.4.1 Calculating the systematic and random set-up error for an individual patient

For each individual patient in the study the mean of all the shifts recorded during treatment for each separate direction was calculated. This defines the **systematic set-up error** (μ) for each individual patient and for each direction. The patient's systematic set-up error (μ) resembles the average shift/deviation of the target volume from the position of the target volume during planning.

The standard deviation (SD) of all the shifts for the individual patient and for each direction defines the patient's **random set-up error** (r). The patient's random set-up error (r) shows the day-to-day variation of the target volume position from the mean position of the target volume.

2.4.2 Calculating the systematic and random set-up error and the variation of the systematic set-up error for a specific population

In order to obtain the **systematic set-up error for a population** (M) the mean of all the systematic set-up errors (μ) of all the individual patients included in this population is calculated for each direction. In other words, the average of all the mean shifts for all the individual patients in the population is calculated. The systematic set-up error for a

population (M) shows the average shift/deviation of all target volumes in the population from their position during planning. The systematic set-up error for a population (M) is an error that affects each patient in the population in the same magnitude or direction.

The **variation of the systematic setup error of the population** (∑), the population error spread, is defined as standard deviation (SD) of all the individual patient systematic errors (i.e. the standard deviation (SD) of all mean shifts (μ) per patient in the population). It indicates the patient-to-patient variation in the systematic deviation from the planning situation.

The **random set-up error of the population** (σ), the random variation, is determined by calculating the root-mean-square (RMS) of the random setup errors observed for each patient in the population (i.e. the RMS of all individual patient standard deviations (SD's)).

2.5 Retrospective evaluation of CTV-PTV margins

The CTV-PTV margin is determined by applying the two margin recipes presented by Stroom et al. (1999) and by van Herk et al. (2000), which account for both population systematic and random errors. The following equations were used:

$$M=2\textstyle\sum+0.7\sigma \text{ (Stroom et al., 1999)}$$

and

$$M=2.5\textstyle\sum+0.7\sigma \text{ (van Herk et al., 2000)}$$

We calculated the CTV-PTV margins for both populations applying the values calculated by means of the alignment data. We further investigated if there was a difference between the calculated margins using the alignment data acquired with the help of the different imaging techniques.

2.6 Study population and alignment data

The present study includes the data of 89 patients receiving image guided radiotherapy (IGRT) at the Department of Radiotherapy and Radiooncology at the Saarland University Medical Center from January 2013 to December 2013. Of these patients, 36 were treated for prostate cancer and 53 for head-and-neck cancer. Overall 3061 radiation fractions were analyzed retrospectively, 1324 for prostate cancer patients and 1737 for head-and-neck cancer patients. For 1260 of these fractions, 609 for prostate cancer patients and 651 for head-and-neck cancer patients, treatment targets were localized prior to radiation using different verification imaging techniques. The set-up verification images were matched with the reference set-up position as defined by the reference images obtained during treatment planning (DRR's or planning CT's), the patient's set-up accuracy was evaluated and necessary couch shifts for optimal alignment of the target volume were determined. The couch was then shifted accordingly in three dimensions, anterior-posterior (AP), superior-inferior (SI) and left-right (LR) to the corrected position. The alignment data of these 1260 x 3 shifts was analyzed for this study in the MS Excel 2010 Software. Table 1 summarizes the number and distribution of fractions and verification images among the two patient populations included in this study.

Table 1: Number and distribution of patients, fractions and verification images

	prostate cancer patients	head-and-neck cancer patients	Total
Number of patients	36	53	89
Number of radiation fractions	1324	1737	3061
Number of set-up verification images	609	651	1260

The 36 patients within the group of prostate cancer patients were treated during January 2013 to October 2013. The average number of fractions for these patients was 37 and they on average received 17.7 set-up verification images during radiation treatment, i.e. images where acquired for approximately every other radiation fraction. The mean and standard deviation for the fractions and verification images for prostate cancer patients are shown in table 2.

Table 2: Prostate cancer patients - Statistic of fractions and images

Prostate cancer patients	Mean	Standard deviation	Minimum	Maximum
Fractions	37	2.6	33	39
Set-up verification images	17.7	3.9	10	34
Percentage of images per fraction	45.30%	12%		

Within the collective of 53 patients with head-and-neck cancer, treated from January 2013 to December 2013, the number of radiation fractions and set-up images varied widely. As shown in table 3, the number of fractions per patient ranged from 17 to 55, and the number of set-up images from 4 to 23. However, on average, 33 radiation fractions and 12.3 set-up images per patient were obtained, i.e. verification images where acquired for approximately every third radiation fraction.

Table 3: Head-and-neck cancer patients - Statistic of fractions and images

Head-and-neck cancer patients	Mean	Standard deviation	Minimum	Maximum
Fractions	33	8.8	17	55
Set-up verification images	12.3	4.5	4	23
Percentage of images per fraction	37.4%	12%		

3. Results

## 3.1 Employment of the different linacs within both groups

Since the three linacs in our clinic offer different imaging techniques it was important to evaluate which amount of the treatment fractions for each group was delivered with each of the different treatment machines. Obviously this distribution has an impact on the different imaging modalities used for each group since not all linacs provide all three imaging energies. Table 4 shows the amount of fractions and images delivered with each of the three different treatment machines for both head-and-neck and prostate cancer patients, as well as the subdivision of the acquired images into the different image modalities used at each treatment machine. Figures 5, 6 and 7 visualize these distributions.

Table 4: Distribution of linacs and imaging modalities for both patient groups

Head-and-neck cancer patients				6MV		IBL		kV	
	fractions	images	images per fractions at each linac	planar images	CBCT	planar images	CBCT	planar images	CBCT
ART1	551	220	40%	29	0	113	16	29	34
ART2	981	357	36%	61	0	221	75	0	0
ONC2	221	75	34%	59	16	0	0	0	0

Prostate cancer patients				6MV		IBL		kV	
	fractions	images	images per fractions at each linac	planar images	CBCT	planar images	CBCT	planar images	CBCT
ART1	590	252	42%	23	0	50	15	87	77
ART2	246	144	59%	12	0	59	73	0	0
ONC2	489	210	43%	150	60	0	0	0	0

Figure 5 Distribution of the linacs used for treatment of the two patient populations

head-and-neck cancer patients

prostate cancer patients
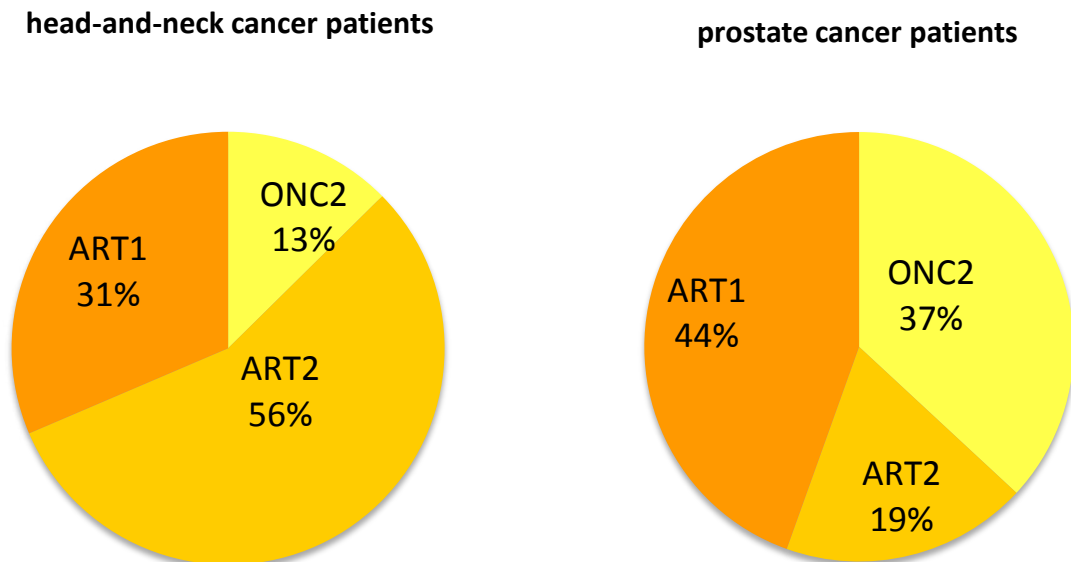
As seen in Figure 5 the radiation treatment for head-and-neck cancer patients was predominantly delivered with the ART2 (56%), followed by the ART1 (31%) and with only a small number of fractions and images obtained with the ONC2 (13%). Radiation treatment for prostate cancer patients was generally delivered with the ART1 (44%) and the ONC2 (37%), the ART2 (19%) was used the least for radiation treatment for prostate cancer patients.

Figure 6: Distribution of planar images versus CBCT for each linac and each population

Head-and-neck cancer patients
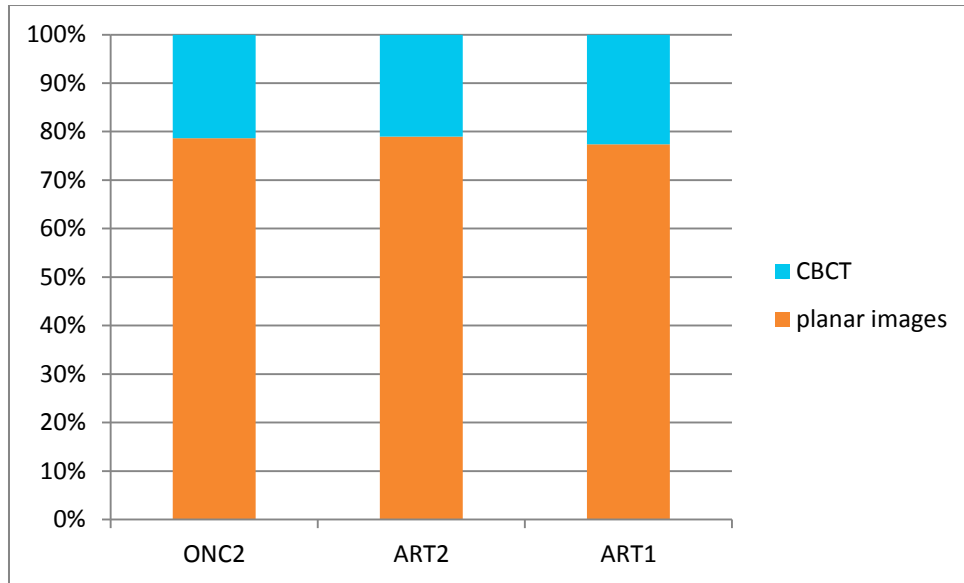
Prostate cancer patients
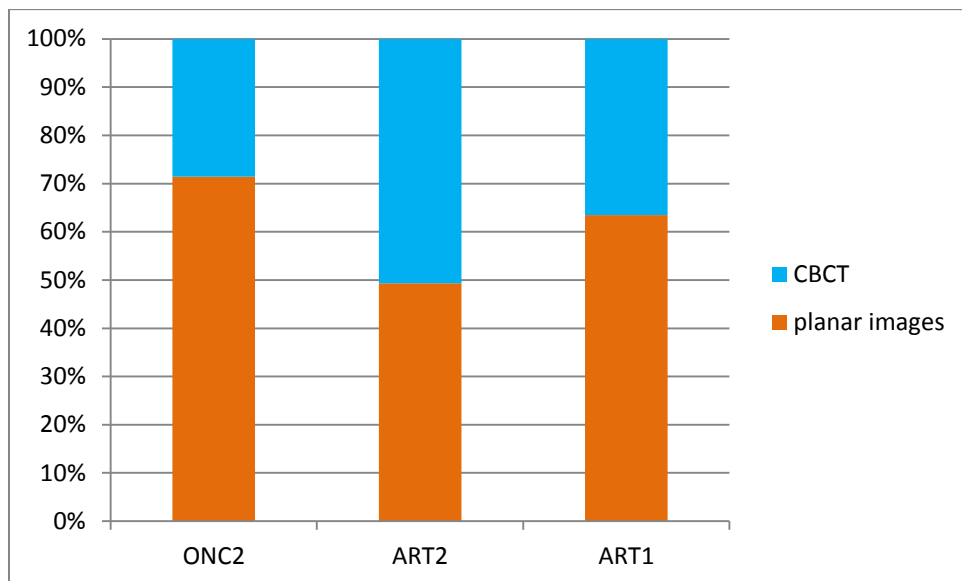
Figure 6 demonstrates that for set-up verification planar imaging is generally used a lot more frequently than three dimensional CBCT imaging for both populations. However, in comparison to head-and-neck cancer patients the frequency of CBCT imaging when treating prostate cancer images is a lot higher. For prostate cancer patients treated with the ART 2 as much as 50 % of the images acquired are CBCT images.

Figure 7: Percentage of each imaging modality used for the different linacs for each population

Head-and-neck cancer patients
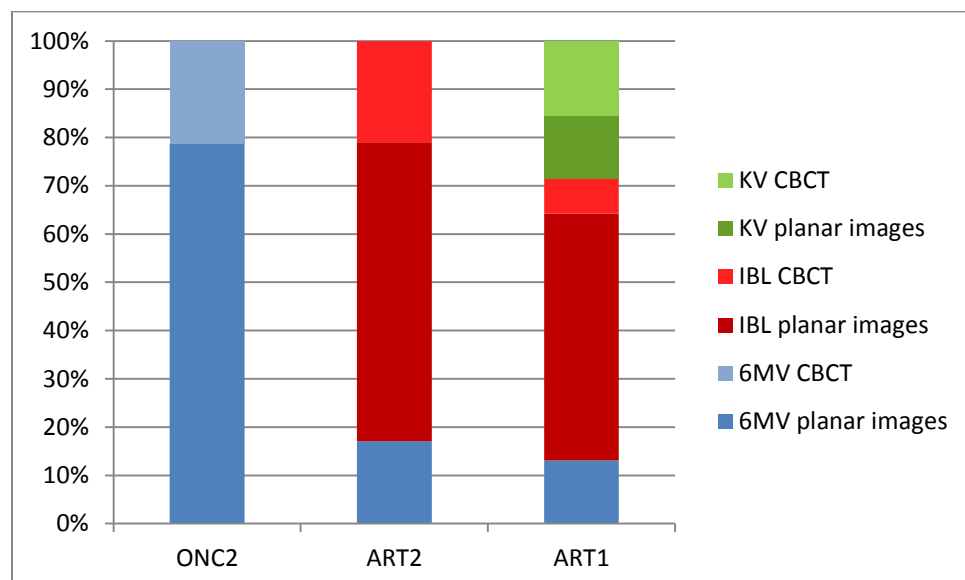
Prostate cancer patients
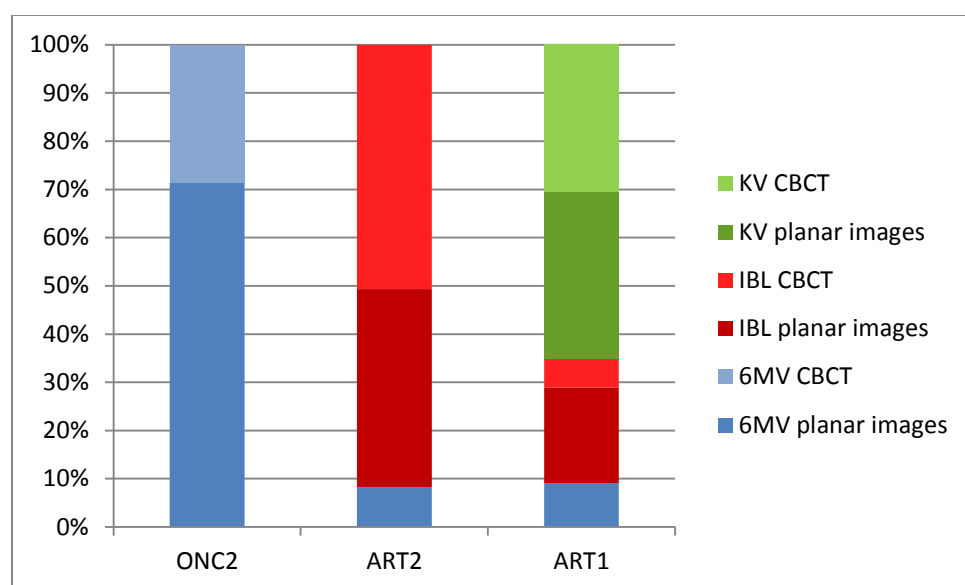
Figure 7 shows that when using the ART1 there were significant differences in the choice of image-modality used within both patient populations. When using the ART1 for treating prostate cancer patients, kilovoltage imaging was utilized in more than half of the treatments. This stands in contrast to the utilization when treating head-and-neck cancer patients. For head-and-neck cancer patients only approximately one third of the imaging technique used was kilovoltage imaging. The most commonly used imaging energy for head-and-neck cancer patients when treated at the ART1 is IBL planar imaging. For both populations at the ART1 and the ART2 only a small amount of imaging used was 6MV, approximately 10-20%, and in these cases only planar images were obtained. For prostate cancer treatment at the ART1 half of the obtained kV imaging was three dimensional CBCT imaging, and at the ART2 half of the obtained IBL imaging was CBCT imaging.

Discussion and Conclusion (3.1)

Selection of treatment machines:

As already discussed and visualized in Figure 5 the distribution of the two patient populations to the individual linacs is very different. Head-and-neck cancer patients are treated at the ART2 in more than half (56%) of the fractions, followed by the ART1 (31%) and with only a small number of treatments delivered at the ONC2 (19%). In comparison prostate cancer patients are irradiated mainly at the ART1 (44%) and the ONC2 (37%) with only a small number of treatments delivered at the ART2 (19%). This constellation is due to different factors:

As previously explained, the 6MV energies are matched at all three machines, but only the ART1 and ONC2 provide the 18MV energy. Therefore, 3DCRT prostate treatment, which is delivered with 18MV, can only be carried out at these two machines. Hence for prostate irradiation the ART2 is used only for the IMRT treatment fractions, which explains the small amount of fractions at the ART2. The ONC2 uses dynamic jaws for IMRT, which results in a slightly longer treatment time than the static jaw setting used by the ART1 and ART2. Therefore, IMRT are preferentially scheduled at the ART1 and ART2, in particular at the ART2. Taken together, as the ART2 only offers 6MV, and has static jaws, this machine is used for a large number of IMRT treatments, while the ONC2 is generally chosen for 3DCRT, especially for simple plans (arthrosis and prosthesis radiation).

Since patients with prostate cancer are mostly treated with a combination of IMRT with 6MV and 3DCRT with 18MV and the linac ART2 is not capable of 18MV 3DCRT treatment, the percentage of treatment fractions at the ART2 is relatively small (19%). Since for head-and-neck cancer treatment all fractions are delivered with IMRT generally the ART1 or the ART2 are preferred over the ONC2.

As the 6MV energy is available at all three treatment machines, and the 18MV energy is provided at both the ART1 and ONC2, there is still a lot of flexibility in choosing the machine for treatment. While it is technically possible to deliver IMRT at the ONC2, the linac ONC2 does not present the first choice for IMRT treatment, due to the longer delivery time

(because of the dynamic jaws). Therefore, the final decision is based on factors such as free treatment slots, machine properties, and – importantly – imaging capability.

Equipped with kilovoltage imaging, the ART1 of course offers the best imaging quality and is, therefore, more important for the treatment of prostate cancer patients, which require a higher soft tissue contrast than for e.g. head-and-neck cancer patients. Therefore, for prostate cancer patients the ART1 is the preferred treatment machine and for head-and-neck cancer patients, where good imaging quality is still necessary, however, not as crucial as for prostate cancer patients, the ART2 is the favored treatment machine. This is reflected in our results which show that most treatment fractions for prostate cancer patients were delivered at the ART1 (44%). For head-and-neck cancer patients over half of the treatments were delivered at the ART2 (56%) and only few treatments took place at the ONC2 (13%).

Planar imaging versus CBCT imaging:

Our evaluation shows that planar imaging is clearly used more often than three dimensional CBCT imaging. The reason for this is simple: Although CBCT offers a much better imaging quality and is, therefore, more capable of detecting geometric inaccuracies, CBCT imaging also involves a much higher radiation dose adding to the toxicity of the radiation therapy. The compromise is to obtain planar imaging on a regular basis with CBCT imaging interspersed, which explains the difference in frequency of the two imaging techniques. Our results have also shown that the frequency of CBCT images is a lot higher within the population of prostate cancer patients, which is plausible since prostate cancer treatment requires better imaging due to higher geometric variability and less rigid fixation methods. As discussed earlier at the ART2 only IMRT fractions can be delivered for prostate cancer treatment. IMRT is a much more complex radiation technique in comparison to 3DCRT and therefore requires a higher accuracy. This is reflected in our results which show that for prostate treatment at the ART2 as much as 50 % of the imaging used is CBCT. A reason for the circumstance that at the ONC2 treatment machine CBCT imaging is less often performed for prostate treatment (approx. 30%) might be the higher dosage involved with 6MV CBCT in comparison to IBL CBCT or kV CBCT. Also it is probable that for cases in which patients were

treated at the ONC2 as an exception, radiation therapists abstained from performing 6MV CBCT imaging, since it has a lower quality and higher dosage and instead performed 6MV planar imaging for this treatment fraction.

Imaging modality used at the different treatment machines:

Generally it is to be expected that for each linac the best imaging quality with the lowest dose is predominantly used and this is indeed the standard operating procedure (SOP) at our department. Figure 7 shows that this is the case for treatment at the ART2, which uses predominantly IBL imaging. At the ONC2 there is only 6MV imaging energy available which consequently is used for all imaging obtained at this machine. However for IGRT at the ART1 this cannot be confirmed. Although one would expect kV imaging to represent the highest percentage of imaging at the ART1, for head-and-neck cancer patients the dominant imaging technique used is IBL imaging with approximately 60%. For prostate cancer patients mostly kV imaging is used (approx. 60%), however, still a very large fraction of the images are IBL (approx. 30%). Since this result differs from our expectations it requires further discussion.

Possible reasons for this result may be found in the general work flow. For patients that are treated at a linac for the first time, set-up fields need to be created in order to obtain kV images. Since this is time consuming it may not be worthwhile in some situations, for example, if the patient is usually treated at a different machine and using the ART1 for a treatment fraction presents an exception. As shown in Figure 5 and discussed above, head-and-neck cancer patients were treated for the most part at the ART2, therefore when treated at the ART1 this often presented an exception for the patient. It is likely that in these situations IBL imaging may have been preferred due to already existing set-up fields for IBL imaging.

Also the total time necessary for the acquisition of kV images is slightly larger than the time required for IBL imaging. Therefore, in the daily routine, in situations with limited time, IBL imaging might have been preferred. Another reason leading to the result in our study is the fact that at the beginning of the year 2013 the time necessary for the acquisition of kV planar image was much larger due to necessary gantry rotations of 180° in order to match

the images to the created set-up fields, hence adding to the difference in time and workload between IBL and kV imaging. This, however, has been modified and is now no longer necessary. The discrepancy between our expectation and the actual employment of the different imaging modalities might also be simply due to lack of experience with kV imaging. KV imaging was still relatively new in our clinic and there might have been a habitual impact on the employment of imaging modalities. However, the radiation therapists in our clinic have confirmed that today more kV imaging is realized at the ART1 and generally, wherever possible, the best imaging technique available is used.

When looking at the fraction of IBL imaging for head-and-neck cancer patients at the ART1 it can be noted that almost all of the IBL images are planar images in comparison to the fraction of kV images, where CBCT and planar images are evenly distributed. A possible reason for this may be that since geometrical uncertainties are not as common for head-and-neck cancer patients and planar imaging is often sufficient for set-up verification, IBL planar images might have been realized under the assumption that an IBL planar imaging might have a sufficiently low dose in comparison to kV CBCT imaging. However, although planar IBL images may imply a reduced dose in comparison with CBCT imaging, Ames (2015) and Dzierma et al. (2015) have shown that this is not necessarily the case, for head-and-neck cancer treatment the dose of kV CBCT imaging is still significantly lower than the dose of IBL planar images.

Apart from the reasons mentioned above, the preference of using the better imaging techniques when treating prostate cancer is, of course, due to the fact that a higher soft-tissue contrast is necessary in order to correctly align the target volume. In contrast, when aligning head-and-neck cancer patients, bony structures are often used as reference points. Also there is a much higher variability of inner organ movement in prostate cancer treatment. This is due to the anatomic site with differences in rectum and bladder movement and to the positioning of the patient on the treatment couch, which is not as reproducible as for head-and-neck cancer patients, where with the use of thermoplastic masks, better immobilization methods can be applied. Therefore in general the linac ART1 and in particular kV imaging is used more frequently for prostate cancer patients.

3.2 Analysis of 3-dimensional conformal radiation therapy (3DCRT) versus intensity-modulated radiation therapy (IMRT) for prostate cancer patients

While all patients within the head-and-neck cancer group were treated with IMRT, most of the prostate cancer patients received a 3 field 3DRCT with 18 MV for part of their radiation treatment, usually followed by a boost treatment with IMRT. We were interested in analyzing the employment of the different imaging modalities used for the two radiation techniques at our clinic. Table 5 and Figure 8 show the subdivision of 3DCRT and IMRT within the total number of radiation fractions for prostate cancer patients and the number of set-up verification images acquired for each group. Also the distribution within the different types of imaging modalities is shown for 3DCRT and IMRT treatment fractions.

Table 5: Distribution of IMRT and 3DCRT fractions for prostate cancer patients and number of different image modalities used within each group

	fractions	images	6MV		IBL		KV	
			planar images	CBCT	planar images	CBCT	planar images	CBCT
3DCRT	979	399	158	56	70	23	59	33
IMRT	347	202	24	7	38	61	27	45

Figure 8: Number of images acquired during treatment with 3DCRT and IMRT and the distribution of these images within the different image modalities available
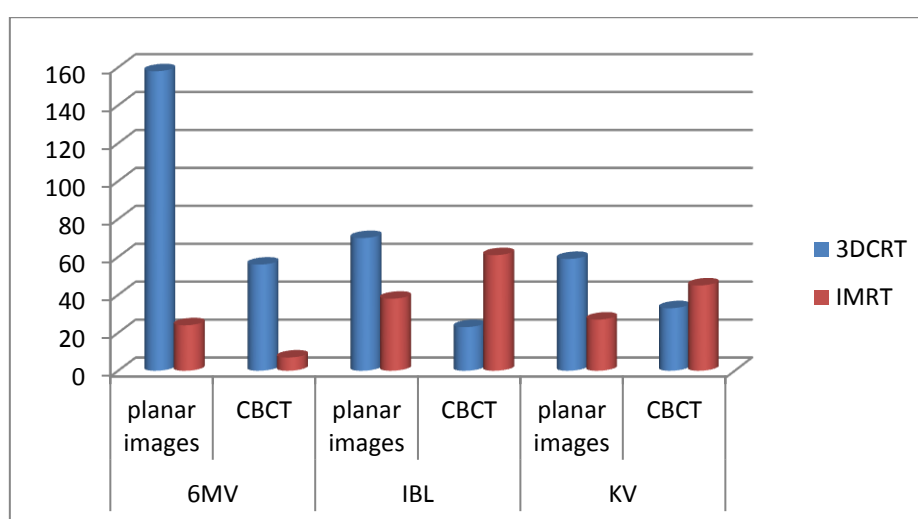
Table 6 shows the distribution and percentage of images obtained for each treatment fraction for 3DCRT and IMRT and the subdivision of these images into two dimensional planar and three dimensional CBCT imaging. The amount of images per fraction obtained is higher for IMRT than for 3DCRT. 58 % of the radiation fractions delivered with IMRT received verification imaging prior to treatment. In comparison, only 41 % of the radiation fractions delivered with 3DCRT received verification imaging. While for 3DCRT treatment predominantly planar imaging is used as a means for set-up verification (72%), for IMRT this is not the case. For IMRT treatment fractions three dimensional CBCT imaging is used more frequently than planar imaging with 56% of the imaging being CBCT in comparison to 44 % planar imaging. Figure 9 visualizes the distribution of CBCT versus planar images for both treatment techniques.

Table 6: Distribution and percentage of images per fraction for 3DCRT and IMRT and the subdivision into planar images and CBCT images for each treatment technique

	fractions	images	CBCT	planar images	Percentage of images per fraction	Percentage of planar images per images	Percentage of CBCT per images
3DCRT	979	399	112	287	41%	72%	28%
IMRT	347	202	113	89	58%	44%	56%

Figure 9: Percentage of CBCT versus planar images within 3DCRT and IMRT
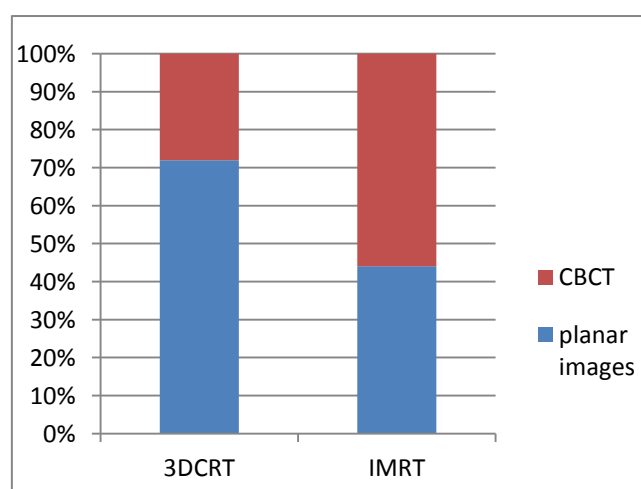
As shown in Figure 10 the distribution of CBCT versus planar images for 3DCRT and IMRT is different within the different imaging energies. For 6MV imaging is mostly planar and the percentage of CBCT images versus planar images is similar for both 3DCRT and IMRT, with approximately 80% being planar images. For IBL and kV imaging the distribution of CBCT and planar imaging is different for both treatment techniques. When acquiring IBL or kV images during 3DCRT mostly planar images are used (IBL = approx. 80% and kV = approx. 60%) in comparison to imaging during IMRT, where predominantly CBCT images are obtained (for both IBL and kV approx. 60% of the imaging obtained is CBCT).

Figure 10: Percentage of CBCT images versus planar images for each imaging modality divided into 3DCRT and IMRT treatment fractions
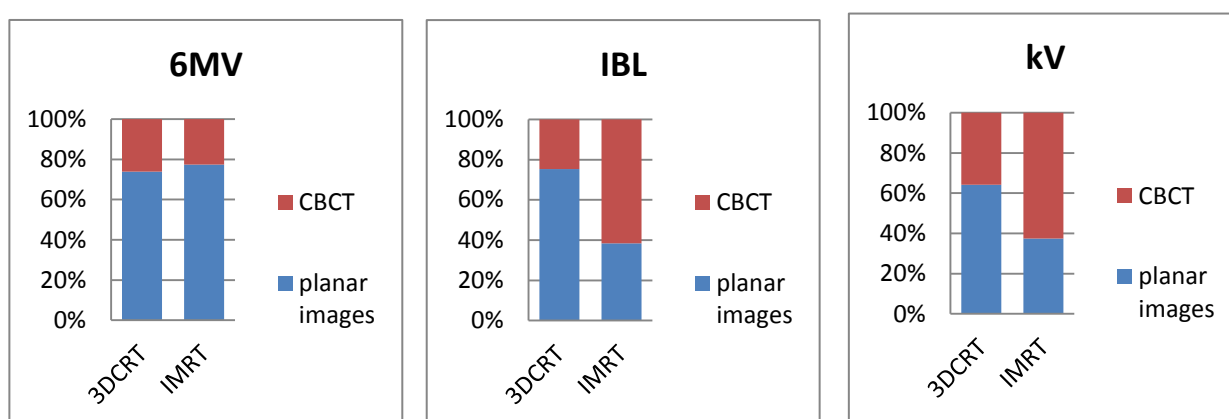
Table 7 shows the percentage of each of the different imaging types available within the images acquired for the group of 3DCRT and IMRT treatment fractions. The histogram in Figure 11 shows these percentages within the total number of treatment fractions delivered with 3DCRT and with IMRT.

Table 7: Percentage of the different types of imaging modalities used for 3DCRT and IMRT factions

	6MV		IBL		kV	
	planar images	CBCT	planar images	CBCT	planar images	CBCT
3DCRT	39.6%	14.0%	17.5%	5.8%	14.8%	8.3%
IMRT	11.9%	3.5%	18.8%	30.2%	13.4%	22.3%
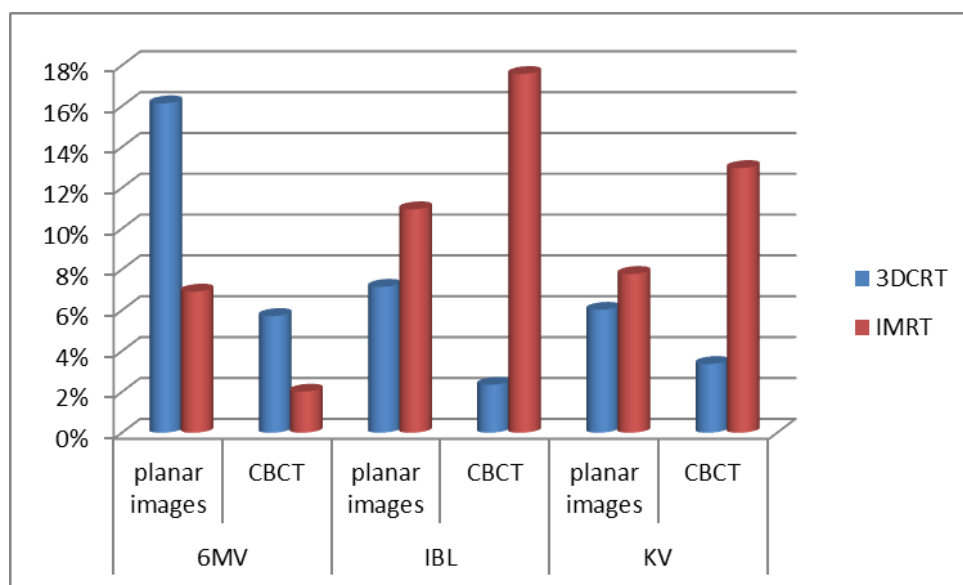
The histogram in Figure 12 and the pie-chart in Figure 13 visualize the percentages listed in table 7. They show the distribution of the percentages of each different image modality used, for the number of images obtained during radiation treatment, within the group of radiation fractions treated with 3DCRT and within the group of radiation fractions treated with IMRT.

Figure 12: Percentage of image modality used within the total amount of images acquired during 3DCRT and IMRT fractions
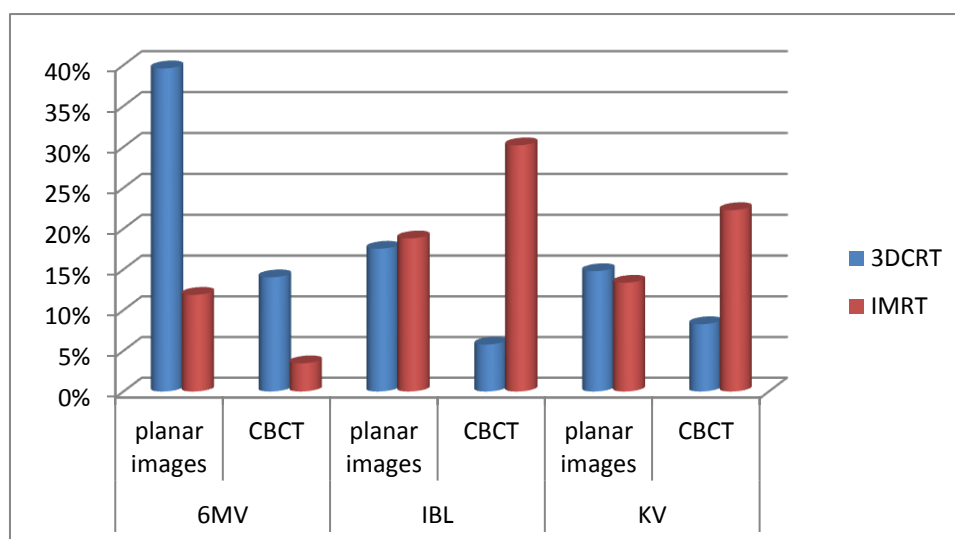
3DCRT

IMRT
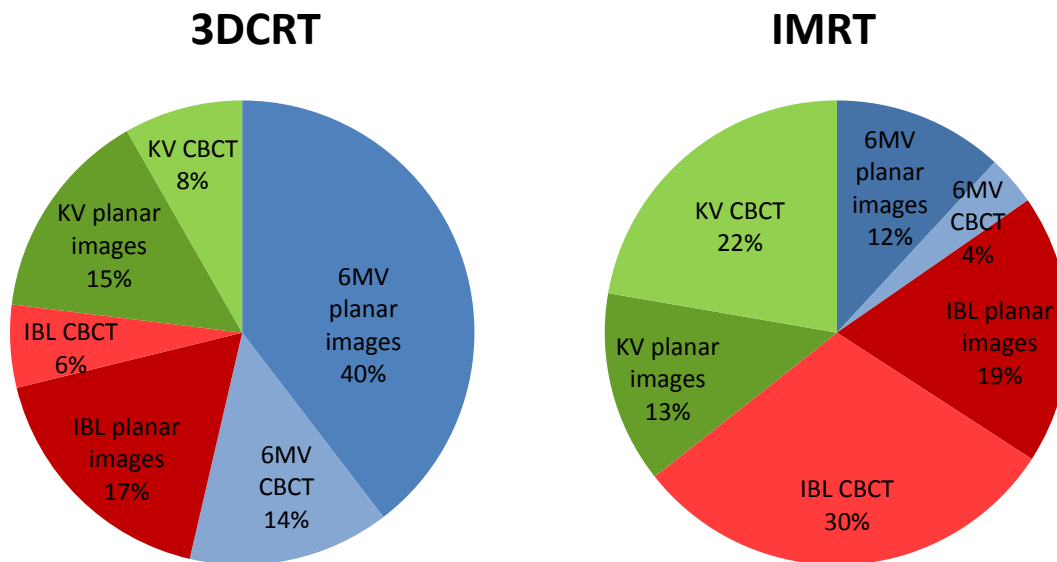
As can be seen in Figure 13, for 3DCRT predominantly 6MV planar imaging was used as method for set-up position verification. 39.6 % of all images acquired during 3DCRT are 6MV planar images. IBL planar images (17.5%) and KV planar images (14.8%) represent the next two largest groups within the total amount of images acquired during 3DCRT. With more than half of the images (54%), 6MV images (planar + CBCT) represent the largest group within images acquired during 3DCRT. This result differs from the group of images obtained during IMRT. For IMRT fractions the preferred imaging techniques used for position verification were IBL CBCT imaging (30.2%) and kV CBCT imaging (22.3%). Only a few images obtained during IMRT were 6MV images (16%), and in cases where 6MV images were obtained these were mostly planar images (11.9%). On the other hand, three dimensional CBCT imaging was favored for IBL and kV images obtained during IMRT, with 30% IBL CBCT in comparison to 19% IBL planar images and 22% kV CBCT in comparison to 13% kV planar images.

Discussion and Conclusion (3.2)

The amount of imaging acquired prior to each treatment is significantly higher for IMRT (58%) in comparison to 3DCRT (41%). For 3DCRT mostly planar imaging is used as a means for set-up verification (72%), whereas for IMRT the amount of planar imaging versus CBCT imaging is different, as 56% of the obtained imaging is three-dimensional CBCT, in comparison to 44% planar imaging. The results show that at our clinic, for 3DCRT, the most commonly used imaging modality for position verification is planar imaging with 6MV. In contrast, for IMRT radiation the preferred imaging techniques used for set-up verification are three dimensional CBCT images with IBL and kV energies. These imaging techniques offer a much higher resolution and, therefore, allow a much more precise alignment of the target volume prior to radiation. It makes sense that the better imaging modalities are used for set-up verification because IMRT is found to require a more precise positioning and alignment of the target volume since it is a more complex radiation technique in comparison to 3DCRT radiation. Another factor influencing these results is the distribution to the different linacs. As mentioned earlier only the ONC2 and the ART1 are capable of delivering 3DCRT with 18MV. This might explain the large amount of IBL imaging within the group of IMRT, since IMRT fractions were predominantly delivered at the ART2 and the best imaging modality available at the ART2 is IBL imaging. For prostate cancer 35% of the imaging realized during IMRT is delivered with kV energy. This suggests that when treated at the ART1, in most cases, the best imaging quality was used. These results confirm that in our clinic, when using more complex radiation techniques such as IMRT, better imaging techniques are applied for set-up verification imaging, allowing better alignment of the target volume.

3.3 Analysis of the different types of image modalities used for each group over the course of time

In order to determine if there was a trend development within the different techniques of imaging modalities used for set-up verification in our clinic, the employment of the different image modalities was evaluated in relation to the course of time for the group of head-and-neck cancer patients and for the group of prostate cancer patients. First the results for the population of head-and-neck cancer patients will be presented. This will be followed by the results for the population of prostate cancer patients.

3.3.1   Head-and-neck cancer patients

Table 8 shows the monthly amount of radiation fractions delivered to head-neck cancer patients throughout the study and the total amount and percentage of set-up verification images per radiation fraction obtained each month. Most radiation fractions were delivered during the months of June to September. As can be seen in table 8 the months of October to December are shaded since only very few radiation fractions were analyzed during this time. Therefore, the radiation fractions during these three months are not representative for the group of head-and-neck cancer patients included in our study and as a result not taken into account in the further presentation of our findings. The percentage of images acquired per radiation fraction each month ranges between 32.1% and 53%. On average 37.9% of verification images per radiation fraction were obtained every month. Apart from the months of October to December, which have been excluded, the month of June differs from the rest of the months with 53.4% of images acquired per fractions. An increase or decrease in the amount of images obtained per radiation fraction cannot be observed over the course of the year, there is no specific time trend regarding the amount of images per fraction. On average, for every third radiation fraction, a set-up verification image is obtained prior to radiation delivery.

Table 8: Radiation fractions and set-up images per month, percentage of images per monthly radiation fractions for head-and-neck cancer patients

month	fractions per month	images per month	percentage of images per fractions
January	211	82	38.9%
Febuary	293	94	32.1%
March	149	58	38.9%
April	102	38	37.3%
May	124	41	33.1%
June	176	94	53.4%
July	279	92	33.0%
August	209	78	37.3%
September	139	51	36.7%
October	35	12	34.3%
November	15	9	60.0%
December	5	2	40.0%
MEAN	187	70	37.9%

Comparison of CBCT imaging and planar imaging for head-and-neck cancer patients

The collected data was evaluated in terms of preferences for two dimensional planar imaging versus three dimensional conebeam CT (CBCT) imaging over time. Table 9 and Figure 14 show that the percentage of CBCT images and planar images remains relatively consistent throughout the different months. An average of 78 % of the images acquired each month for set-up verification are two dimensional planar images, 22 % are cone beam CT images. No increasing or decreasing in the employment of either imaging technic is observed over time.

Table 9: Amount and percentage of planar images versus CBCT images acquired each month for head-and-neck cancer patients

Month	planar images	CBCT
January	59	23
Febuary	78	16
March	41	17
April	32	6
May	32	9
June	73	21
July	74	18
August	62	16
September	39	12
October	10	2
November	8	1
December	2	0
MEAN	54	15

Month	planar images	CBCT
January	72.0%	28.0%
Febuary	83.0%	17.0%
March	70.7%	29.3%
April	84.2%	15.8%
May	78.0%	22.0%
June	77.7%	22.3%
July	80.4%	19.6%
August	79.5%	20.5%
September	76.5%	23.5%
October	83.3%	16.7%
November	88.9%	11.1%
December	100,0%	0.0%
MEAN	78.0%	22.0%

Figure 14: Percentage of planar images and CBCT per month for head-and-neck cancer patients
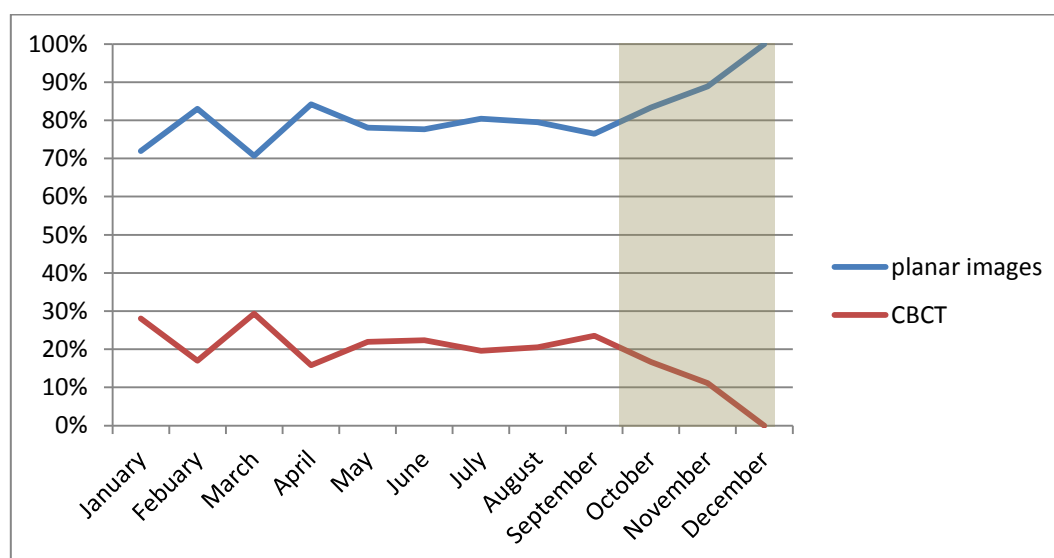
Comparison of monthly 6MV, IBL and kV imaging for head-and-neck cancer patients

A summary, of the amount and percentages of 6MV, IBL and kV images obtained each month for head-and-neck cancer patients, is provided in Table 10. Figure 15 shows a visualization of the quantities of 6MV, IBL and KV images obtained each month.

Table 10: Amount and percentage of 6MV, IBL and kV images acquired each month within the group of head-and-neck cancer patients

Month	fractions per month	absolute number of images			percentage of images per images total monthly images		
		6MV	IBL	kV	6MV	IBL	kV
January	211	16	56	10	19.5%	68.3%	12.2%
Febuary	293	18	70	6	19.1%	74.5%	6.4%
March	149	19	33	6	32.8%	56.9%	10.3%
April	102	9	27	2	23.7%	71.1%	5.3%
May	124	18	20	3	43.9%	48.8%	7.3%
June	176	27	52	15	28.7%	55.3%	16%
July	279	27	57	8	29.3%	62%	8.7%
August	209	14	57	7	17.9%	73.1%	9%
September	139	10	38	3	19.6%	74.5%	5.9%
October	35	4	5	3	33.3%	41.7%	25%
November	15	2	7	0	22.2%	77.8%	0%
December	5	0	2	0	0%	100%	0%
MEAN	187	18	46	7	26.0%	62.0%	12.5%

Figure 15: 6MV, IBL and kV images obtained each month for head-and-neck cancer patients
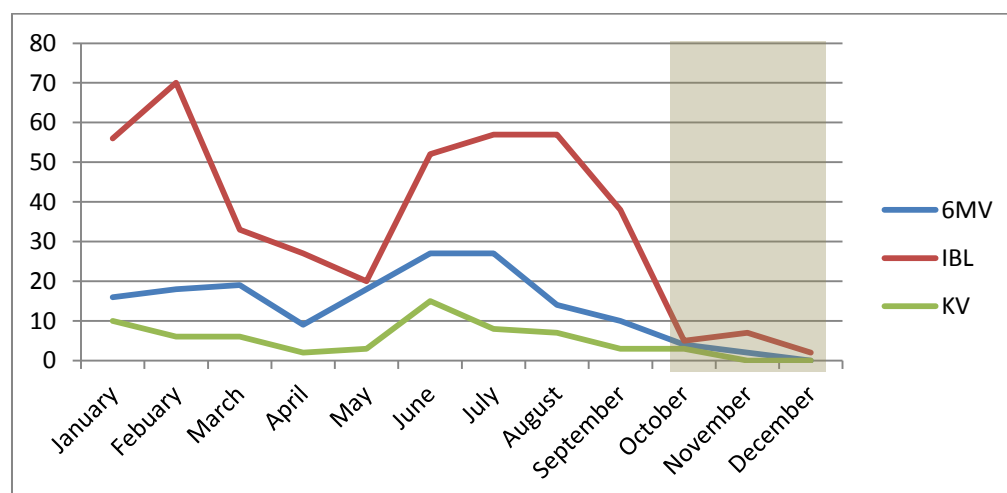

44

Figure 16 and Figure 17 compare and visualize the percentage of 6MV, IBL and kV imaging modalities applied during each month for head and neck cancer patients. IBL imaging is the most commonly used imaging technic every month, an average of 60-70 % of the monthly acquired images are IBL images. 6MV images represent the second largest amount of images with an average of 20-30 % of monthly images. The percentage of monthly obtained kV images ranges between 5.9 % and 16 %. In general, however, only a small number of the monthly obtained images are kV images, approximately an average of 10%. An exception is the month of June where 16 % of the imaging is kV.

Figure 16: Percentage of 6MV, IBL and kV images per total of the monthly set-up images for head-and-neck cancer patients
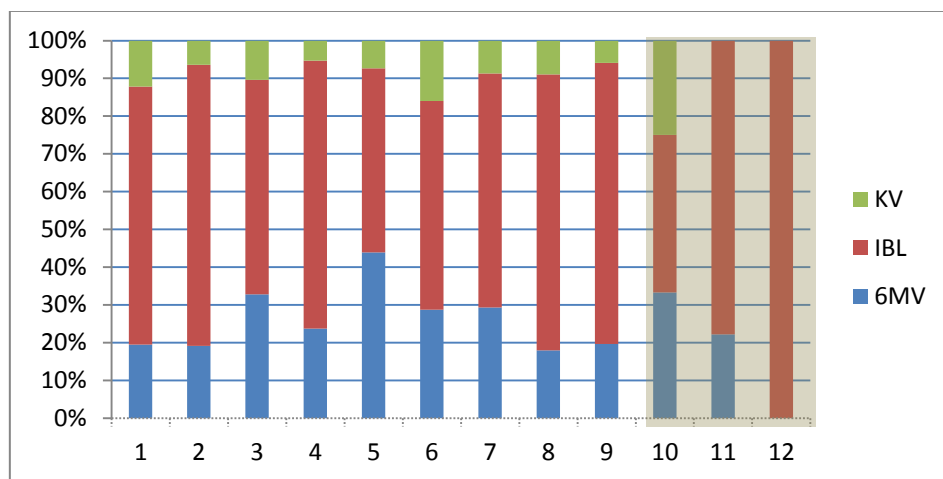
Figure 17: Development of employment of the different imaging modalities over time for head-and-neck cancer patients
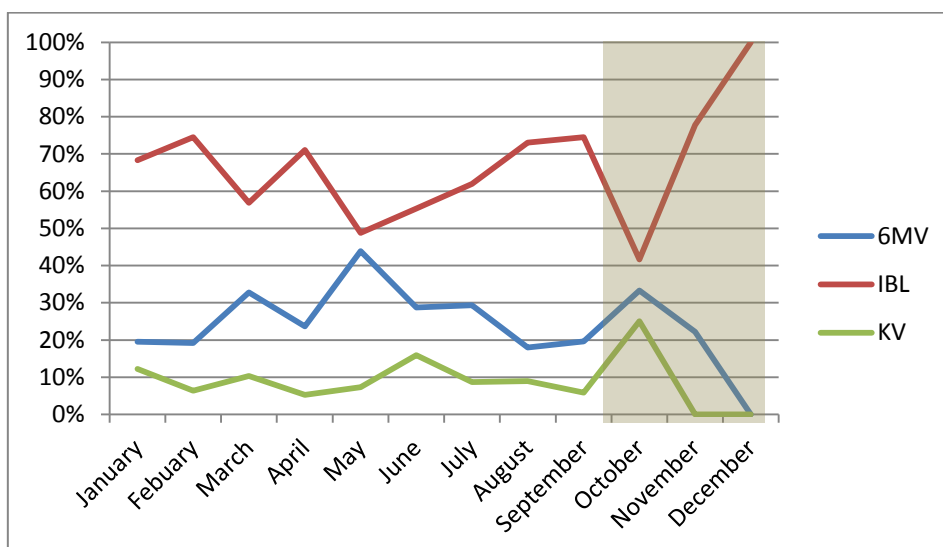
Comparison of 6MV planar images and CBCT, IBL planar images and CBCT images and kV planar and CBCT images for head-and-neck cancer patients

The imaging techniques used for radiation therapy were evaluated not only in terms of the energy used (6MV, IBL and kV), but also it was investigated whether two-dimensional planar images or three-dimensional CBCT images were acquired for set-up verification imaging. A summary, of the monthly number of times each of the six different image modalities was used, is provided in Table 11 and Figure 18. Table 12 shows the percentage of the images in relation to the total amount of images obtained each month.

Table 11: Amount of images per imaging modality and per month for of head-and-neck cancer patients

Month	fractions per month	6MV		IBL		kV	
		planar images	CBCT	planar images	CBCT	planar images	CBCT
January	211	12	4	44	12	3	7
Febuary	293	16	2	61	9	1	5
March	149	18	1	19	14	4	2
April	102	8	1	22	5	2	0
May	124	16	2	15	5	1	2
June	176	26	1	40	12	7	8
July	279	26	1	43	14	5	3
August	209	12	2	46	11	4	3
September	139	9	1	30	8	0	3
October	35	3	1	5	0	2	1
November	15	2	0	6	1	0	0
December	5	0	0	2	0	0	0
MEAN	187	16	2	36	10	3	4

Figure 18: Number of 6MV-, IBL- and kV-planar images and number of 6MV-, IBL- and kV CBCT obtained each month for head-and-neck cancer patients
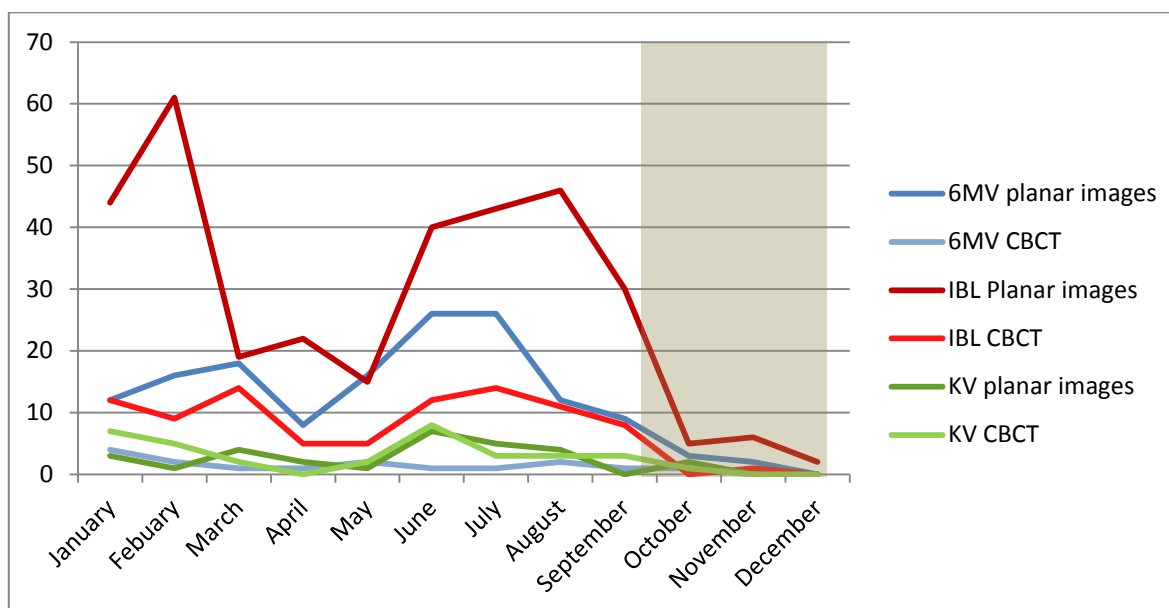

Table 12: Percentage of different image modalities per total monthly images within the group of head-and-neck cancer patients

Month	6MV		IBL		KV	
	planar images	CBCT	Planar images	CBCT	planar images	CBCT
January	14.6%	4.9%	53.7%	14.6%	3.7%	8.5%
Febuary	17.0%	2.1%	64.9%	9.6%	1.1%	5.3%
March	31.0%	1.7%	32.8%	24.1%	6.9%	3.4%
April	21.1%	2.6%	57.9%	13.2%	5.3%	0%
May	39.0%	4.9%	36.6%	12.2%	2.4%	4.9%
June	27.7%	1.1%	42.6%	12.8%	7.4%	8.5%
July	28.3%	1.1%	46.7%	15.2%	5.4%	3.3%
August	15.4%	2.6%	59.0%	14.1%	5.1%	3.8%
September	17.6%	2.0%	58.8%	15.7%	0%	5.9%
October	25.0%	8.3%	41.7%	0%	16.7%	8.3%
November	22.2%	0%	66.7%	11.1%	0%	0%
December	0%	0%	100%	0%	0%	0%
MEAN	23.5%	2.6%	50.3%	14.6%	4.1%	4.8%

Figure 19 and Figure 20 compare and visualize the percentages of the six different imaging techniques used each month for the group of head-and-neck cancer patients in this study. IBL planar imaging is by far the most commonly used technique for set-up verification imaging within the group of head-and-neck cancer patients. With an average of 50.3 %, half of the images obtained each month were IBL planar images. With an average of 23.5 %, 6MV planar images represent the second most commonly used imaging technique, followed by IBL CBCT imaging with a monthly average of 14.6 %. The other three imaging techniques available, 6MV CBCT and KV planar images and KV CBCT were rarely used for set-up verification imaging, with a monthly average of 2.6 % for 6 MV CBCT, 4.8 % for KV CBCT and 4.1 % for KV planar imaging. The percentage each of the different imaging modalities was used every month is relatively consistent over the course of time. A specific time trend for the employment of the different image modalities is not apparent.

Figure 19: Percentage of images obtained in each different image modality per total monthly images for head-and-neck cancer patients
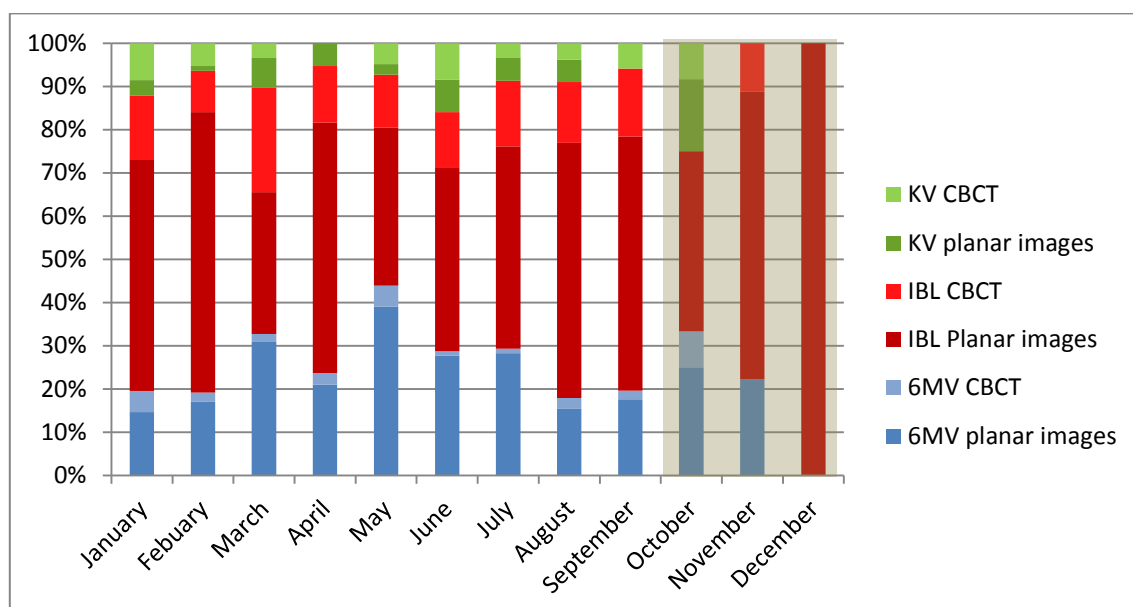
Figure 20: Development of employment of the different image modalities over time for head-and-neck cancer patients
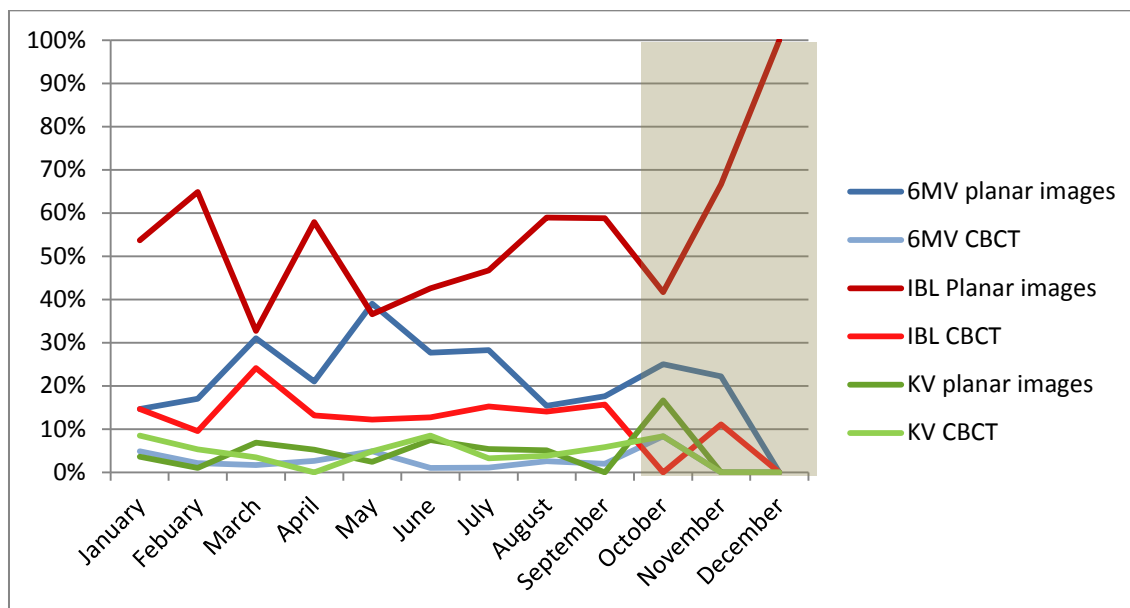
3.3.2 Prostate cancer patients

Table 13 summarizes the monthly amount of radiation fractions delivered to prostate cancer patients throughout the study and the total amount and percentage of monthly set-up verification images per radiation fraction. Most radiation fractions were delivered during the months of May, June and July. The percentage of images acquired per radiation fraction each month varies from 41 % to 50 %, with an average of 46.7 % images per fraction. The month of March presents a clear exception. During March 58.8 % percent of treatment fractions received set-up verification imaging. However, it can be generally noted, that verification imaging is obtained for nearly every other fraction. There is no evident trend development over the course of time regarding the number of images per radiation fraction. For the months of January and February the number of fractions is so small since only patients that started treatment during these months were included in the study. Patients with already ongoing treatment, which was begun in the end of the year 2012, were not included.

Table 13: Radiation fractions and set-up images per month, percentage of images per monthly radiation fractions for prostate cancer patients

Month	fractions per month	images per month	percentage of images per fractions
January	23	10	43.5%
February	53	22	41.5%
March	68	40	58.8%
April	193	98	50.8%
May	223	105	47.1%
June	232	108	46.6%
July	242	99	40.9%
August	165	68	41.2%
September	91	42	46.2%
October	34	17	50.0%
MEAN	132.4	60.9	46.7%

Comparison of CBCT imaging and planar imaging for prostate cancer patients

In addition, the data was evaluated in terms of the preference for two dimensional planar imaging versus three dimensional CBCT imaging over time. Table 14 and Figure 21 show that two-dimensional planar images are more commonly used than three-dimensional CBCT. The percentage of conebeam CT images and planar images is consistent throughout the different months. About 60-70 % of the images acquired each month for set-up verification were two dimensional planar images, 30-40 % were conebeam CT images. The mean monthly employment rates for the two different imaging techniques were 64 % for planar imaging versus 36 % for CBCT imaging. The largest deviation is seen in the months of February and August. In February only 22.7 % of the imaging is CBCT and in August as much as 48.5 % of the images are CBCT images. Apart from these months the distribution of the two imaging techniques remains similar. No increasing or decreasing employment of either imaging technique is observed over time.

Table 14: Amount and percentage of planar images versus CBCT images acquired each month for prostate cancer patients

Month	planar images	CBCT
January	6	4
February	17	5
March	24	16
April	58	40
May	63	42
June	72	36
July	65	34
August	35	33
September	29	13
October	12	5
MEAN	38.1	22.8

Month	planar images	CBCT
January	60.0%	40.0%
February	77.3%	22.7%
March	60.0%	40.0%
April	59.2%	40.8%
May	60.0%	40.0%
June	66.7%	33.3%
July	65.7%	34.3%
August	51.5%	48.5%
September	69.0%	31.0%
October	70.6%	29.4%
MEAN	64.0%	36.0%

Figure 21: Percentage of planar images and CBCT per month for prostate cancer patients
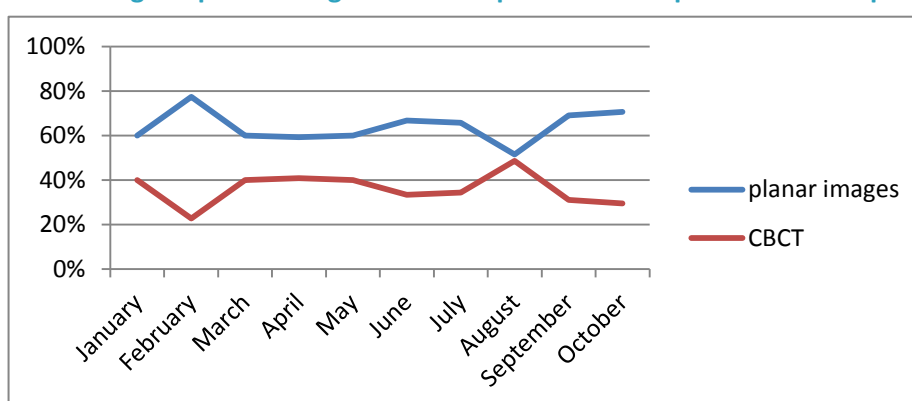
Comparison of monthly 6MV, IBL and kV imaging technique for prostate cancer patients

A summary of the number and percentage of 6MV, IBL and kV images, obtained each month for prostate cancer patients, is provided in Table 15. Figure 22 shows a visualization of the number of 6MV, IBL and kV images obtained each month.

Table 15: Number and percentage of 6MV, IBL and kV images acquired each month within the group of prostate cancer patients

Month	absolute number of images			percentage of images per images total monthly images		
	6MV	IBL	kV	6MV	IBL	kV
January	6	0	4	60.0%	0%	40.0%
February	12	7	3	54.5%	31.8%	13.6%
March	10	24	6	25.0%	60.0%	15.0%
April	20	53	25	20.4%	54.1%	25.5%
May	49	31	25	46.7%	29.5%	23.8%
June	48	24	36	44.4%	22.2%	33.3%
July	62	7	30	62.6%	7.1%	30.3%
August	17	28	23	25.0%	41.2%	33.8%
September	14	16	12	33.3%	38.1%	28.6%
October	10	7	0	58.8%	41.2%	0%
MEAN	24.8	19.7	16.4	43.1%	32.5%	24.4%

Figure 22: Quantity of 6MV, IBL and kV images obtained each month for prostate cancer patients
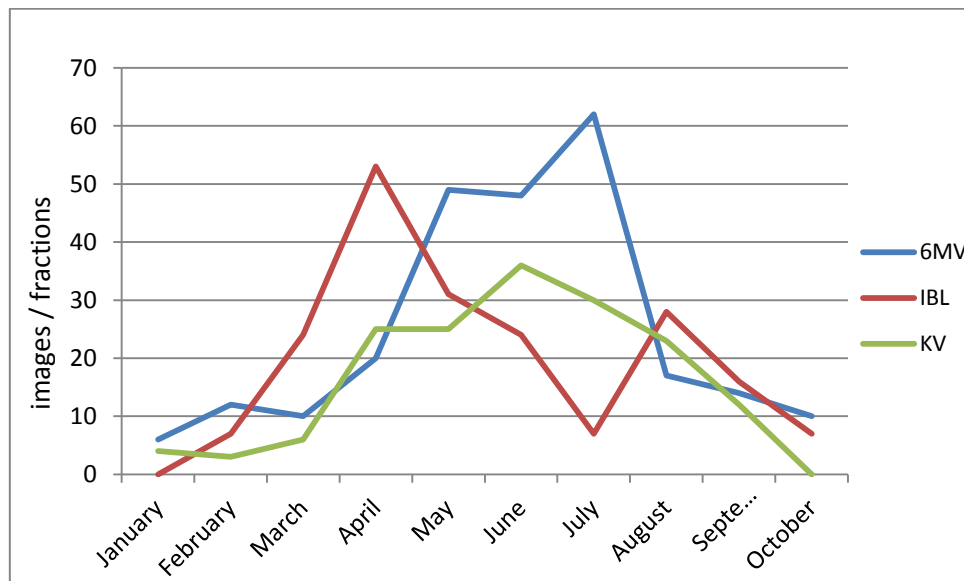
Figure 23 and Figure 24 visualize the distribution of the percentage of 6MV, IBL and kV images within the total of set-up verification images obtained during each month. 6MV imaging represents the most commonly applied imaging technique within the group of prostate cancer patients in this study, with an average of 43.1 % of the total monthly obtained images. The mean percentage of monthly IBL images is 32.5 % and the mean percentage of monthly kV images is 24.4 %. However the percentage of the different image modalities used throughout the different months varies greatly. In the months of May, June and July 6MV imaging is clearly the most commonly used imaging technique, whereas during the months of March and April more IBL images were obtained. After falling from 40 % in January to about 14 % in February the percentage of kV imaging steadily increases again during the course of the year until October where it decreases once more. There is no visible development of a specific trend for the employment of an imaging modality over time. However, due to the small amount of fractions analyzed the month of October may not be representative.

Figure 23: Percentage of 6MV, IBL and kV images per total of the monthly set-up images for prostate cancer patients
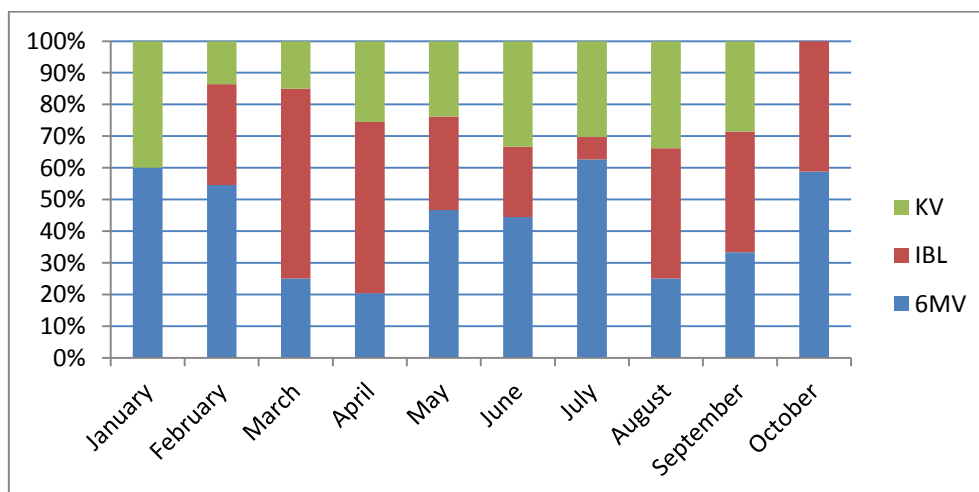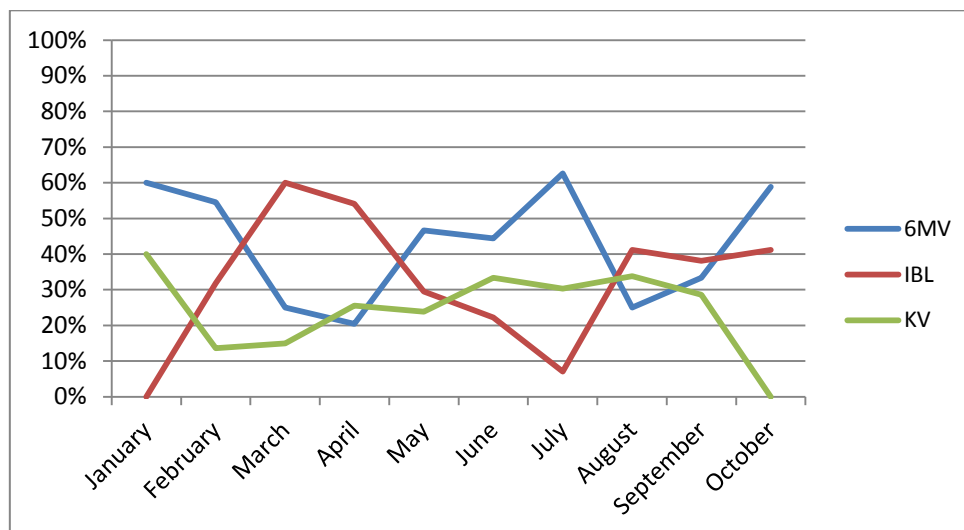
Figure 24: Development of employment of the different image modalities throughout time for prostate cancer patients

Comparison of 6MV planar images and CBCT, IBL planar images and CBCT images and kV planar and CBCT images for prostate cancer patients

Table 16 and Figure 25 show the amount of each of the three different image modalities used for set-up verification imaging. Each of the energies is further divided into two-dimensional planar imaging and three-dimensional CBCT imaging.

Table 16: Absolute number of images per image modality and per month for prostate cancer patients

Month	6MV		IBL		kV	
	planar images	CBCT	planar images	CBCT	planar images	CBCT
January	5	1	0	0	1	3
February	11	1	5	2	1	2
March	7	3	12	12	5	1
April	16	4	29	24	13	12
May	33	16	14	17	16	9
June	38	10	15	9	19	17
July	44	18	6	1	15	15
August	12	5	13	15	10	13
September	12	2	10	6	7	5
October	7	3	5	2	0	0
TOTAL	185	63	109	88	87	77

Figure 25: Number of 6MV-, IBL- and kV-planar images and number of 6MV-, IBL- and KV CBCT obtained each month for prostate cancer patients
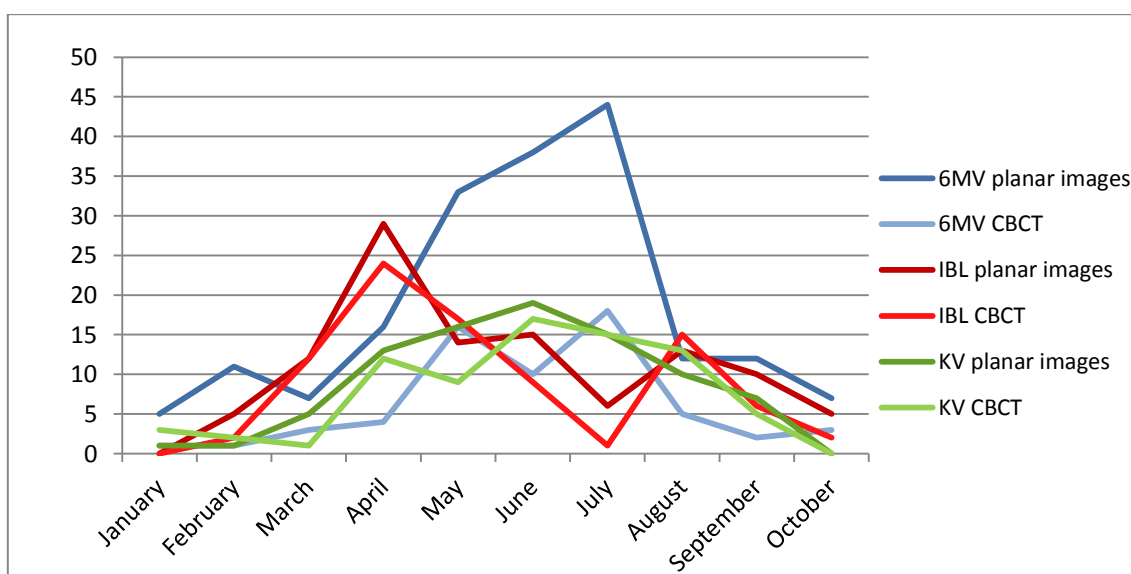
Table 17 summarizes the percentage of the images obtained with the six different imaging techniques in relation to the total amount of monthly images. Figure 26 and Figure 27 compare and visualize these percentages. 6MV planar imaging is the most commonly used technic for set-up verification imaging within the group of prostate cancer patients included in this study, with an average of 33.2 %, followed by IBL planar imaging with an average of 18.8% of the total monthly images. The monthly average of the other four imaging techniques is similar and ranges from 9.9 % (6MV CBCT imaging) to 13.7 % (IBL CBCT imaging). A specific time trend for the employment of the different image modalities is not visible. As can be seen in the diagrams the amount of each different imaging technique used every month varies greatly.

Table 17: Percentage of different image modalities per total monthly images within the group of prostate cancer patients

Month	6MV		IBL		KV	
	planar images	CBCT	planar images	CBCT	planar images	CBCT
January	50.0%	10.0%	0%	0%	10.0%	30.0%
February	50.0%	4.5%	22.7%	9.1%	4.5%	9.1%
March	17.5%	7.5%	30.0%	30.0%	12.5%	2.5%
April	16.3%	4.1%	29.6%	24.5%	13.3%	12.2%
May	31.4%	15.2%	13.3%	16.2%	15.2%	8.6%
June	35.2%	9.3%	13.9%	8.3%	17.6%	15.7%
July	44.4%	18.2%	6.1%	1.0%	15.2%	15.2%
August	17.6%	7.4%	19.1%	22.1%	14.7%	19.1%
September	28.6%	4.8%	23.8%	14.3%	16.7%	11.9%
October	41.2%	17.6%	29.4%	11.8%	0%	0%
MEAN	33.2%	9.9%	18.8%	13.7%	12.0%	12.4%

Figure 26: Percentage of images obtained in each different image modality per total monthly images for prostate cancer patients
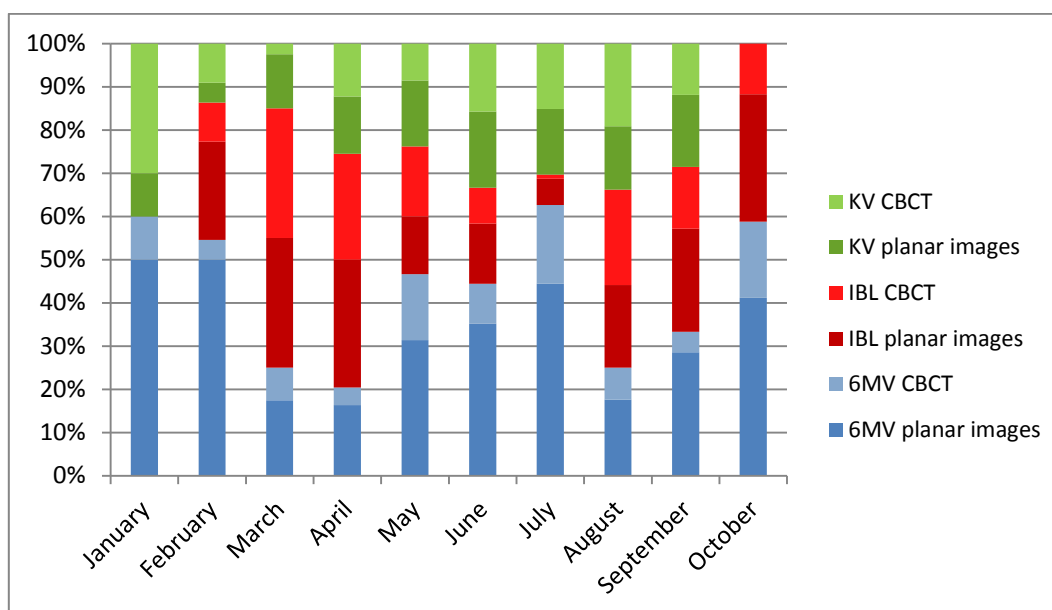
Figure 27: Development of employment of the different image modalities throughout time for prostate cancer patients
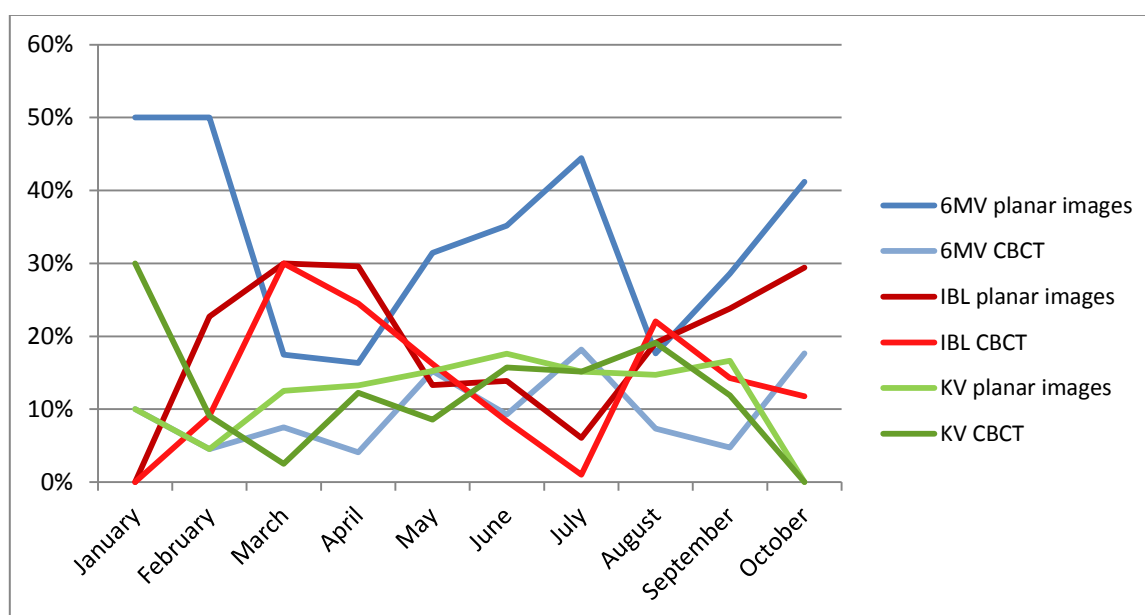
Discussion and Conclusion (3.3)

These results have shown that the frequency of performing verification imaging prior to delivering the radiation treatment is very different for head-and-neck cancer patients versus prostate cancer patient. While prostate cancer patients receive set-up verification imaging for approximately every other treatment fraction, for head-and-neck cancer patients set-up verification imaging is only performed for approximately every third treatment fraction.

When comparing the employment of two dimensional planar imaging versus three dimensional conebeam imaging for both populations, the results show that although the amount of each of the two imaging techniques remains largely consistent over the course of the months, there is a significant difference in the amount of the imaging techniques used between both patient populations. For prostate cancer patients a mean of 36.0 % of CBCT images acquired every month. The amount of three dimensional imaging is much higher than that of head-and-neck cancer patients with a monthly mean of 18.8%. As discussed earlier these results are due to the fact that prostate irradiation requires a much higher accuracy due to greater geometric variability.

Our analysis of the employment of the different imaging techniques used at our clinic did not show any clear development or trend over the course of the time evaluated in our study. After introduction of kV imaging, a new and better high resolution imaging technique, a clear change in the employment rates of the different imaging techniques was not visible over the course of the evaluated months. This might be due to the fact that by January 2013 the new imaging modality was already well established in the daily routine. Another possibility might be that the time period of 9 months was not long enough. An evaluation of a longer time period might bring different results.

For head-and-neck cancer patients IBL planar images consistently make up more than half (55.5 %) of the monthly images, with 6MV planar imaging (21.6 %) coming in second place and IBL CBCT imaging in third (11.9 %). This differs from the distribution within the group of prostate cancer patients in our study. Here the most commonly used imaging technique throughout the months evaluated in this study is 6MV planar imaging with an average of

58

33.2 % and IBL planar imaging with an average of 18.8 %. Only one out of three lincas available in our clinic has the ability of obtaining images with kV energy, whereas two out of three linacs are equipped for IBL imaging and all three linacs are able obtain 6MV images. Taking this into consideration explains the generally small number of kV images. Within the group of head-and-neck cancer patients kV imaging makes up an average of 8 % of the show a much higher percentage of kV imaging per month. 24 % of the monthly set-up verification images for prostate cancer patients are kV images. The amount of planar and CBCT images is approximately even. Certainly the distribution of the imaging modalities used is impacted to some extent by the different employment of the three linacs within both patient populations. As shown earlier (Figure 5) prostate cancer patients were irradiated much more frequently at the ART 1 linac, which is the only one of the three machines in our clinic equipped for kV imaging. This obviously has an influence on the result that the amount of kV imaging within the prostate cancer group is almost three times as high as within the head-and-neck cancer group. In conclusion these results are, to a considerable extent, due to the distribution of the two patient groups to the different linac machines, as well as due to the fact that for prostate cancer patients better imaging techniques are required in comparison to head-and-neck cancer patients. Also, as mentioned earlier, the radiation therapists have confirmed that today the amount of kV imaging at the ART1 has increased and generally the SOP to always use the best imaging technique for each treatment machine is followed.

3.4 Evaluation of the alignment data

### 3.4.1 Overview of all recorded couch shifts

Figure 28, Figure 29 and Figure 30 visualize the range of size of all individual couch shifts recorded during radiation treatment for both patient groups in the S-I, L-R and A-P directions.

Figure 28 shows that for the group of head-and-neck cancer patients the range of couch shifts administered to compensate for the alignment of the target volume prior to the radiation ranges between -1 cm and 1 cm for all three directions. There are no major outliers within this group.

As can be seen in Figure 29 the set-up error shifts for prostate cancer patients, with a few exceptions, all range within the same size, between -2 cm and 2 cm. These exceptions, however, are limited to three patients. Since the variations are so drastic compared to the average size of shifts among the rest of the prostate patients and therefore are not representative for the population of prostate cancer patients in this study, these three patients were excluded in the further evaluation of the data. Figure 30 shows the distribution of set-up errors measured for prostate cancer patients without inclusion of the three patients, further referred to as "outlier".

In Figure 30 it can be seen that, even after eliminating the three "outlier" patients in the prostate cancer patients group, there is still a wide range of size within the individual couch shifts administered for this group. The smallest variation within the couch shifts for prostate cancer patients can be seen in the anterior-posterior (A-P) direction. Here, with few exceptions the couch shifts range between -0.7 cm and 0.7 cm. For the superior-inferior (S-I) direction and for the left-right (L-R) direction the couch shifts are larger, with a range mainly between -1.5 cm to 1.5 cm, with a few exceptions, remaining between -2 cm to 2 cm.

Figure 28: Distribution of all individual set-up error shifts (in cm) in each direction for all head-and-neck cancer patients
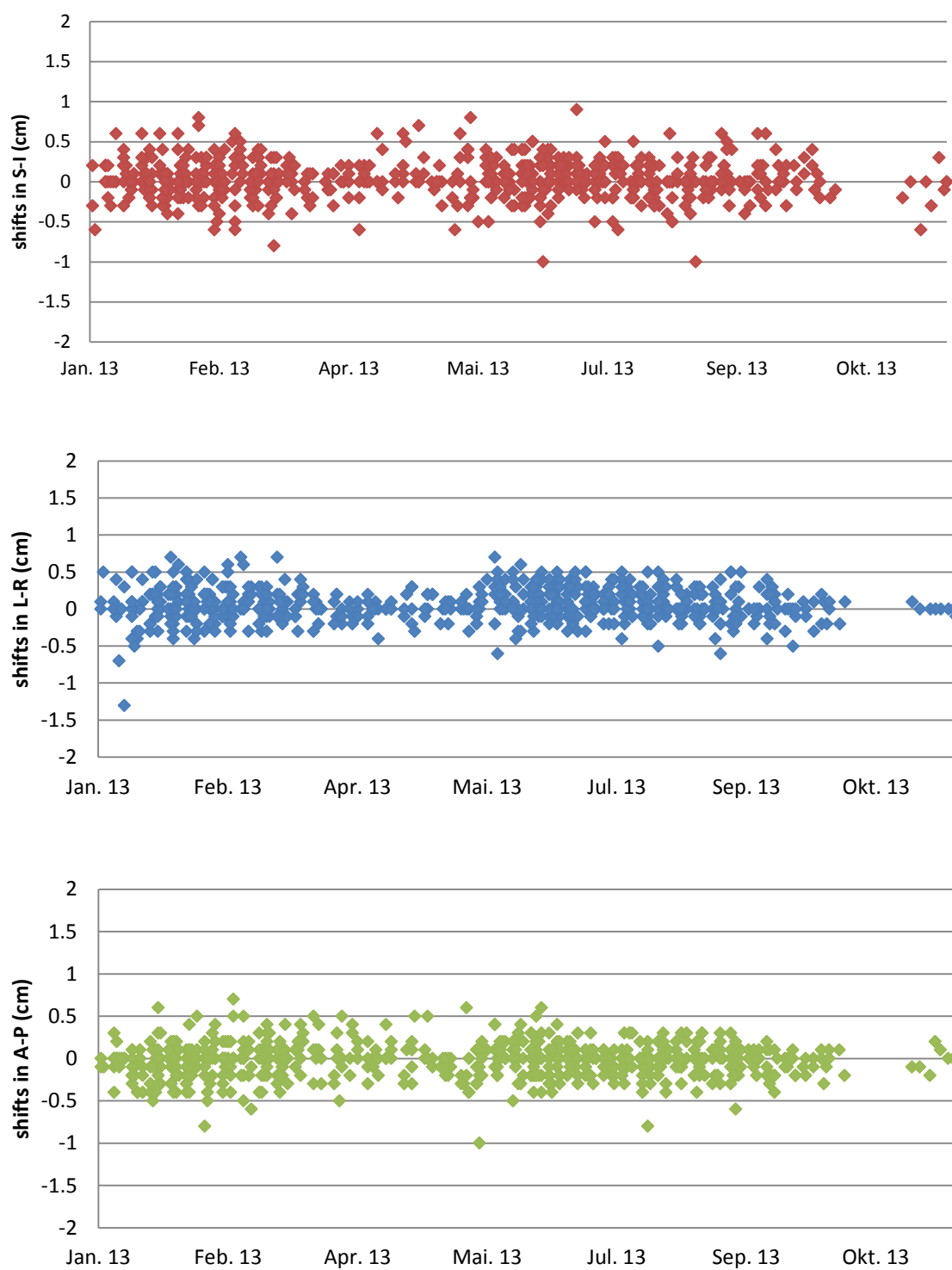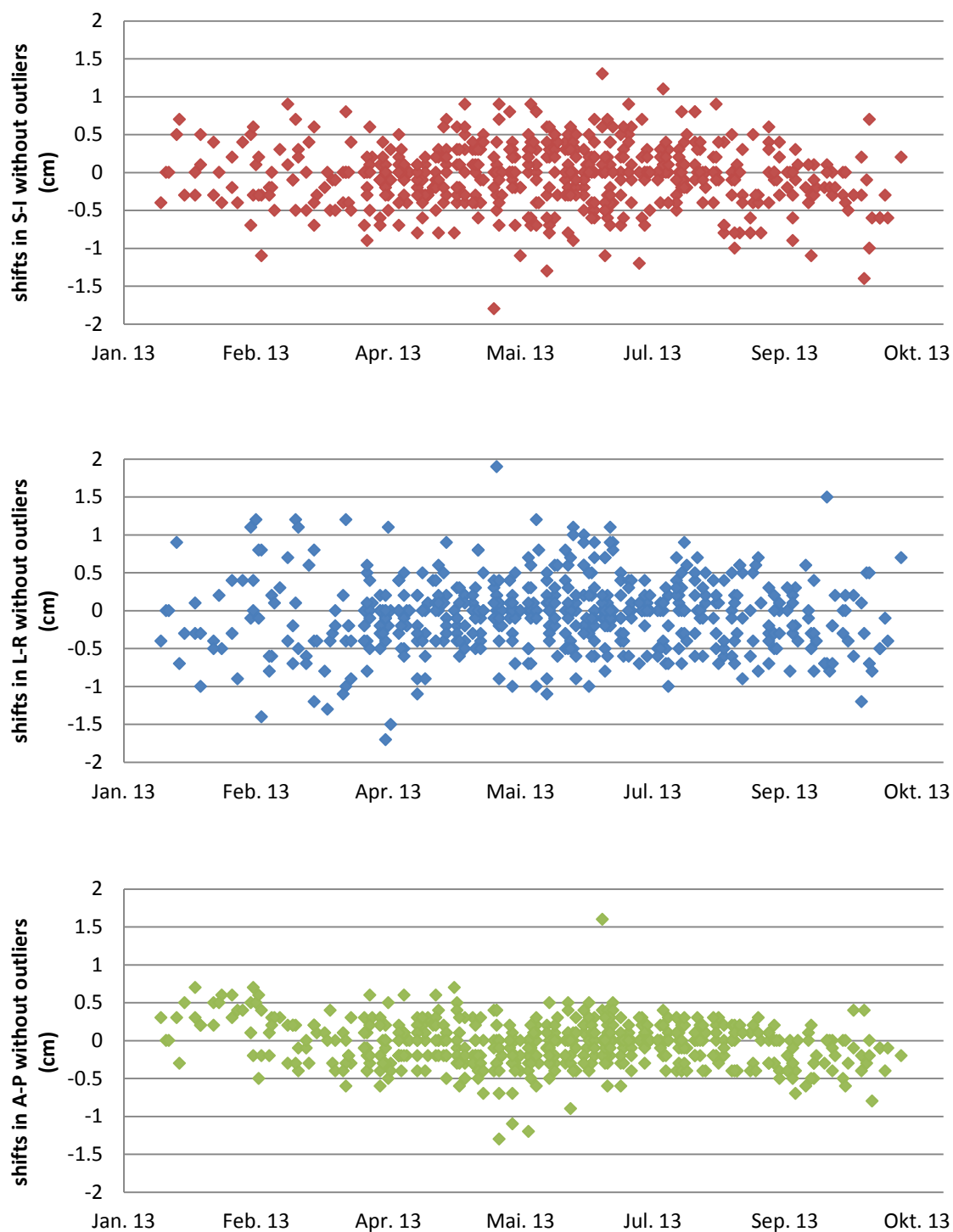
Figure 29: Distribution of all individual set-up error shifts (in cm) in each direction for all prostate cancer patients included in the study
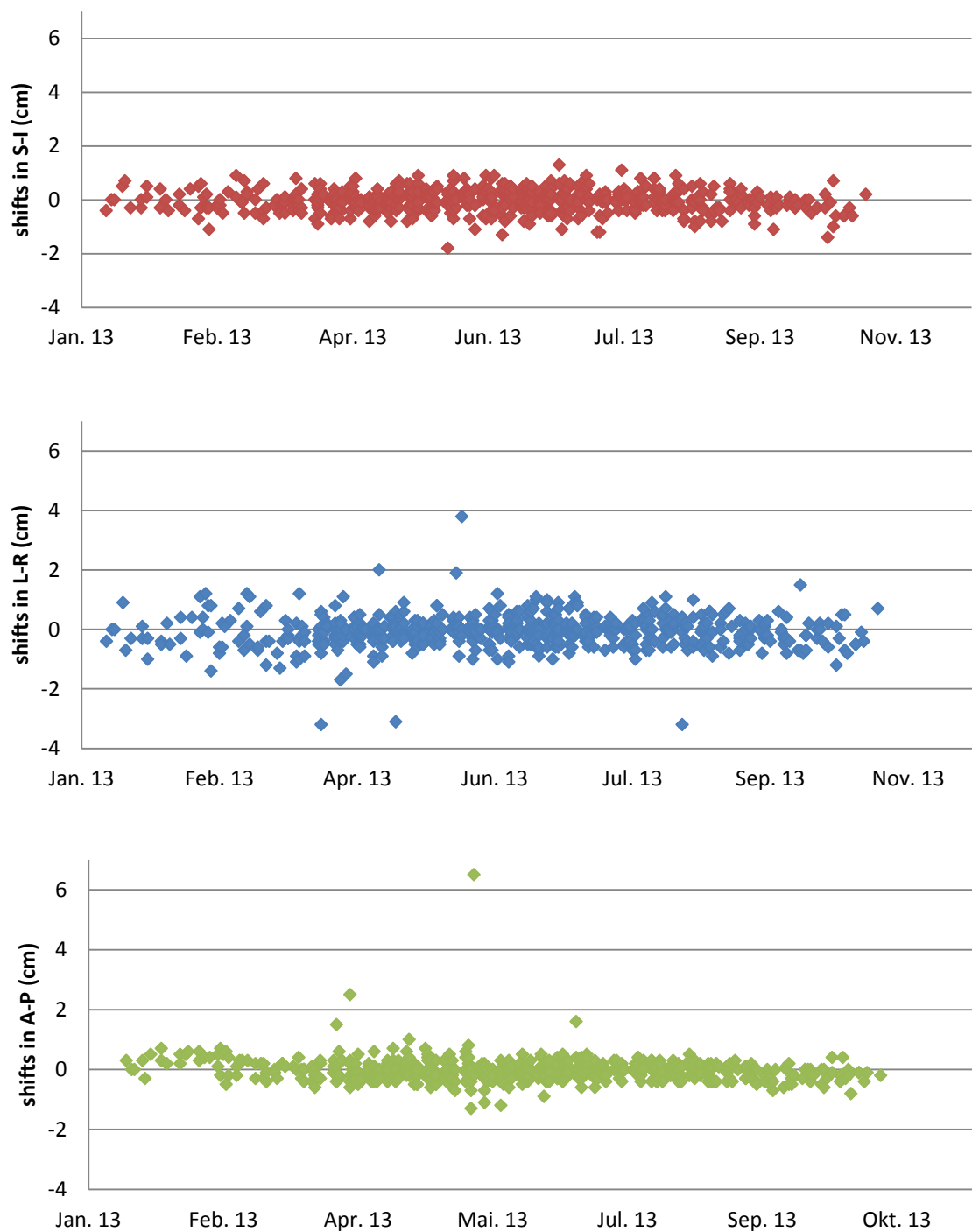
Figure 30: Distribution of all individual set-up error shifts (in cm) in each direction for all prostate cancer patients included in the study without the three outliers

Discussion and conclusion (3.4.1)

Comparing Figure 28 and Figure 30 it becomes obvious that there is a lot less variation in couch shift size within the population of heads-and-neck cancer patients in proportion to the population of prostate cancer patients. For head-and-neck cancer patients the couch shifts range between -1 cm and 1 cm for all three dimensions. For prostate cancer after exclusion of the three "outlier" patients" the couch shifts range generally between -1.5 cm and 1.5 cm. In the A-P dimension the couch shifts for prostate cancer patients are smallest ranging between -0.7 cm and 0.7 cm.

These results are, as previously discussed, due to the fact that the target volume in head-and-neck cancer patients is a lot more rigid in relation to the bony anatomy than the target volume in prostate cancer. Also the immobilization methods used in head-and-neck cancer treatment are more successful in reproducing the position of the target volume acquired during planning due to the better immobilization techniques (i.e. thermoplastic mask). In prostate cancer treatment there is also a much larger variability of the position of the target volume due to internal organ movement (i.e. rectum and bladder filling).

3.4.2 Systematic and random set-up error

For each patient included in this study and for each patient population the systematic and random setup error was calculated according to the methodology by van Herk (2004) explained in methods and materials.

Systematic (μ) and random (r) set-up errors for each individual patient

Table 18 and Table 19 show the mean set-up error for each individual patient and for each of the three dimensions (S-I, L-R and A-P) in the two patient populations, defined as the systematic set-up error (μ) of the patient. Additionally, the standard deviation (SD) of the mean shift for each individual patient is listed, defined as the random error (r) for each individual patient.

The mean set-up error, the systematic set-up error for each individual patient (μ), reveals the exact direction in which the couch was shifted after image verification at an average. This means the average size (in cm) and direction in which the target volume during the individual treatment fractions deviated from the position of the target volume during treatment planning. It is consistent for all individual fractions and therefore is called the systematic set-up error (sometimes also referred to as the preparation set-up error).

The random set-up error (r) is considered the daily variation of the patient's set-up from the mean target volume position. Random set-up errors vary from fraction to fraction. As mentioned earlier, in order to determine the random set-up error (r) for each patient in the two populations, the standard deviation (SD) of the patients mean set-up error (i.e. the systematic setup error (μ)) is calculated.

Figure 31 and Figure 33 show the range of the individual patient's systematic errors (μ) for each direction for head-and-neck cancer and prostate cancer patient populations respectively. Figure 32 and Figure 34 show the range of the systematic errors (μ) of the individual patients compared with Gaussian distribution curves, for each patient population and for each direction.

Table 18: Systematic (μ) and random (r) set-up errors for all individual head-and-neck cancer patients in each direction

mean shift in each direction (cm)			
patient	S-I	L-R	A-P
1	0.07	0.00	-0.03
2	0.09	-0.07	-0.01
3	-0.09	-0.05	-0.12
4	0.17	0.02	0.07
5	0.06	0.26	-0.07
6	0.03	0.15	-0.05
7	-0.02	0.01	-0.12
8	-0.04	0.07	0.04
9	0.10	0.22	0.04
10	-0.02	0.05	-0.05
11	0.16	0.23	0.20
12	0.03	-0.02	0.09
13	-0.02	0.13	-0.03
14	0.23	-0.03	-0.03
15	0.05	0.11	-0.13
16	0.17	0.27	-0.12
17	0.06	0.01	0.11
18	0.14	0.23	0,04
19	-0.12	0.12	-0.09
20	0.11	0.01	0.02
21	-0.08	0.10	0.14
22	-0.01	-0.01	-0.12
23	-0.03	0.08	0.00
24	0.02	0.24	0,21
25	0.01	0.11	-0.08
26	-0.02	0.18	-0.10
27	0.02	0.14	-0.06
28	0.09	0.04	-0.08
29	0.09	0.24	-0.06
30	0.20	0.00	-0.16
31	0.04	0.00	-0.03
32	-0.02	0.10	-0.23
33	0.21	0.16	0.01
34	0.07	0.16	-0.07
35	-0.19	0.08	-0.05
36	0.03	-0.13	-0.03
37	0.03	0.03	-0.05
38	0.07	-0.07	-0.10
39	0.00	-0.05	0.08
40	0.02	0.00	-0.06
41	0.00	0.05	-0.02
42	0.09	0.05	-0.11
43	-0.07	-0.03	-0.03
44	0.08	-0.08	-0.06
45	0.01	0.04	-0.06
46	0.01	0.22	-0.01
47	0.33	0.13	-0.30
48	0.00	-0.03	0.00
49	-0.02	-0.03	0.07
50	-0.13	0.05	0.24
51	-0.04	0.09	-0.02
52	-0.22	-0.03	-0.15
53	-0.03	0.02	-0.02

SD of mean shifts in each direction (cm)			
patient	S-I	L-R	A-P
1	0.17	0.14	0.14
2	0.29	0.22	0.21
3	0.13	0.19	0.17
4	0.38	0.14	0.27
5	0.23	0.35	0.15
6	0.09	0.16	0.11
7	0.09	0.11	0.11
8	0.32	0.14	0.26
9	0.13	0.27	0.12
10	0.40	0.14	0.21
11	0.18	0.19	0.12
12	0.17	0.15	0.14
13	0.12	0.15	0.12
14	0.19	0.16	0.14
15	0.30	0.23	0.31
16	0.14	0.18	0.11
17	0.27	0.25	0.26
18	0.13	0.14	0.13
19	0.21	0.12	0.30
20	0.14	0.23	0.22
21	0.19	0.22	0.16
22	0.22	0.30	0.40
23	0.14	0.26	0.10
24	0.23	0.22	0.27
25	0.38	0.48	0.18
26	0.15	0.19	0.17
27	0.15	0.17	0.14
28	0.11	0.17	0.14
29	0.14	0.13	0.13
30	0.18	0.15	0.09
31	0.14	0.08	0.18
32	0.15	0.17	0.17
33	0.29	0.20	0.11
34	0.17	0.15	0.23
35	0.33	0.23	0.16
36	0.11	0.18	0.16
37	0.11	0.14	0.13
38	0.38	0.24	0.15
39	0.16	0.14	0.11
40	0.25	0.21	0.20
41	0.15	0.07	0.04
42	0.43	0.10	0.13
43	0.25	0.09	0.16
44	0.12	0.16	0.10
45	0.26	0.15	0.19
46	0.18	0.21	0.19
47	0.27	0.12	0.36
48	0.06	0.07	0.08
49	0.16	0.16	0.17
50	0.18	0.17	0.27
51	0.17	0.22	0.09
52	0.23	0.04	0.21
53	0.12	0.12	0.26

Figure 31: Range of all systematic set-up errors (μ) for each individual head-and-neck cancer patient in each direction in cm.
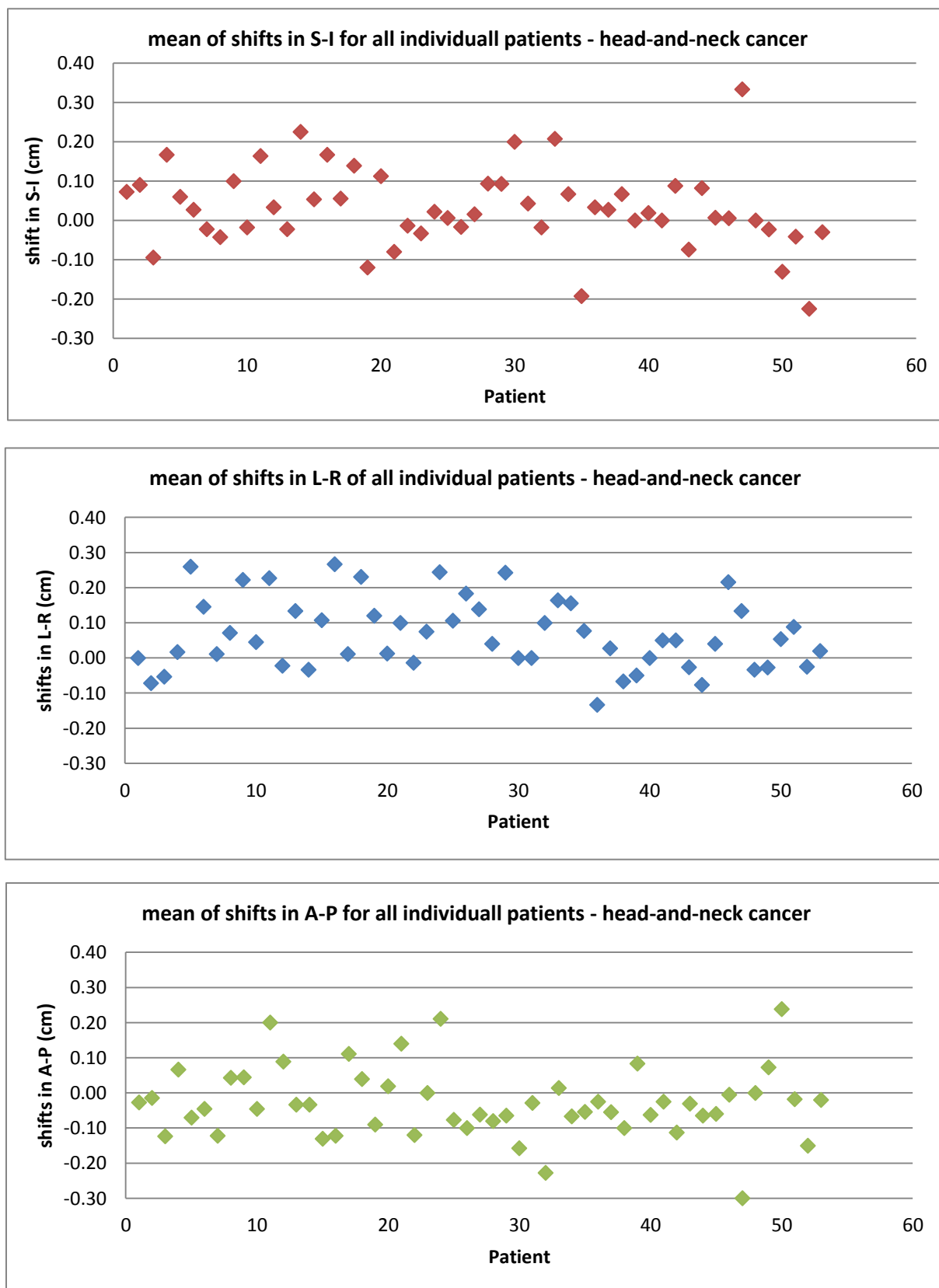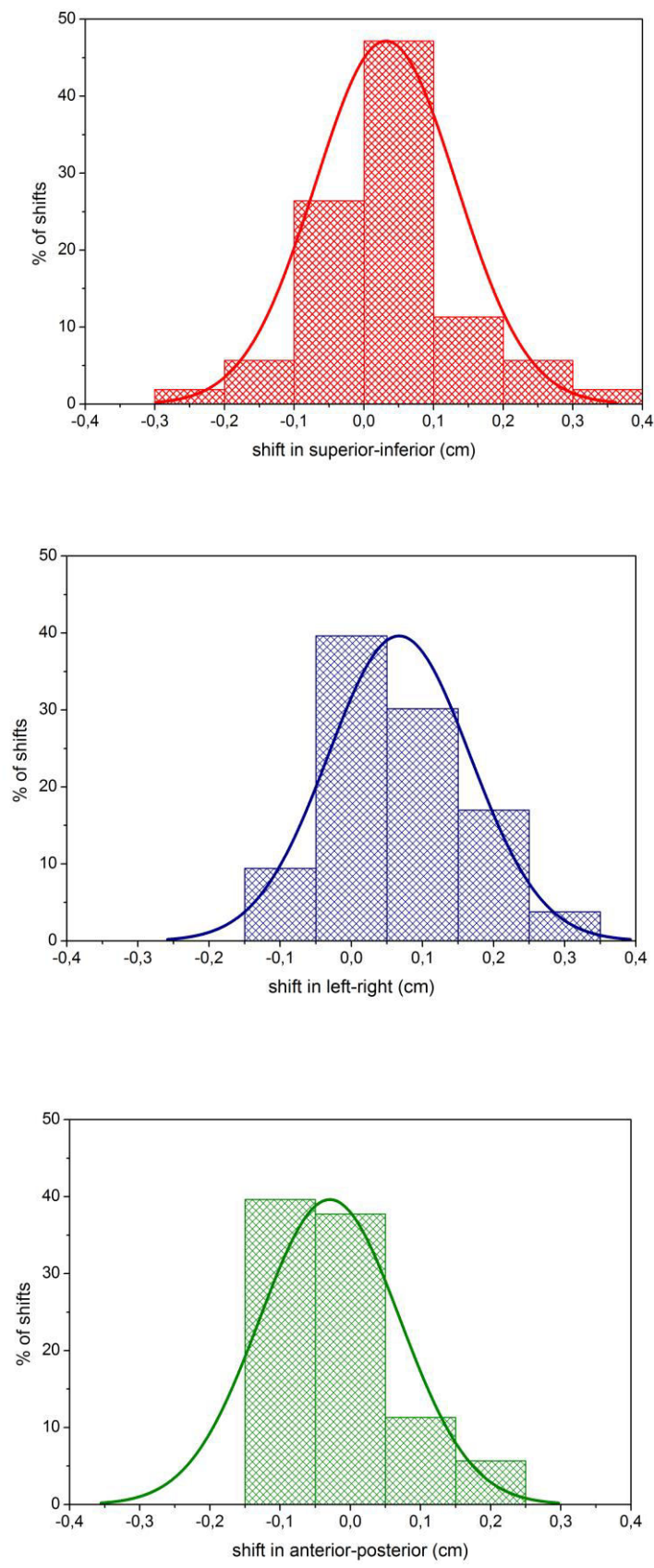
Figure 32: Distribution of shifts for head-and-neck cancer patients and Gaussian fit

Table 19: Systematic (μ) and random(r) set-up errors for all individual prostate cancer patients in each direction

mean of shifts in each direction (cm)			
patient	S-I	L-R	A-P
1	0.08	0.02	-0.02
2	-0.08	-0.30	-0.09
3	-0.05	0.16	0.01
4	0.21	-0.16	-0,06
5	0.09	0.08	-0.06
6	-0.08	0.00	0.13
7	-0.05	0.08	0.24
8	-0.07	-0.13	-0.16
9	0.07	0.11	0.00
10	-0.03	0.06	-0.02
11	-0.29	-0.04	-0.21
12	-0.38	-0.18	-0.29
13	0.02	-0.18	-0.28
14	0.23	-0.06	-0.19
15	-0.14	0.31	-0.12
16	0.11	-0.10	0.16
17	-0.04	0.29	-0.15
18	-0.22	-0.06	0.10
19	0.23	0.07	-0.03
20	-0.18	-0.13	0.02
21	0.02	0.21	0.22
22	-0.33	-0.10	-0.22
23	-0.22	-0.17	-0.29
24	-0.23	-0.03	-0.13
25	0.25	-0.02	0.07
26	-0.35	-0.33	-0.05
27	-0.06	-0.63	-0.02
28	0.08	0.08	0.28
29	0.05	-0.12	-0.09
30	0.00	0.04	0.09
31	-0.07	-0.01	-0.05
32	-0.13	-0.19	0.04
33	0.13	-0.12	-0.29
Outlier patients			
34	0.08	-0.31	-0.09
35	0.03	0.14	0.42
36	0.08	-0.26	0.04

SD of mean shifts in each direction (cm)			
patient	S-I	L-R	A-P
1	0.35	0.32	0.24
2	0.28	0.30	0.20
3	0.36	0.37	0.22
4	0.15	0.30	0.18
5	0.34	0.21	0.16
6	0.40	0.41	0.16
7	0.33	0.40	0.26
8	0.29	0.39	0.18
9	0.27	0.35	0.13
10	0.29	0.23	0.15
11	0.28	0.46	0.25
12	0.46	0.60	0.32
13	0.30	0.24	0.21
14	0.18	0.43	0.20
15	0.31	0.38	0.15
16	0.28	0.29	0.20
17	0.36	0.38	0,.17
18	0.43	0.30	0.42
19	0.22	0.27	0.11
20	0.37	0.49	0.16
21	0.50	0.71	0.32
22	0.37	0.24	0.41
23	0.52	0.53	0.16
24	0.46	0.48	0.17
25	0.48	0.52	0.30
26	0.32	0.41	0.23
27	0.19	0.39	0.23
28	0.36	0.47	0.30
29	0.19	0.28	0.17
30	0.41	0.41	0.22
31	0.72	0.53	0.51
32	0.48	0.37	0.16
33	0.28	0.83	032
Outlier patients			
34	0.38	0.99	0.21
35	0.38	0.88	1.42
36	0.30	0.88	0.59

Figure 33: Range of all systematic set-up errors (μ) for each individual prostate cancer patient in each direction in cm.
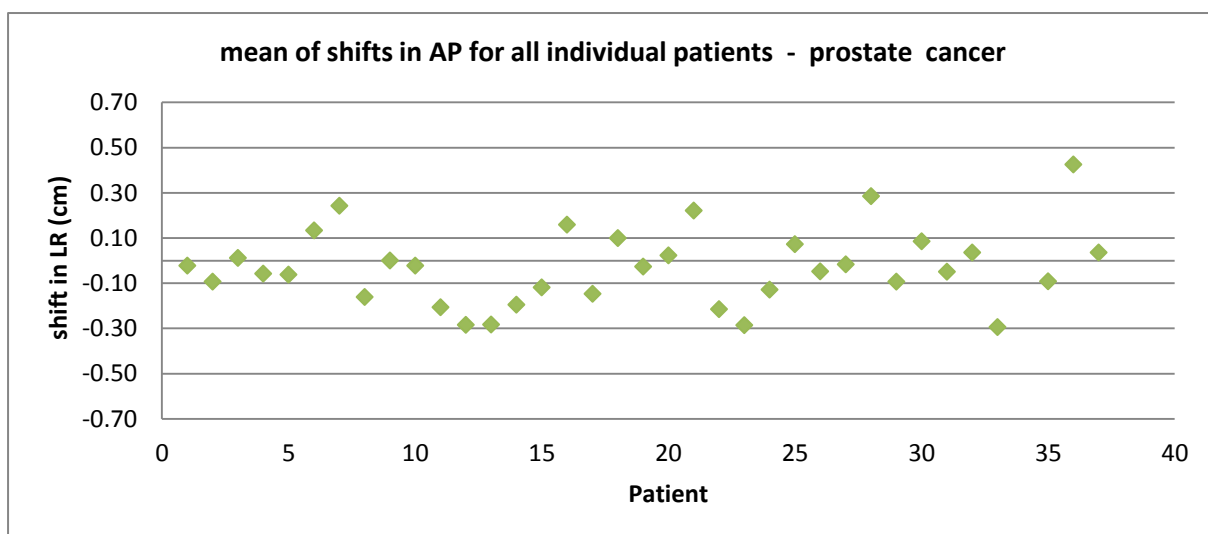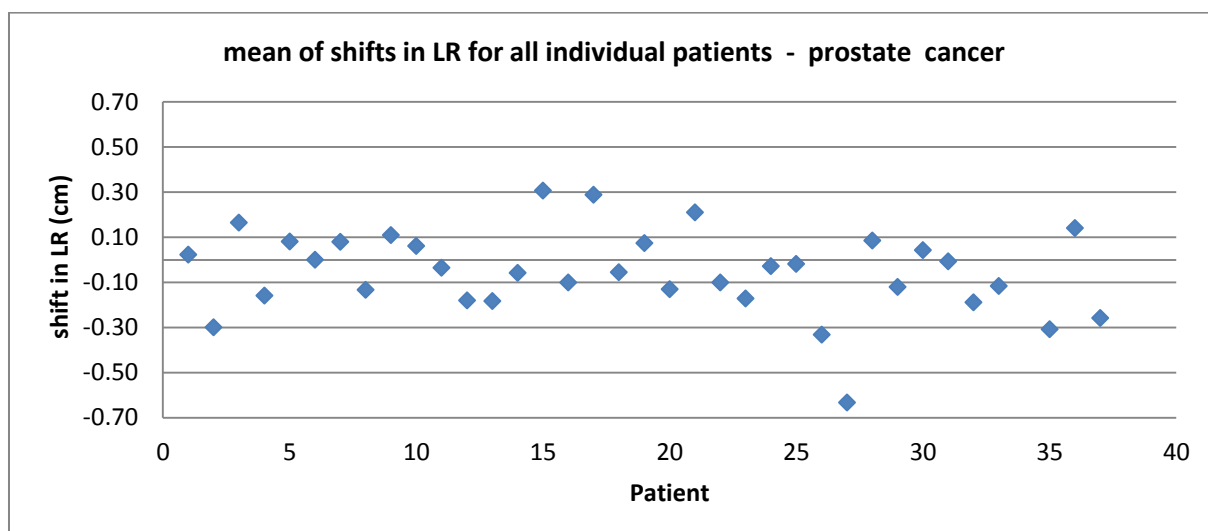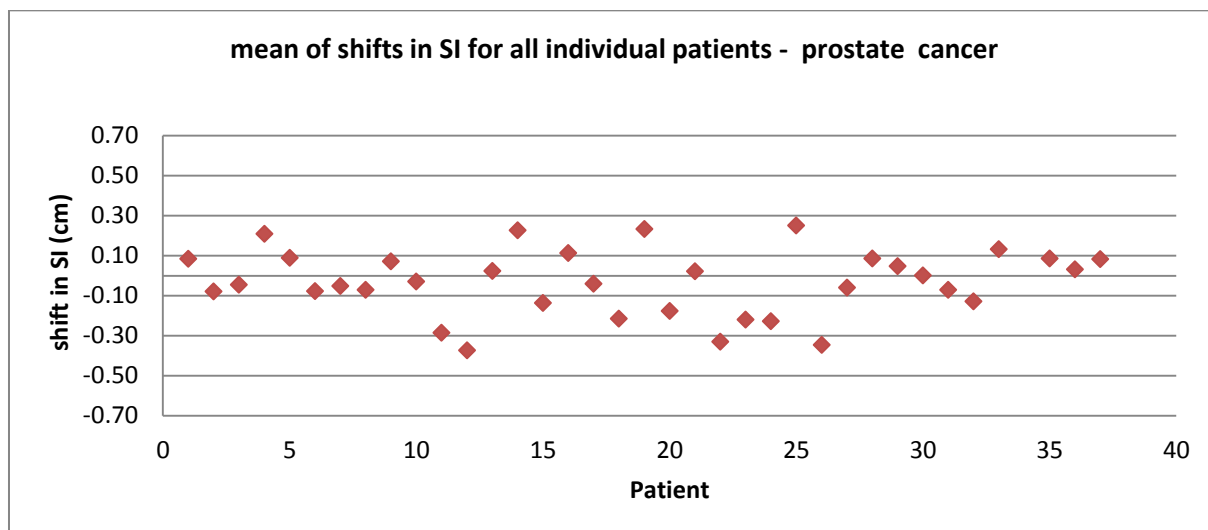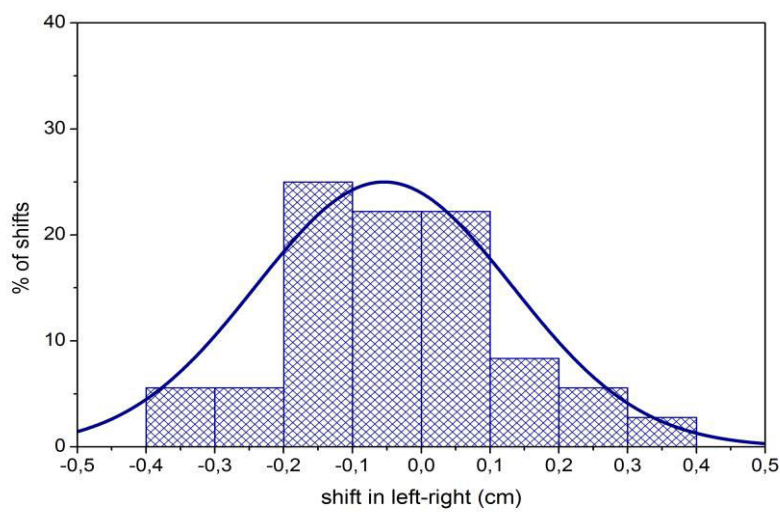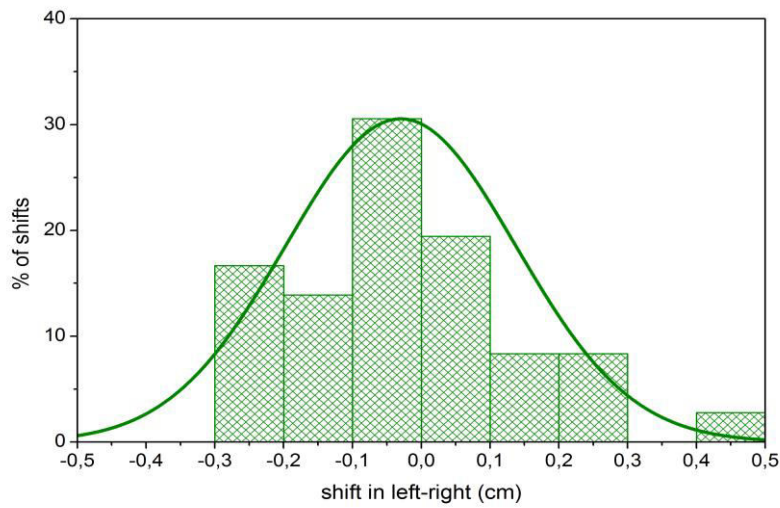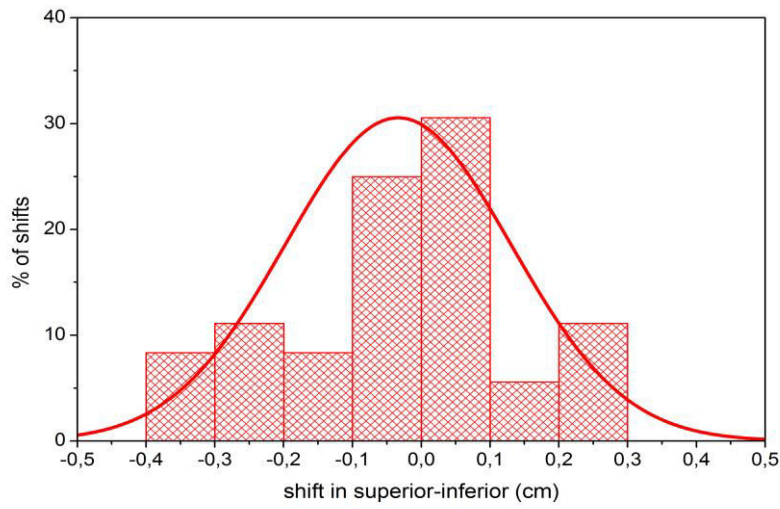
Figure 34: Distribution of shifts for prostate cancer patients and Gaussian fit

Discussion and conclusion (3.4.2)

Figure 31 shows that the systematic set-up errors (μ) for the individual head-and-neck cancer patients range mainly (with few exceptions each), within -0.15 cm and 0.2 cm for the S-I direction, within -0.1 cm and 0.3 cm for the L-R direction and within -0.1 cm and 0.1 cm for the A-P direction. For head-and-neck cancer patients the systematic set-up error (μ), therefore, is smallest in the A-P direction. As mentioned earlier, for prostate cancer patients, the range of the systematic set-up errors (μ) in each direction is larger in comparison to head-and-neck cancer patients. Figure 33 shows that the range is within -0.4 cm and 0.25 cm in the S-I direction, within -0.3 cm and 0.1 cm in the L-R direction and -0.3 cm and 0.2 cm in the A-P direction.

The random error (r) for head-and-neck cancer patients ranges from 0.06 cm to 0.43 cm in the S-I direction, from 0.07 cm to 0.48 cm in the L-R direction and from 0.09 cm to 0.40 cm in the A-P direction. The random error (r) for prostate cancer patients (without the outlier patients) ranges from 0.15 cm to 0.72 cm for the S-I direction, from 0.21 cm to 0.83 cm for the L-R direction and from 0.11 cm to 0.51 cm for the A-P direction. Consistently with the results for the systematic set-up errors (μ) for both patient populations, these results reveal that the random set-up error (r) is considerably larger for prostate cancer patients in comparison to head-and-neck cancer patients.

The random error (r) differs distinctly for each patient and each direction, with values smaller than 0.5 cm for head-and-neck cancer patients and smaller than 0.9 cm for prostate cancer patients. Some individual patients have a larger random error, for example head-and-neck cancer patient 25 with random errors of 0.38 cm, 0.48 cm and 0.18 cm for the S-I, L-R and A-P directions. For other patients the calculated random error is close to zero, i.e. head-and-neck cancer patient 48 with values of 0.06 cm, 0.07 cm and 0.08 cm for the S-I, L-R and A-P directions. This is due to the fact that the different factors affecting the position of the target volume in each patient have a different impact on each individual patient. These factors include weight loss, internal organ motion, tumor shrinkage or other anatomic changes, the fit of the fixation mask, and the agitation of a patient during treatment.

The Gaussian distribution curves in ₍Figure 32₎ and ₍Figure 34₎ show that the sizes of the individual couch shifts realized after set-up verification imaging in order to compensate for geometrical variations are distributed around zero for both populations. However, when comparing the Gaussian curves clear differences can be seen between the two populations. Again it can be seen that the sizes of the mean individual shifts for prostate cancer patients are more widely spread in comparison to the head-and-neck cancer shifts.

3.4.3   The mean absolute shift for each individual patient

In addition to the individual systematic set-up error (μ) (the mean shift) the mean absolute shift for each individual patient was calculated. The "absolute shift" refers to the actual size (in cm) the couch was shifted in order to align the target volume correctly to the reference image, without taking into consideration the sign of the shift value. Calculating the mean absolute shift for each patient discloses how much in actual size (in cm) the position of the target volume differed from the reference target volume position defined during treatment planning as an average.
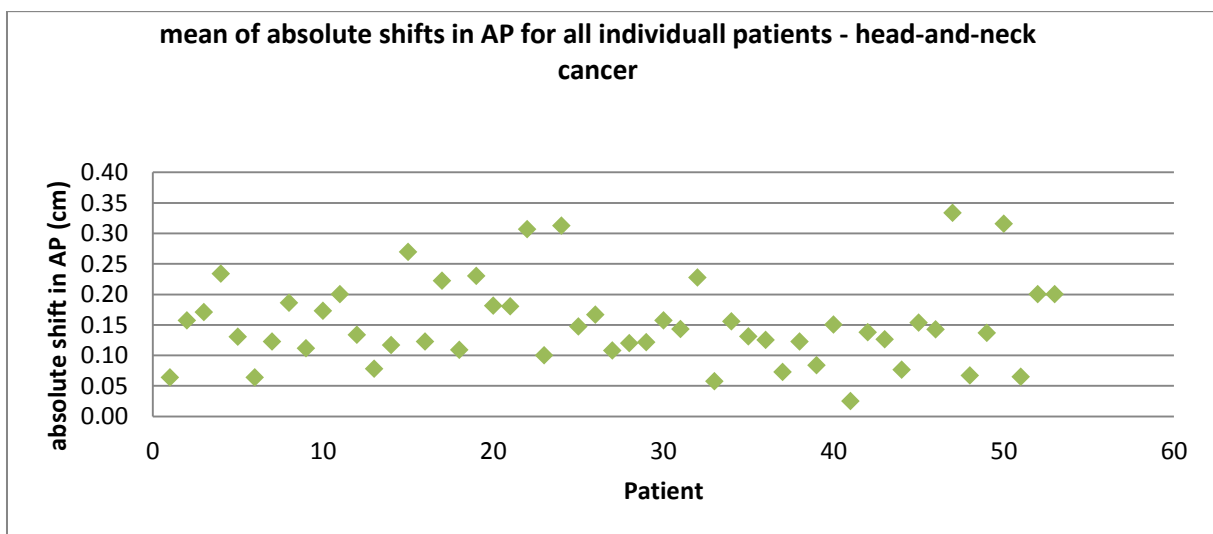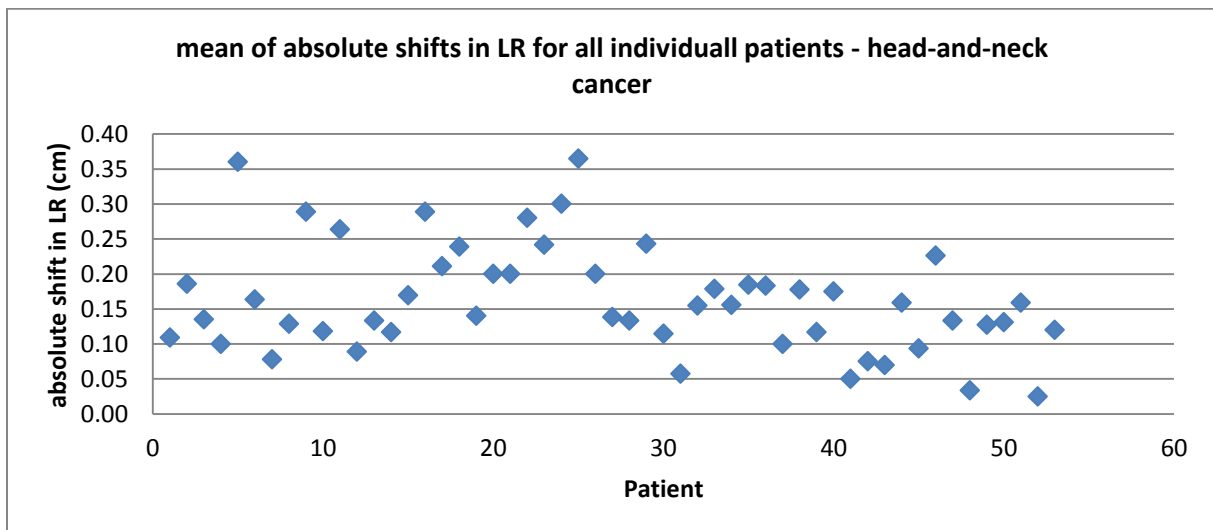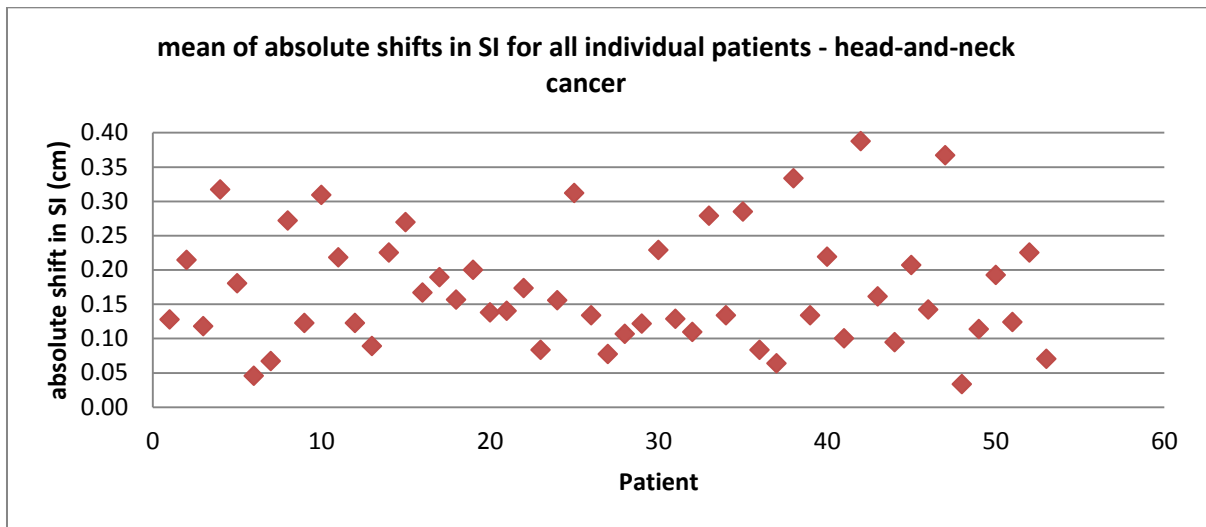
Table 20 and Table 21 show the mean absolute shift for all individual patients in each population and in each direction, as well as the standard deviation of the mean absolute shift in each direction for each individual patient, thus the average absolute size of the daily variation is shown for each patient. Figure 35 and Figure 36 show the range of the individual patient's mean absolute shifts for each direction.

Table 20: Mean absolute shift and standard deviation of the mean absolute shift for all individual head-and-neck cancer patients in each direction

mean shift in each direction (cm)				SD of mean shifts in each direction (cm)			
patient	S-I	L-R	A-P	patient	S-I	L-R	A-P
1	0.13	0.11	0.06	1	0.13	0.09	0.12
2	0.21	0.19	0.16	2	0.21	0.14	0.14
3	0.12	0.14	0.17	3	0.11	0.15	0.12
4	0.32	0.10	0.23	4	0.27	0.10	0.16
5	0.18	0.36	0.13	5	0.16	0.24	0.10
6	0.05	0.16	0.06	6	0.08	0.14	0.10
7	0.07	0.08	0.12	7	0.07	0.08	0.11
8	0.27	0.13	0.19	8	0.18	0.09	0.19
9	0.12	0.29	0.11	9	0.11	0.19	0.06
10	0.31	0.12	0.17	10	0.26	0.09	0.12
11	0.22	0.26	0.20	11	0.11	0.14	0.12
12	0.12	0.09	0.13	12	0.12	0.13	0.09
13	0.09	0.13	0.08	13	0.09	0.15	0.09
14	0.23	0.12	0.12	14	0.19	0.12	0.08
15	0.27	0.17	0.27	15	0.14	0.19	0.21
16	0.17	0.29	0.12	16	0.14	0.14	0.11
17	0.19	0.21	0.22	17	0.20	0.14	0.18
18	0.16	0.24	0.11	18	0.11	0.13	0.09
19	0.20	0.14	0.23	19	0.14	0.09	0.21
20	0.14	0.20	0.18	20	0.11	0.12	0.13
21	0.14	0.20	0.18	21	0.15	0.14	0.12
22	0.17	0.28	0.31	22	0.13	0.11	0.28
23	0.08	0.24	0.10	23	0.11	0.12	0.00
24	0.16	0.30	0.31	24	0.17	0.17	0.18
25	0.31	0.36	0.15	25	0.22	0.33	0.13
26	0.13	0.20	0.17	26	0.07	0.17	0.10
27	0.08	0.14	0.11	27	0.12	0.17	0.11
28	0.11	0.13	0.12	28	0.10	0.11	0.11
29	0.12	0.24	0.12	29	0.12	0.13	0.09
30	0.23	0.11	0.16	30	0.14	0.10	0.09
31	0.13	0.06	0.14	31	0.07	0.05	0.12
32	0.11	0.15	0.23	32	0.11	0.12	0.17
33	0.28	0.18	0.06	33	0.22	0.19	0.10
34	0.13	0.16	0.16	34	0.12	0.15	0.18
35	0.28	0.18	0.13	35	0.25	0.15	0.11
36	0.08	0.18	0.13	36	0.08	0.13	0.11
37	0.06	0.10	0.07	37	0.10	0.10	0.12
38	0.33	0.18	0.12	38	0.19	0.17	0.13
39	0.13	0.12	0.08	39	0.09	0.09	0.11
40	0.22	0.18	0.15	40	0.13	0.12	0.15
41	0.10	0.05	0.02	41	0.11	0.07	0.04
42	0.39	0.08	0.14	42	0.21	0.08	0.10
43	0.16	0.07	0.13	43	0.20	0.07	0.11
44	0.09	0.16	0.08	44	0.11	0.08	0.09
45	0.21	0.09	0.15	45	0.16	0.12	0.12
46	0.14	0.23	0.14	46	0.12	0.20	0.12
47	0.37	0.13	0.33	47	0.22	0.12	0.32
48	0.03	0.03	0.07	48	0.05	0.07	0.05
49	0.11	0.13	0.14	49	0.11	0.10	0.12
50	0.19	0.13	0.32	50	0.11	0.10	0.14
51	0.12	0.16	0.06	51	012	0.17	0.07
52	0.22	0.03	0.20	52	0.23	0.04	0.16
53	0.07	0.12	0.20	53	0.10	0.10	0.19

.

Figure 35: Range of all mean absolute shifts for each individual head-and-neck cancer patient in each direction in cm.

Table 21: Mean absolute shift and standard deviation of the mean absolute shift for all individual prostate cancer patients in each direction

mean of absolute shifts in each direction (cm)				SD of absolute shifts in each direction (cm)			
patient	S-I	L-R	A-P	patient	S-I	L-R	A-P
1	0.26	0.23	0.18	1	0.25	0.22	0.16
2	0.20	0.34	0.16	2	0.22	0.26	0.15
3	0.27	0.35	0.19	3	0.25	0.20	0.12
4	0.21	0.24	0.16	4	0.15	0.24	0.11
5	0.24	0.13	0.10	5	0.26	0.18	0.14
6	0.30	0.30	0.18	6	0.28	0.28	0.10
7	0.27	0.31	0.31	7	0.20	0.26	0.18
8	0.24	0.32	0.17	8	0.18	0.26	0.17
9	0.21	0.27	0.08	9	0.19	0.25	0.10
10	0.23	0.17	0.12	10	0.18	0.16	0.09
11	0.36	0.34	0.28	11	0.18	0.31	0.17
12	0.48	0.52	0.37	12	0.36	0.35	0.22
13	0.26	0.27	0.31	13	0.15	0.14	0.17
14	0.23	0.29	0.24	14	0.18	0.33	0.15
15	0.24	0.39	0.13	15	0.25	0.28	0.14
16	0.21	0.25	0.21	16	0.22	0.17	0.16
17	0.31	0.34	0.19	17	0.19	0.34	0.11
18	0.36	0.23	0.23	18	0.33	0.20	0.36
19	0.24	0.19	0.08	19	0.21	0.21	0.08
20	0.33	0.41	0.13	20	0.25	0.30	0.10
21	0.41	0.64	0.36	21	0.29	0.37	0.15
22	0.39	0.21	0.38	22	0.30	0.15	0.25
23	0.48	0.49	0.30	23	0.31	0.26	0.14
24	0.43	0.40	0.20	24	0.29	0.26	0.08
25	0.46	0.42	0.26	25	0.29	0.31	0.16
26	0.42	0.36	0.21	26	0.21	0.38	0.12
27	0.15	0.63	0.19	27	0.14	0.39	0.13
28	0.32	0.41	0.36	28	0.20	0.24	0.20
29	0.14	0.21	0.13	29	0.14	0.21	0.14
30	0.34	0.29	0.17	30	0.23	0.30	0.17
31	0.57	0.38	0.36	31	0.45	0.37	0.36
32	0.34	0.29	0.11	32	0.36	0.29	0.13
33	0.22	0.66	0.34	33	0.22	0.52	0.27
Outlier patients				Outlier patients			
34	0.33	0.66	0.17	34	0.21	0.80	0.16
35	0.31	0.39	0.54	35	0.22	0.80	1.38
36	0.23	0.54	0.35	36	0.21	0.75	0.48

mean of absolute shifts in SI for all individual patients - prostate cancer

mean of absolute shifts in LR for all individual patients - prostate cancer

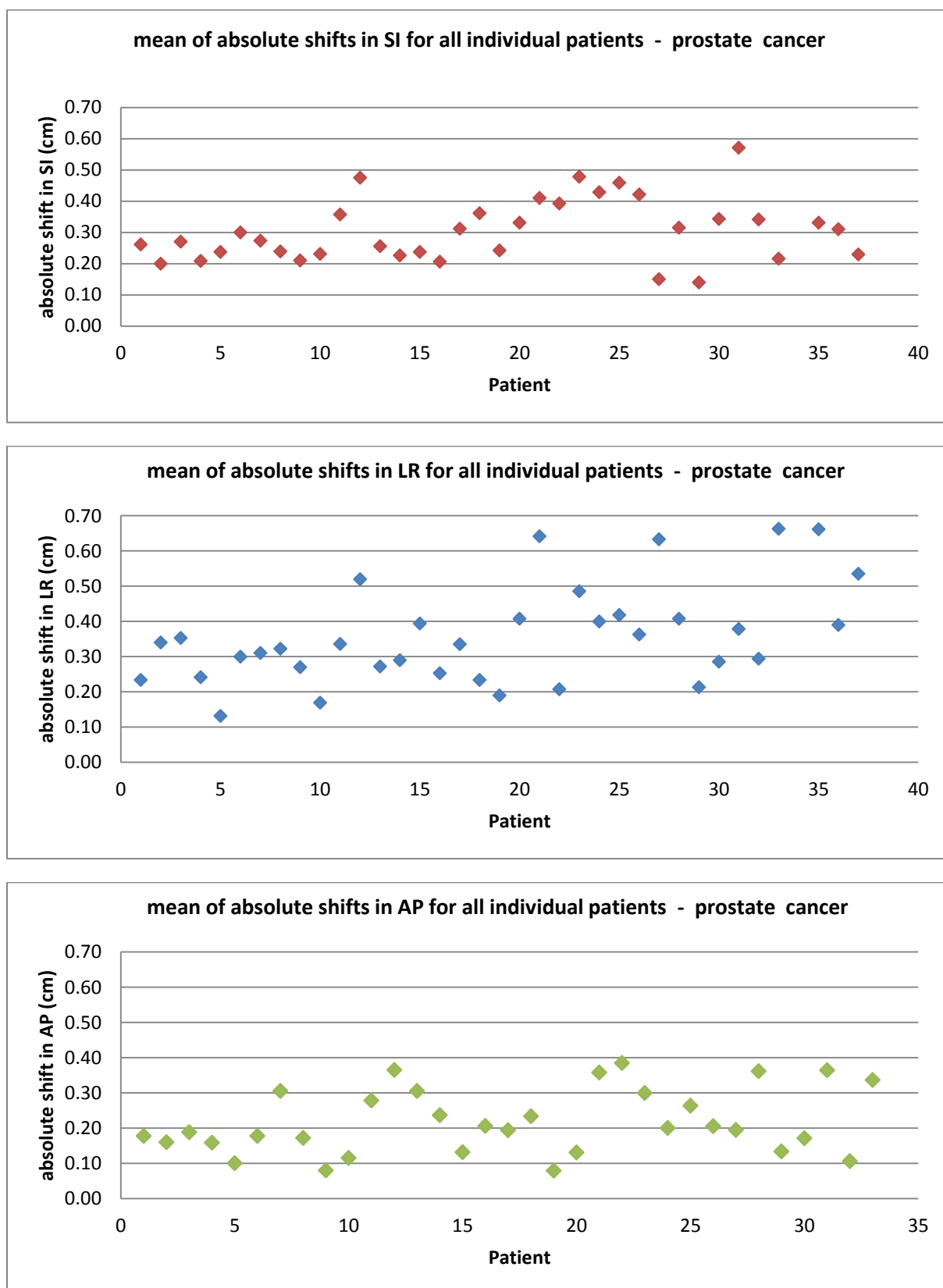mean of absolute shifts in AP for all individual patients - prostate cancer

Figure 35 shows that the sizes of the average absolute shifts for the individual head-and-neck cancer patients are similar within the three directions, the A-P direction having the smallest variation ranging mainly from 0.05 cm to 0.25 cm, in comparison to the S-I direction with values between 0.05 cm and approximately 0.35 cm and to the L-R direction with values ranging mainly from 0.05 cm to 0.30 cm. For prostate cancer patients the mean absolute shifts are larger in all three dimensions. In Figure 36 the average absolute shifts for each individual patient are shown to be largest in the L-R direction, ranging mainly within 0.1 cm and 0.65 cm, in comparison to 0.2 cm and 0.45 cm in the S-I direction and 0.1 cm to 0.4 cm in the A-P direction.

3.4.4 Differences in set-up errors shown in the example of individual patients

In order to demonstrate the large differences between individual patients within a patient population a boxplot (Figure 37) was created. The boxplot shows examples of a patient with a very large set-up variability (poor) and a patient with a very small set-up variation (good), as well as a representative average set-up error (total) for both head-and-neck cancer patients and prostate cancer patients.

Figure 37: Boxplot showing the range of set-up errors within both patient populations - showing sample patients with good, poor and average (total) set-up accuracy
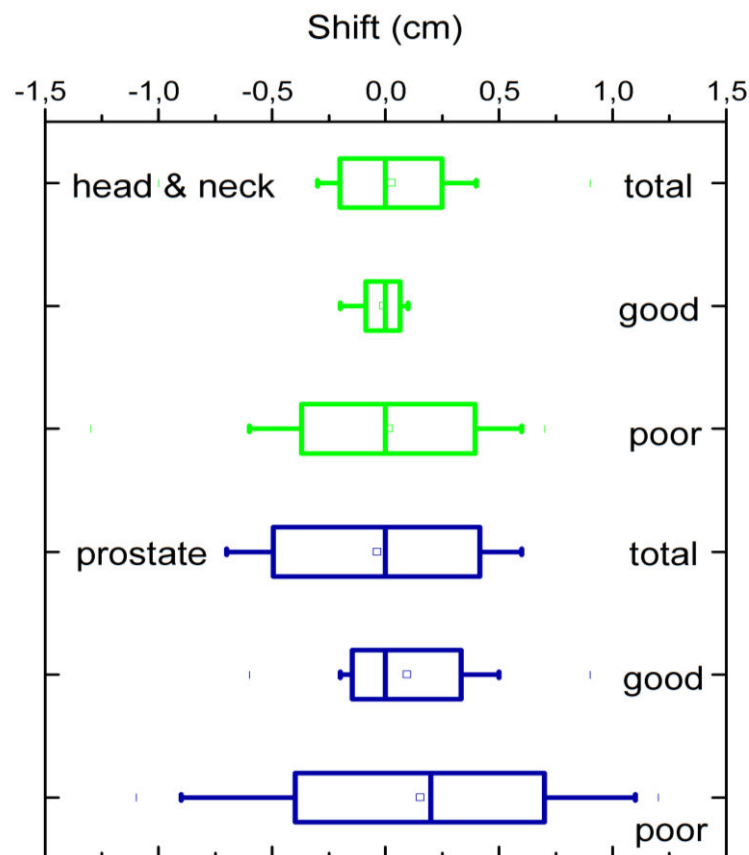
Discussion and conclusion: (3.4.3 and 3.4.4)

Overall, these results show that the dimension of the systematic set-up errors (μ) for both head-and-neck cancer patients and prostate cancer patients is minor, with values close to zero in all of the three directions. In addition, there is no specific trend visible that would indicate a dominant deviation in a certain direction, thus a systematic set-up error which results in a systematic deviation of the target volume to a certain direction is not evident. These are important results confirming the quality assurance of the delivery of radiation therapy at our clinic. Furthermore, these results have confirmed that the random error is a lot larger for prostate cancer patients in comparison to head-and-neck cancer patients due to larger geometric variability of target volumes for prostate cancer patients in comparison to head-and-neck cancer patients. However, our results also show that for individual patients within a population the random set-up error might be very different. Some individual patients have a large random set-up error with large couch shifts necessary in order to compensate for these set-up errors. For other patients there is only a minimal variation of the position of the target volume evident after set-up verification imaging. The fact that random errors might be very different for individual patients needs to be taken into consideration when treating patients.

3.5 Population systematic errors (M), variation of population systematic errors (∑) and population random errors (σ)

3.5.1 Errors of both populations for combined imaging techniques

As previously explained in Methods and Materials, according to van Herks (2004) methodology, the systematic set-up error within a population of patients (M) is determined by calculating the mean of all the individual patient's systematic set-up errors (μ). The population systematic error (M) indicates any potential systematic error that affects all patients and all fractions within a specific population. The variation (∑) of the population systematic set-up error (M) is obtained by calculating the standard deviation (SD) of all the individual patient systematic errors. The variation (∑) of the population systematic set-up error indicates the patient-to-patient variation in the systematic deviation from the planning situation. The random set-up error (σ) for a population of patients is defined by calculating the root-mean-square (RMS) of the random set-up errors recorded for each patient in the population. Table 22 shows the results of the calculations for the population systematic setup error (M), variation of population systematic error (∑) and population random set-up error (σ) for head-and-neck cancer and prostate cancer patients in all three directions.

Table 22: population systematic setup error (M), variation of population systematic error (∑) and population random error (σ) for head-and-neck cancer and prostate cancer patients in the S-I, L-R and A-P directions

	population systematic setup error (M) (cm)			variaton of population systematic error (∑) (cm)			population random error (σ) (cm)		
	S-I	L-R	A-P	S-I	L-R	A-P	S-I	L-R	A-P
Head-and-neck cancer patients	0.03	0.07	-0.03	0.10	0.10	0.10	0.22	0.19	0.19
Prostate cancer patients	-0.03	-0.05	-0.03	0.16	0.18	0.17	0.37	0.49	0.35

As anticipated the population systematic set-up error (M) for both populations is approximately zero in all three directions. The values for the population of head-and-neck cancer patients are 0.03 cm for the S-I direction, 0.07 cm for the L-R direction and -0.03 cm

for the A-P direction. The values for the population of prostate cancer patients are -0.03 cm for the S-I direction, -0.05 cm for the L-R direction and -0.03 cm for the A-P direction. All values are smaller than 1 mm.

For the results of the variation of the population systematic error (Σ) differences can be seen within both patient population errors. The variation of the population systematic error (Σ) is larger for prostate cancer patients with values of 0.16 cm (S-I), 0.18 cm (L-R), and 0.17 cm (A-P) in comparison to 0.10 cm in all three directions for head-and-neck cancer patients. The biggest difference between the two patient groups can be found in the calculation of the population random error (σ). For head-and-neck cancer patients, the population random error (σ) is 0.19 cm for the L-R and A-P direction and slightly larger with 0.22 cm for the S-I direction. In contrast, the population random error (σ) for prostate cancer patients is considerably larger with values of 0.37 cm (S-I), 0.49 cm (L-R) and 0.35 cm (A-P).

Discussion and conclusion (3.5.1)

The results for the population systematic error M is nearly zero for both patients populations. This confirms that there is no relevant systematic set-up error (M) in our clinic which systematically affects the entire patient population. This means there is practically no error in the individual patient set-up that affects all the patients of a specific population in the same way. This confirms the efficiency of the quality assurance measures realized at our clinic. These results also reveal that the variation of the population systematic error (∑) is slightly larger for prostate cancer patients. The biggest difference our results show is, as mentioned earlier, the large difference between the population random errors (σ) for both patient groups. The target volume in prostate cancer patients is subject to a much wider set-up variation in comparison to head-and-neck cancer patients. This has been shown earlier in the results shown in figures 31, 32, 33 and 34 presenting the mean set-up error for individual patients of both populations. The largest random population error (σ) for prostate cancer patients can be found in the L-R dimension (0.49 cm). In comparison, for head-and-neck cancer patients the random population error (σ) is found to be slightly larger in the S-I dimension. However, the random population error (σ) for head-and-neck cancer patients is very similar for all three dimensions. A possible reason for this might be that the thermoplastic immobilization masks used for head-and-neck cancer patients allow more movement of the head in the S-I dimension than in the other two dimensions. Of course the reason for the larger population random error for prostate cancer patients is due to the larger geometric variability of the target volume caused by internal organ motion, rectum and bladder filling and other factors previously discussed.

.

3.5.2 Comparison of error calculations for the different imaging techniques

In order to determine whether the individual imaging modalities had an impact on these results, the population systematic errors (M), variation of population systematic errors (∑) and population random errors (σ) using the alignment data acquired with each of the different imaging modalities separately, were calculated. The results of this calculation are shown in Table 23 for head-and-neck cancer patients and in Table 24 for prostate cancer patients.

Table 23: population systematic setup error (M), variation of population systematic error (∑) and population random error (σ) for the different imaging modalities – head-and-neck cancer patients

IMAGING MODALITY	population systematic setup error (M) (cm)			variaton of population systematic error (∑) (cm)			population random error (σ) (cm)		
	S-I	L-R	A-P	S-I	L-R	A-P	S-I	L-R	A-P
6MV	-0.01	0.04	-0.03	0.15	0.16	0.14	0.16	0.15	0.13
IBL	0.04	0.08	-0.03	0.13	0.11	0.14	0.21	0.18	0.18
kV	0.06	0.05	-0.03	0.23	0.18	0.15	0.12	0.11	0.13

IMAGING MODALITY	population systematic setup error (M) (cm)			variaton of population systematic error (∑) (cm)			population random error (σ) (cm)		
	S-I	L-R	A-P	S-I	L-R	A-P	S-I	L-R	A-P
Planar imaging	0.03	0.07	-0.03	0.11	0.11	0.10	0.22	0.19	0.19
CBCT	0.05	0.03	0.01	0.15	0.16	0.15	0.14	0.14	0.15

IMAGING MODALITY	population systematic setup error (M) (cm)			variaton of population systematic error (∑) (cm)			population random error (σ) (cm)		
	S-I	L-R	A-P	S-I	L-R	A-P	S-I	L-R	A-P
6MV Planar imaging	0.00	0.03	-0.02	0.15	0.15	0.12	0.16	0.15	0.14
6MV CBCT	-0.01	-0.09	-0.07	0.17	0.19	0.22	0.07	0.07	0.08
IBL Planar imaging	0.06	0.08	-0.03	0.14	0.13	0.13	0.22	0.18	0.18
IBL CBCT	0.02	0.04	0.01	0.16	0.16	0.21	0.11	0.12	0.10
kV Planar imaging	-0.03	0.04	-0.11	0.18	0.12	0.14	0.11	0.09	0.09
kV CBCT	0.14	0.04	0.03	0.25	0.21	021	0.07	0.09	0.07

Table 24: population systematic setup error (M), variation of population systematic error (∑) and population random error (σ) for the different imaging modalities – prostate cancer patients

IMAGING MODALITY	population systematic setup error (M) (cm)			variaton of population systematic error (∑) (cm)			population random error (σ) (cm)		
	S-I	L-R	A-P	S-I	L-R	A-P	S-I	L-R	A-P
6MV	-0.08	-0.13	-0.06	0.19	0.24	0.22	0.34	0.34	0.21
IBL	-0.03	-0.01	-0.02	0.25	0.40	0.21	0.28	0.42	0.36
kV	0.09	-0.09	-0.02	0.20	0.29	0.22	0.29	0.40	0.20

IMAGING MODALITY	population systematic setup error (M)			variaton of population systematic error (∑)			population random error (σ) (mm)		
	S-I	L-R	A-P	S-I	L-R	A-P	S-I	L-R	A-P
Planar imaging	-0.02	-0.02	-0.04	0.17	0.20	0.17	0.33	0.43	0.24
CBCT	-0.03	-0.10	-0.02	0.28	0.38	0.27	0.38	0.50	0.39

IMAGING MODALITY	population systematic setup error (M) (cm)			variaton of population systematic error (∑) (cm)			population random error (σ) (cm)		
	S-I	L-R	A-P	S-I	L-R	A-P	S-I	L-R	A-P
6MV Planar imaging	-0.09	-0.12	-0.09	0.19	0.25	0.28	0.30	0.35	0.19
6MV CBCT	-0.03	-0.15	-0.09	0.38	0.34	0.30	0.28	0.28	0.13
IBL Planar imaging	-0.01	0.01	-0.03	0.22	0.44	0.19	0.24	0.38	0.22
IBL CBCT	-0.06	-0.05	-0.01	0.37	0.33	0.27	0.32	0.45	0.46
kV Planar imaging	0.09	-0.04	-0.05	0.21	0.29	0.24	0.28	0.30	0.21
kV CBCT	0.09	-0.19	0.07	0.24	0.70	0.20	0.30	0.28	0.17

Discussion and conclusion(3.5.2)

The population systematic error (M) calculated with different imaging techniques

These results show that in terms of calculating the systematic error for both populations the different imaging modalities applied offer very similar results. The systematic error is always close to zero, no matter which imaging modality was used.

Comparing errors calculated with 6MV, IBL and KV imaging

Within the groups of head-and-neck cancer patients the variation of the population systematic errors ($\sum$) is found to be slightly larger with the alignment data obtained from kV imaging, with values of 0.23 cm (S-I), 0.18 cm (L-R) and 0.15 cm (A-P) in comparison to the values obtained from 6MV and IBL alignment data, which range between 0.11 cm to 0.16 cm for all three directions. For prostate cancer patients we find different results for the variation of population systematic errors ($\sum$) calculated with 6MV, IBL and kV alignment data separately. In correspondence to the results calculated with all imaging modalities together the values are a lot larger for prostate cancer patients as opposed to head-and-neck cancer patients. The results for the L-R direction are notably larger in comparison to the S-I and A-P direction for all three imaging modalities. With 0.40 cm, the variation of population systematic error ($\sum$) for the L-R direction determined with IBL imaging is considerably larger than the rest. This is followed by 0.29 cm with KV and 0.24 cm with 6MV imaging. IBL also offers the largest variation of population systematic errors ($\sum$) for the S-I dimension, where it is 0.25 cm in comparison to 0.19 cm for 6MV and 0.20 cm for kV.

Comparing the values for the population random errors (σ) determined with the different imaging energies for head and neck cancer patients, the largest variation can be found in the S-I dimension with values ranging from 0.12 for kV imaging, to 0.16 cm for 6MV imaging and 0.21 cm for IBL imaging. The largest population random error (σ) can be found in the results of the alignment data obtained with IBL imaging (0.21 cm for S-I, 0.18 cm for L-R and A-P).

The smallest population random error (σ) is found with the results of the alignment data obtained with kV imaging (0.12 cm for S-I, 0.11 cm for L-R and 0.13 cm for A-P). These results are similar to the results found within the population of head-and-neck cancer patient. Here for the L-R and the A-P direction IBL imaging leads to the largest population random error (σ) with values of 0.42 cm for L-R and 0.36 cm for A-P. However, for the S-I direction, IBL imaging leads to the smallest population random error (σ) with 0.28 cm in comparison to 0.34 cm for 6MV and 0.29 cm for kV. For kV imaging there is a great difference of the population random error (σ) evaluated for the three dimensions. For example, in the A-P direction the population random error (σ) is as little as 0.20 cm in comparison to 0.29 cm for S-I and as much as 0.40 cm for the L-R direction.

Comparing errors calculated with planar imaging versus CBCT imaging

Our results comparing the variation of population systematic error (∑) for head-and-neck cancer patients determined with the alignment data obtained from planar, versus the alignment data obtained from CBCT imaging show that the values are smaller for planar imaging. For planar imaging the values are 0.11 cm for the S-I and the L-R direction and 0.10 cm for the A-P direction. For CBCT imaging the values are 0.15 cm for the S-I and A-P direction and 0.16 cm for the L-R direction. This is consistent with our results for the population of prostate cancer patients. The variation of population systematic error (∑) calculated with planar imaging is 0.17 cm for the S-I and A-P direction and 0.20 cm for the L-R direction. For CBCT the results are considerably larger for all three dimensions with values of 0.28 cm for S-I, 0.38 cm for L-R and 0.27 cm for A-P. These results, therefore, show that for both patient populations three dimensional CBCT imaging leads to larger values for the variation of population systematic error (∑). For the population random errors (σ) determined with the two different imaging techniques it is the opposite way. Three dimensional CBCT imaging is shown to lead to smaller population random errors (σ), in comparison to planar imaging. For head-and-neck cancer patients the results for CBCT are 0.14 cm (S-I and L-R) and 0.15 (A-P) in comparison to planar imaging with 0.22 cm (S-I) and 0.19 cm (L-R and A-P). For prostate cancer patients the calculated values for CBCT are 0.38 cm (S-I), 0.50 cm (L-R) and 0.39 cm (A-P), in comparison to planar imaging with 0.33 cm (S-I),

0.43 cm (L-R) and 0.24 cm (A-P). The results show that for both imaging techniques the L-R dimension offers the largest population random errors (σ). An interpretation for this might be that perhaps patient positioning is more reproducible when using CBCT imaging than when using planar imaging.

Comparing the different errors calculated with all six different imaging techniques

Our analysis of the variation of population systematic error (∑) and the population random error (σ) obtained with the alignment data of each of the six different imaging techniques available (the three different energies 6MV, IBL and kV each subdivided into planar imaging and CBCT imaging) shows that for head-and-neck cancer patients the largest variation of population systematic error (∑) can be found with kV CBCT imaging, the imaging offering the highest soft tissue contrast available (0.25 cm for S-I, 0.21 for L-R and 0.21 for A-P). The smallest variation of population systematic error (∑) values is found with IBL planar imaging (0.14 cm for S-I, 0.13 cm for L-R and 0.13 cm for A-P)

For the population of prostate cancer patients, the results for the variation of population systematic error (∑) obtained with the different imaging techniques show a much wider variation. The highest value can be found with kV CBCT imaging with a value for the variation of population systematic error (∑) of 0.70 cm for L-R. The smallest values are found for 6MV planar imaging in the S-I dimension (0.19 cm) and kV planar imaging in the A-P direction (0.19 cm). For the population random error (σ), evaluated with the different imaging techniques, these results show the smallest values for head-and-neck cancer patients for the 6MV CBCT and KV CBCT imaging, with values ranging from 0.07 and 0.09 in all directions. For prostate cancer patients there is again a large variation within the values evaluated with the alignment data different imaging techniques. Results range from 0.13 cm for 6MV CBCT in A-P to 0.45 cm for IBL CBCT in L-R.

The large variation in these results may be due to the fact that the amount of the set-up verification images obtained with the different imaging techniques was too little. Additionally, there is a large variation within the amount of set-up images acquired with the different imaging techniques. In conclusion these results have shown that there are no clear

differences found in the calculation of set-up errors when using different imaging modalities. The detection of misalignment of the target volume appears to be independent from the imaging modality used for set-up verification imaging. The main limitation in this comparison is, that the set-up shifts compared are all from different treatment fractions. There is no direct comparison of the different imaging techniques within the same treatment fraction. Differences within the imaging modalities, therefore, may be due to different patient set-up on different treatment days. A comparison of all six different imaging techniques within the same treatment fraction would be beneficial, however, would excessively increase the imaging dose and is, therefore, not possible. Additionally, this would require more time during which shifts and changes of the patient position may occur. This retrospective study reflects the realistic clinical case in which imaging is performed at our institution.

3.6 Margin calculation applying the margin recipes by Stroom et al. (1999) and van Herk et al. (2000)

After calculating the values for the variation of population systematic error (Σ) and the population random error (σ) for both head-and-neck cancer patients and for prostate cancer patients the results were applied to the two margin recipes by Stroom et al. (1999): $M=2\Sigma+0.7\sigma$ and van Herk et al. (2000): $M=2.5\Sigma+0.7\sigma$ introduced earlier. Table 25 shows the margins calculated for both patient populations and for all three directions (S-I, L-R and A-P). For head-and-neck cancer patients margins of 0.35 cm for the S-I direction and 0.33 cm for the L-R and A-P direction (according to Stroom et al., 1999) and margins of 0.4 cm for the S-I direction and 0.38 cm for the L-R and A-P direction (according to van Herk et al., 2000) were calculated. For prostate cancer patients the calculated margins are 0.57 cm, 0.70 cm and 0.58 cm for the S-I, L-R and A-P direction (according to Stroom et al.,1999) and 0.66 cm, 0.79 cm and 0.67 cm for the S-I, L-R and A-P direction (according to van Herk et al., 2000).

Table 25: Observed set-up errors and calculated margins

	population systematic setup error (M) (cm)			variaton of population systematic error (Σ) (cm)			Population random error (σ) (cm)			Margin calculation by Stroom et.al./van Herk $2\Sigma+0.7\sigma$ / $2.5\Sigma+0.7\sigma$ (in cm)		
	S-I	L-R	A-P	S-I	L-R	A-P	S-I	L-R	A-P	S-I	L-R	A-P
Head-and-neck cancer	0.03	0.07	-0.03	0.10	0.10	0.10	0.22	0.19	0.19	0.35/0.4	0.33/0.38	0.33/0.38
Prostate cancer	-0.03	-0.05	-0.03	0.16	0.18	0.17	0.37	0.49	0.35	0.57/0.66	0.70/0.79	0.58/0.67

Discussion and conclusion (3.6)

After application of the margin recipe our results reveal, that when planning the CTV-PTV margin for head-and-neck cancer patients, margins of 0.35 cm in the S-I direction, and of 0.33 cm in the L-R and A-P directions are necessary according to Stroom et al. (1999) in order to account for set-up variation sufficiently. According to van Herk et al. (2000) the margins need to be slightly larger in order to be adequate, with values of 0.4 cm in the S-I dimension and 0.38 cm in the L-R and A-P dimensions. As explained in methods and materials, at our department, margins between 0.5 cm and 1 cm are applied for head-and-neck cancer patients in order to account for geometrical uncertainties. For prostate cancer patients our results, after application of the margin recipe, have revealed margins in the size of 0.57 cm for S-I, 0.70 cm for L-R and 0.58 cm to be adequate according to Stroom et al. (1999) and again slightly larger according to van Herk et al. (2000) with 0.66 cm and 0.67 cm in the S-I and A-P dimension and 0.79 cm in the L-R dimension. In our clinic the PTV for radiation therapy of prostate cancer is usually created by adding a margin of approx. 1 cm to the CTV.

These results, therefore, show that the CTV-PTV margins used at our institution are sufficient. According to the margin recipe presented by Stroom et al. (1999) and even according to the larger margins required by van Herk et al. (2000) our margins are found to successfully account for potential geometrical inaccuracies and set-up errors. These results might be taken into consideration in future planning of radiation therapy for head-and-neck and prostate cancer patients at our clinic. For example a reduction of the CTV-PTV margin applied to head-and-neck cancer patients between 0.5 cm and 1 cm to a smaller margin between 0.4 cm and 0.5 cm for all directions might be possible. This would help sparing of the OAR's and other healthy tissue. An interesting result, revealed by our analysis, is that the margin required for prostate cancer in the L-R dimension is considerably larger (with at least 0.70 cm) in comparison to the S-I (0.57 cm) and A-P (0.58 cm) dimensions. This means that for prostate cancer patients the variation of the position of the target volume varies more in the left-right direction than in the other two directions. This is interesting since factors affecting the position of the target volume, such as bladder and rectum filling should primarily affect the superior-inferior direction. The fact that the calculations of adequate CTV-PTV margins have resulted in larger margins for prostate cancer patients in comparison

to head-and-neck cancer patients is consistent to our previous results and, of course, due to the greater geometric variability of the target volume in prostate cancer patients.

4. Discussion

Because of the substantial amount of different results this study has procured, a separate discussion was presented at the end of each chapter/section. In this chapter the previously discussed arguments are recapitulated and summarized. Additionally, further aspects that need to be taken into consideration when looking at the results of this study are elaborated.

4.1 Recapitulation of previous discussion

4.1.1   Employment of the different linacs

The evaluation of the distribution of the two population groups included in this study showed that significantly more patients with prostate cancer (44%) were treated at the linac ART1, in comparison to head-and-neck cancer patients (31%). Out of the three linear accelerators available in our clinic the ART1, with the capability of kV imaging, offers the best imaging quality. There are multiple factors that have an impact on the distribution of the patients to the different treatment machines and that influence the choice of the imaging modality used. The differences of the various anatomic sites need to be accounted for when choosing between treatment machines equipped with different technologies. Some target volume locations have higher rates of geometrical variations and uncertainties than others. For these target volumes better imaging techniques with a higher soft tissue contrast are required. This study demonstrates that this is taken into consideration when distributing the different patient populations to the individual treatment machines. The target volume in prostate cancer patients is subject to a much higher geometric variation, due to internal organ movement and differences in bladder and rectum filling, and therefore, in this case bony structures are not ideal as surrogates when aligning a patient on a treatment couch. To reduce set-up errors, high resolution imaging is necessary so that the target volume itself or other relevant anatomic structures can be visualized in the verification images. In comparison, head-and-neck tumors are fairly rigid in their anatomic position and patient

alignment is much more reproducible, due to better immobilization devices such as the thermoplastic masks used. Therefore, when making a decision on the treatment machine that should be used for which patient, these differences need to be taken into consideration.

The results of this study also demonstrated, that when using a treatment machine with "better" imaging technology, the highest imaging resolution available for the particular treatment machine was not always used. As shown in Figure 5, when treated with the ART1, as many as 26 % of the verification images for prostate cancer patients and more than half (58 %) of the verification images for head-and-neck cancer patients were IBL images. There are multiple reasons possible for this discrepancy in the utilization of the best imaging technique available and the imaging technique actually used. Generally, the choice of the image guidance method used is at the discretion of the operating radiation therapist. However, certain protocols with predefined guidelines by the radiation oncologist are provided. Possible reasons for these results may be found in the differences of work- and time-load. At the beginning of 2013 the time necessary to perform kV imaging was considerably larger in comparison to IBL imaging. This was due to the fact that in order to match the set-up verification images to the reference images time consuming gantry rotations of 180° were necessary. Also, for patients treated at the ART1 for the first time, new set-up fields need to be created in order to use kV imaging. Therefore, IBL imaging might have been preferred due to already existing set-up fields and time constraints. Additionally, as discussed earlier, the radiation therapists might have wrongly assumed that the dose of IBL planar imaging is similarly low in comparison to kV CBCT imaging and, therefore, for patients with a presumed lower geometric variation, such as head-and-neck cancer patients, IBL planar imaging was performed. The work of Ames (2015) and Dzierma et al. (2015), however, has demonstrated that this is not the case for head-and-neck imaging. Another possible reason for this result may simply be the lack of experience with the "new" imaging device, resulting in a habitual preference for the familiar imaging technique. However, we expect that having been introduced in November 2012 kilovoltage imaging should have already been successfully incorporated in the daily routine by the beginning of 2013, and indeed, as the results have shown, there is no time trend visible in the evaluation over the course of time. On an optimistic note, the radiation therapists in our clinic have

confirmed that today kV imaging is used much more frequently. Wherever possible the SOP to always use the best imaging technique available at each treatment machine is followed. Furthermore, the time necessary for kV imaging has been decreased with the elimination of the 180° gantry rotation previously necessary for image matching.

These results, however, have also demonstrated that the differences in anatomic sites and the differences in the complexity of the radiation technique used are taken into consideration when choosing treatment machines and imaging modalities. For example, for prostate cancer patients treated at the ART2, as many as half of the imaging is CBCT imaging. As discussed earlier, the ART2 was used exclusively for the IMRT fractions in prostate cancer treatment. IMRT is a much more complex radiation technique in comparison to 3DCRT. At the ONC2 and ART1 where 3DCRT prostate treatment was performed, the amount of CBCT imaging is distinctly smaller in comparison to planar imaging. When comparing the amount of three dimensional CBCT imaging for head-and-neck cancer patients and prostate cancer patients our results have demonstrated that prostate cancer patients received CBCT imaging much more frequently; also the amount of kV imaging is much higher for prostate cancer patients in comparison to head-and-neck cancer patients. As already largely discussed prostate cancer patients are much more prone to set-up errors due to a larger geometric variability of the target volume. Therefore, the results show that anatomic differences are taken into account when choosing the different imaging techniques.

4.1.2   Employment of imaging modalities over the course of time

Our expectation, that after introduction of a new imaging technique there would be a change in the employment of the different imaging modalities, was not confirmed. The amount of kV verification images varied from month to month for both populations. No image modality asserted itself as being superior to others for the different patient populations. In particular there was no visible increase in the amount of kV imaging obtained every month. A possible reason for this might be that the evaluation time was not sufficient. However, as mentioned before, by the beginning of 2013, kV should have already been sufficiently established and fully integrated into the daily routine. Again, according to the

radiation therapists, kV imaging is now used much more frequently in the daily routine. Potentially a new evaluation in a few years covering a greater time span would have a different result regarding the employment of the different imaging modalities.

4.1.3 Evaluation of the alignment data, systematic and random set-up errors

The retrospective evaluation of the couch shifts, performed in order to correctly align the target volume to the position intended and defined during treatment planning, has shown very different results for the two populations included in this study. The range of couch shifts was found to be a lot larger for prostate cancer patients in comparison to head-and-neck cancer patients. This is the case, not only for the range of all the individual couch shifts, but also for the mean set-up error for each individual patient. The calculations of the systematic and random set-up error for the entire populations have shown corresponding results. The variation of the systematic set-up error, as well as the random set-up error for the population of prostate cancer patients was found to be considerably larger in comparison to head-and-neck cancer patients. This result was to be expected since the variation of the position of the target volume is a lot larger in comparison to head-and-neck cancer patients, due to larger internal organ movement in prostate cancer patients and better immobilization methods for head-and-neck cancer patients.

The systematic set-up error was close to zero for both patient populations and in all three directions. Therefore, these results have proven that there is no systematic error affecting all patients and all treatment fractions in the same way. This is a result that was expected and is proof of the efficiency of the quality assurance methods in our institution.

Additionally, the results of this study have shown that the type of imaging technique used does not have a clear impact on the systematic and random set-up errors calculated. There were no clear differences found in the evaluation of the set-up errors using the alignment data obtained separately with the different imaging techniques.

Although our results have proven that the geometric variability is generally larger for prostate cancer patients in comparison to head-and-neck cancer patients, with larger set-up errors found within the population of prostate cancer patients, our analysis of the range of

couch shifts found in individual sample patients for each population, has demonstrated that even within a certain patient population there are large differences in the geometric variability. This is due to the fact that the anatomic predisposition and factors influencing the reproducibility of the target volume are very different for individual patients in a patient population. This is an important aspect that needs to be taken into consideration in radiation therapy. Since it is not always clear which patients will have larger set-up errors than others, researchers have suggested performing multiple imaging during the first few treatment fractions in order to calculate systematic and random set-up errors for individual patients, and possibly adapt the treatment plan or perform more frequent imaging for patients with large set-up errors (Kupelian et al., 2008; Castadot et al., 2010).

4.1.4   Margin calculation

The calculations performed in order to calculate adequate CTV-PTV margins according to Stroom et al. (1999) and van Herk et al. (2000) have demonstrated that, generally, the margins which are currently used for head-and-neck cancer patients and prostate cancer patients are sufficient and ensure an adequate delivery of the radiation dosage to the target volume. As expected, the application of the margin recipes has resulted in larger margins for prostate cancer treatment in comparison to head-and-neck cancer treatment since set-up errors are larger for prostate cancer patients. Interesting, however, is the fact that the calculations have shown that the largest margin for prostate cancer patients is necessary in the L-R dimension, with approx. 0.8 cm in comparison to approx. 0.6 cm in the S-I and A-P dimension. For head-and-neck cancer patients the calculated margins are similar in all three dimensions with approx. 0.4 cm.

Of course, the radiation oncologists take the OAR's and other anatomic structures into account when defining the CTV. Therefore, the CTV-PTV margin is not always the same in all directions. For example, for prostate cancer patients margins near rectum and bladder and for head-and-neck cancer patient's margins near the salivary glands or the brain are smaller than margins near anatomic structures with less importance. The results of our margin calculations could be taken into consideration in future treatment planning for head-and-

neck cancer and prostate cancer treatment in our clinic and might help or influence the decision making of radiation oncologist during CTV definition in the treatment planning. The results might even be taken further. They could be used as guidelines to perform a margin reduction for the treatment planning of prostate and head-and-neck cancer patients. Our results have demonstrated that according to van Herk et al. (2000), in our institution, margins of 0.4 cm in all three directions should be sufficient for head-and-neck cancer patients and for prostate cancer patients margins of 0.7 cm for the S-I and A-P direction and margins slightly larger (0.8 cm) for the L-R direction should be sufficient. This could be discussed with the responsible radiation oncologists and possibly be applied in the future.

4.1.5   Comparison to other studies

Multiple studies have investigated the observed set-up errors by analyzing the alignment data of the preformed couch shifts after imaging and have calculated adequate CTV-PTV margins accordingly to these set-up errors. Table 26 shows a comparison of different studies. The random and systematic set-up errors observed in this study are generally consistent with previous studies. In general, CTV-PTV margins based on van Herk's margin recipe where found to be in the order of 2.0-6.1 mm (3.8-4.0 mm in this study) for head-and-neck cancer patients and 3.5-13.4 mm (6.7-7.9 mm in this study) for prostate cancer patients.

Table 26: Overall systematic and random set-up errors (for all imaging modalities together) with corresponding PTV margins (in mm), compared with previous studies. Asterisk denotes values not given by the authors, but calculated here based on the set-up errors and margin recipes. †values are given for different anatomical landmarks used for image registration.

Head-and-neck cancer patients														
	M (mm)			Σ (mm)			σ (mm)			margin (Stroom) (mm)			margin (van Herk) (mm)		
	AP	SI	LR	AP	SI	LR	AP	SI	LR	AP	SI	LR	AP	SI	LR
This study	0.3	0.7	0.3	1.0	1.0	1.0	2.2	1.9	1.9	3.5	3.3	3.3	4.0	3.8	3.8
Suzuki†	-0.1/ -0.8	0.2/ 0.8	0.2/ -0.7	0.8/ 0.9	1.2/ 1.3	0.9/ 1.0	0.6/ 1.2	0.9/ 1.3	0.7/ 1.6	2.7	3.0	3.3			
Polat	-0.8	-0.5	0.0	1.6	1.3	1.6	1.6	1.4	2.1				5.1*	4.2	5.5
Gupta				1.0	1.2	1.0	1.9	2.5	2.0	3.3	4.1	3.3	3.8	4.7	3.8
Li 2DkV	-0.2	0.1	0.1	0.5	0.6	0.6	1.2	1.2	0.7				2.1	2.3	2.0
Li CBCT	-1.1	0.1	0.2	1.6	1.5	1.3	1.6	1.6	1.2				5.1	4.9	4.1
Pehlivan	0.9	1.2	0.9	1.8	2.3	1.9	3.9	5.0	4.2	3.1	4.0	3.1	3.6	4.6	3.6
Wang	-0.3	-0.7	-0.7	1.2	1.3	1.1	1.1	1.3	1.1				3.8	4.2	3.5
Strbac				1.4	1.5	1.9	1.8	1.9	1.8	4.1	4.3	5.1	4.8	5.1	6.1
Dionisi	0.5	0.9	-0.5	1.8	1.7	1.4	1.9	1.9	1.4				4.5	5.6	5.8

Prostate cancer patients														
	M (mm)			Σ (mm)			σ (mm)			margin (Stroom) (mm)			margin (van Herk) (mm)		
	AP	SI	LR	AP	SI	LR	AP	SI	LR	AP	SI	LR	AP	SI	LR
This study	0.3	0.3	0.5	1.7	1.6	1.8	3.5	3.7	4.9	5.8	5.7	7.0	6.7	6.6	7.9
Remeijer	0.9	-0.7	0.2	1.9	1.9	1.5	1.6	1.9	2.5				6.2*	6.1*	5.5*
Nederveen	-1.0	1.1	0.0	4.4	3.7	2.4	3.4	2.7	2.1				13.4*	11.1*	7.5*
Poulsen				1.0	1.0		1.6	1.4					3.6	3.5	
Schallenkamp				2.5	1.9	2.0	3.5	2.0	1.6				7.3	5.1	5.0
Osei	1.2	-0.8	-0.1	2.2	2.6	1.4	1.6	1.3	1.3				6.6*	7.4*	4.4*
Graf (set-up)	-1.2	0.1	0.8	2.4	2.1	1.6	2.7	2.7	2.3				7.9*	7.1*	5.6*
Fox (set-up)				2.5	2.4	1.8	2.7	2.7	2.3				8.1*	7.9*	6.1*
Huang	-2.0	0.8	0.1	2.2	1.5	0.5	2.7	2.6	1.2				7.4	5.6	2.0
Perks				2.6	1.6	2.2	2.4	1.9	3.5				8.2*	5.3*	8.0*
Ost (set-up)	-0.5	-1.1	1.5	2.6	1.8	2.7	1.8	1.2	1.9				7.7	5.4	8.0
Mayyas (CBCT)	-1.2	0.2	1.1	3.0	2.7	2.4	3.2	2.2	2.5				9.7	8.3	7.8
Mayyas (kV)	-2.9	-0.4	0.5	3.4	3.1	2.6	2.9	2.0	2.4				10.5	11.2	8.2
Oehler (bones,CBCT)				1.9	1.7	0.6	1.9	1.7	0.9				6.1*	3.7*	2.1*
Oehler (bones, kV)				1.8	1.4	0.8	2.0	2.3	0.9				5.9*	5.1*	2.6*

4.2 General aspects that have an impact on the results

4.2.1 Workflow

Another factor that needs to be taken into consideration when discussing these results is the general workflow, an aspect that should not be underestimated and has been previously discussed. When treating large numbers of patients every day, it is important that the workflow is efficient. In the daily clinical routine this has an impact on the distribution of the patients to the different treatment machines. There is no room for time delay; potential vacancies need to be filled; and the treatment machines need to be used in an efficient manner. Also manpower and organization is an important factor leading to the circumstance that all three treatment machines are not always in constant in use. The time necessary to obtain a CBCT image and to correct the corresponding set-up variations is much larger in comparison to that needed for two dimensional planar imaging. All these factors obviously have an effect not only on the distribution to the different treatment machines but also on the image modality chosen.

4.2.2 Importance of education and training of health professionals

For the practice of radiation therapy a coordinated multidisciplinary team consisting of radiation oncologists, medical physicists, radiation therapists, dosimetrists and planning experts, and other professionals is necessary. Each professional group has its own field of expertizes. However, IGRT has led to significant changes in the practice of radiation therapy. With the introduction of new imaging techniques, new challenges for the different health care professionals have emerged and the roles of the different professionals have evolved accordingly. Adequate education and training of health professionals has become essential as new devices requiring specialized knowledge and skills are introduced.

Especially the role of the radiation therapists professional has considerably changed with the new IGRT technologies. Specialized knowledge when operating volumetric imaging devices is necessary. The radiation therapist hast to be familiar with the operation of the hardware and software, has to be able to acquire good quality images and must be aware of the dose

associated with the imaging. Even when following protocols, a radiation therapist needs to make individual decisions at the time of imaging and verification when performing online corrections. With IGRT the responsibility of radiation therapists has increased. One of the major advantages of volumetric imaging is the ability to identify the soft-tissue anatomy. Therefore, the target volume itself can be identified rather than depending on surrogates, such as bony landmarks, for the target. Unfortunately, radiation therapists often are not accustomed to identifying soft-tissue anatomy on images. This limits the advantage volumetric imaging may have on systematic and random errors. In our institution the matching of a verification image mostly relays on matching it to bony landmarks. The potential of the volumetric imaging is, therefore, not fully exhausted. Consequently, it is important to train the radiation therapists in soft-tissue identification. A suggested strategy is to first perform an alignment to bony anatomy and then perform the alignment to soft tissue, the soft tissue alignment being in a predefined tolerance, relative to the bony anatomy.

Obviously, the radiation oncologist needs similar specialized knowledge, since the radiation oncologist is responsible for the protocols defining the imaging frequency and imaging technique. Also the radiation oncologist must be present for the delivery of the first treatment fraction for each patient and is required to supervise the procedure. With advanced radiation techniques such as conformal radiation therapy, the radiation oncologist needs to be aware of the impact different set-up errors may have on the dose distribution. For example, the importance of correct target delineation during treatment planning is crucial for the success of the radiation therapy. The radiation oncologist must be aware of the different factors affecting the errors introduced through target delineation, such as inter- and intra-observer variability. Therefore, training knowledge on systematic- and random errors, inter-and intra-observer errors, both at the target delineation and image registration stage is advised (White E et al., 2007).

4.2.3 Reducing errors: Imaging frequency and adaptive radiotherapy

The frequency of the verification images realized for the patients in our study was individually defined prior to treatment for each patient. In general, set-up verification images were obtained about twice a week. The fact that the number and frequency of verification imaging is different for each patient has an impact on our results. There are different protocols presented in the literature concerning the ideal frequency for imaging (e.g. Kupelian et al., 2008). With verification imaging and online correction preformed on a daily basis, the systematic and random errors could be minimized. However, this would considerably increase the radiation dose delivered to the patient and is very time consuming. For this reason studies have investigated the feasibility of using the couch shift measurements from several of the initial verification images to estimate and correct the presumed systematic error. Zumsteg et al. found that for head-and-neck cancer patients with large 3D correction vectors (> 5 mm) using the first five CBCT image guided measurements as an estimation, improved the daily set-up accuracy. However, for patients presenting large random errors, daily imaging might be necessary (Zumsteg et al., 2012). This is in agreement to a study by Zeidan et al. showing that imaging protocols with less than daily imaging do not eliminate random error but can effectively reduce systematic errors. The study by Zeidan et al. revealed that, even if every other treatment is image guided, about 11% of all treatments are still subject to three-dimensional (3D) set-up errors of at least 5 mm for head-and-neck cancer from random error, which demonstrated the necessity of daily imaging in addition to reliable immobilization (Zeidan et. al., 2007).

When establishing a treatment plan for an individual patient, the plan is usually based on the imaging performed during treatment planning; in most cases this is the planning CT. This treatment plan, however, does not account for potential changes in the anatomy and position of the target volume occurring throughout the course of the radiation treatment. Reasons for changes are multiple, including decreasing tumor volume, weight loss and alteration in muscle mass and fat distribution. The anatomic changes over the course of the treatment have been proven to be especially large with treatment of head-and-neck cancer patients and have a potential dosimetric impact (Barker JL, 2004). With adaptive radiotherapy a concept to compensate these uncertainties and reduce dosimetric errors is

presented. It consists in re-planning and adapting the treatment plan throughout the course of radiation based on verification imaging realized during the course of treatment. It, therefore, takes into account the anatomic changes occurring. The procedure is very complex and time consuming and further investigation and research is necessary, such as realizing practical guidelines for identifying patients that would profit most from this adaptive treatment, calculating adequate CTV-PTV margins and research on the dose accumulation due to frequent imaging (Castadot et al., 2010). In a comparison of various online IGRT strategies investigating the benefits of plan re-optimization Schulze et al. found that for prostate cancer patients online treatment plan re-optimization may reduce the PTV margin, although for low risk patients, with only the prostate involved, online target alignment IMRT treatment would achieve similar results (Schulze et al., 2009).

5. Conclusion

From the results of this retrospective study several different conclusions may be drawn:

The analysis of the employment of the different treatment machines and imaging modalities has shown that the anatomic differences of target volumes in different patient populations is taken into account when making decisions on the distribution to the different lincas and when choosing the different imaging techniques used. This study has shown that, generally, better imaging techniques are used for IGRT for patients with larger expected set-up errors. However, the study has also revealed that especially at the linac ART1 there is still room for improvement since the best imaging technique was used not always in each situation. On a positive note, the radiation therapists have confirmed that the frequency of kilovoltage imaging has increased further and that currently in most situations the general work SOP to always use the best imaging technique available is pursued.

Furthermore, this study has shown that the target volume in prostate cancer patients is subject to considerably greater geometric variability in comparison to that of the head-and-neck cancer patients. The analysis of the alignment data for both populations has revealed that the couch shifts carried out to correctly position prostate cancer patients are larger by a factor of 1,5-2 in comparison to head-and-neck cancer patients. In addition, the calculation of set-up errors from the alignment data has shown that random population set-up errors are larger for prostate cancer in comparison to head-and-neck cancer patients. Another satisfactory result our study has procured is that for both patient populations there is practically no systematic set-up error. Therefore, the quality assurance measures in our clinic are shown to be successful. Additionally, this study has revealed that the choice of imaging modality used for IGRT does not have a clear effect on the calculation of set-up errors.

Another conclusion that can be drawn from this study is that the CTV-PTV margins applied in our clinic for prostate and head-and-neck cancer patients are sufficient according to the margin recipes by van Herk et al. (2000) and Stroom et al. (1999). This shows that the margins currently used in our clinic ensure that the target volume is adequately treated.

Based on these results one might even consider a margin reduction for future treatment planning. In conclusion, it is also important to state that (as shown in this study) the geometric variability of target volumes, even within a certain patient population, may be very different for individual patients. Some patients are prone to greater set-errors in comparison to other patients. This needs to be taken into consideration when performing IGRT. For these patients the concept of adaptive re-planning or more frequent imaging might be beneficial. More research is necessary, especially in the areas of adaptive re-planning, in order to establish treatment protocols that account for these great differences in the anatomy of individual patients. Also, as already mentioned in the discussion chapter, education of health professionals is essential in order to successfully deliver IGRT and to maximize its benefits.

6. Directory of tables

7. Directory of figures

8. List of abbreviations

ART1	Siemens linear accelerator Artiste 1
ART2	Siemens linear accelerator Artiste 2
CBCT	Cone-beam computer tomography
CT	Computer tomography
CTV	Clinical target volume
DRR's	Digitally reconstructed radiographs
e.g.	exempli gratia = for example
GTV	Gross tumor volume
i.e.	id est = that is
IBL	Imaging beam line
ICRU	International Commission on Radiation Units and Measurements
IGRT	Image-guided radiotherapy
IMRT	Intensity modulated radiation therapy
kV	Kilovoltage
Linacs	Linear accelerators
MRI	Magnetic resonance imaging
MV	Megavoltage
NACP	Nordic Association of Clinical Physics
OAR's	Organs at risk
ONC2	Siemens linear accelerator Oncor 2
PET	Positron emission tomography
PTV	Planning target volume
RMS	Root mean square
SD	Standard deviation
SOP	Standard operating procedure
TBL	Treatment beam line
TPS	Treatment planning system
3DCRT	3-dimensional conformal radiation therapy
(μ)	Individual patient's systematic set-up error
(r)	Individual patient's random set-up error
(M)	Population systematic set-up error
(Σ)	Population variation of the systematic setup error
(σ)	Population random set-up error
(A-P)	Anterior-Posterior
(L-R)	Left-Right
(S-I)	Superior-Inferior

9. References

Aaltonen P, Brahme A, Lax I et al., 1997. Specification of dose delivery in radiation therapy. Recommendation by the Nordic Association of Clinical Physics (NACP). *Acta Oncol* 36 (10):132

Ames E, 2015. In prep. Working title: Evaluation und Vergleich der Dosisbelastung durch die Anwendung unterschiedlicher Bildgebungsmodalitäten für IGRT.

Balter JM and Yue C, 2007. Advanced technologies in image-guided radiation therapy. *Seminars in Radiation Oncology* 17:293-297

Barker JL, Garden AS, Kian Ang K et al., 2004. Quantification of volumetric and geometric changes occuring during fractionated radiotherapy for head-and-neck cancer using an integrated CT/Linear accelerator system. *Int J Radiat Oncol Biol Phys* 59,No.4:960-970

Bel A, Vos PH, Rodrigus PT, Creutzberg CL et al., 1996. High-precision prostate cancer irradiation by clinical application of an offline patient setup verification procedure, using portal imaging. *Int J Radiat Oncol Biol Phys* 35:321-32

Beltran C, Herman MG, Davis BJ, 2008. Planning target margin calculations for prostate radiotherapy based on intrafraction and interfraction motion using four localization methods. *Int J Radiat Oncol Biol Phys* 70:289-95

Castadot P, Lee JA, Geets X et al., 2010. Adaptive radiotherapy of head and neck cancer. *Seminars in Radiation Oncology* 20:84-93

Chen AM, Farwell DG, Quang L et al., 2011. Marginal misses after postoperative intensity-modulated radiotheraphy for head and neck cancer. *Int J. Radiation Oncology Biol Phys* 80:1423-1429

Dawson LA, Sharpe M.B, 2006. Image-guided radiotheraphy: rationale, benefits and limitations. *Lancet Oncol* 7:848-858

De Boer JC, Heijmen BJ, 2002. A new approach to off-line setup corrections: combining safety with minimum workload. *Med Phys* 29:1998-2012

Dionisi F, Palazzi MF, Bracco F et al., 2013. Set-up errors and planning target volume margins in head and neck cancer radiotherapy: a clinical study of image guidance with on-line cone-beam computed tomography. *Int J Clin Oncol* 18:418-427.

Dzierma Y, Ames E, Nuesken F et al., 2015. Image quality and dose distributions of three linac-based imaging modalities. *Strahlenther Onkol (2015)* 191:365–374.

Dzierma Y, Beyhs M, Palm J, Niewald M, Bell K, Nuesken F, Licht N, Rübe Ch: Set-up errors and planning margins in planar and CBCT image-guided radiotherapy using three different imaging systems: a clinical study for prostate and head-and-neck cancer, Physica Medica (European Journal of Medical Physics), in press (accepted 06. Sep 2015).

Fox C, Fisher R, Kron T et al., 2010. Extraction of data for margin calculations in prostate radiotherapy from a commercial record and verify system. *J Medical Imaging Radiat Oncol* 54:161-170

Ghilezan M, Yan D, Liang J et al., 2004. Online image-guided intensity-modulated radiotheraphy for prostate cancer: How much improvement can we expect? A theoretical assessment of clinical benefits and potential dose escalation by providing precision and accuracy of radiation delifery. *Int J Radiat Oncol Biol Phys* 60:162-1610

Graf R, Wust P, Budach V, Boehmer D, 2009. Potentials of on-line repositioning based on implanted fiducial markers and electronic portal imaging in prostate cancer radiotherapy. *Radiat Oncol* 4:13.

Gupta T, Chopra S, Kadam A et al., 2007. Assessment of three-dimensional set-up errors in conventional head and neck radiotherapy using electronic portal imaging device. *Radiat Oncol* 2:44.

Huang K, Palma DA, Scott D et al., 2011. Inter- and Intrafraction Uncertainty in Prostate Bed Image-Guided Radiotherapy. *Int J Radiat Oncol Biol Phys* 84(2):402-407

ICRU-50. International Commission on Radiation Units and Measurements, 1993. ICRU report 50: Prescribing, recording, and reporting photon beam therapy. Bethesda, MD: *International Commission on Radiation Units and Measurement Publications* P.3-16

ICRU-62. International Commission on Radiation Units and Measurements, 1999. ICRU report 62: prescribing, recording, and reporting photon beam therapy (Supplement to ICRU Report 50). Bethesda, MD: *International Commission on Radiation Units and Measurement Publications* P. 3-20

Koper PCM, Stroom JC, van Putten WLJ et al., 1999. Acute morbidity reduction using 3DCRT for prostate carcinoma: A randomized study. *Int J Radiat Oncol Biol Phys* 43:727-734

Korreman S, Rasch C, McNair H et al., 2010. The European Society of Therapeutic Radiology and Oncology-European Institute of Radiotherapy (ESTRO-EIR) report on 3D CT-based in-room image guidance systems: A practical and technical review and guide. *Radiotherapy and Oncology* 94:129-144

Kupelian PA, Langen KM, Zeidan OA et al., 2006. Daily variations in delivered doses in patients treated with radiotheraphy for localized prostate cancer. *Int J Radiat Oncol Biol Phys* 66:876-82

Kupelian PA, Langen KM, Willoughby TR et al., 2008. Image-guided radiotherapy for localized prostate cancer: Treating a moving target. *Semin Radiat Oncol* 18:58-66

Kupelian PA, Lee C, Langen KM et al., 2008. Evaluation of image-guidance strategies in the treatment of localized prostate cancer. *Int J Radiation Oncol Biol Phys* 70:1151-1157

Letourneau D, Martinez AA, Lockman D et al., 2005. Assessment of residual error for online cone-beam CT-guided treatment of prostate cancer patients. *Int J Radiat Oncol Biol Phys* 62:1239-1246

Li H, Zhu X. R, Zhang L et al., 2008. Comparison of 2D radiographic images and 3D cone beam computed tomography for positioning head-and-neck radiotherapy patients. *Int J Radiat Onco Biol Phys* 71(3):916-625

MackieTR, Kapatoes J, Ruchala K et al., 2003 Image guidance for precise conformal radiotherapy. *Int J Radiat Oncol Biol Phys* 56:89-105

Mayyas E, Chetty IJ, Chetvertkov M et al., 2013. Evaluation of multiple image-based modalities for image-guided radiation therapy (IGRT) of prostate carcinoma: A prospective study. *Med Phys* 40, 041707

Nederveen AJ, Dehnad H, van der Heide UA et al., 2003. Comparison of megavoltage position verification for prostate irradiation based on bony anatomy and implanted fiducials. *Radiother Oncol* 68:81-86.

Nutting CM, Convery DJ, Cosgrove VP et al., 2000. Reduction of small and large bowel irradiation using an optimized intensity-modulated pelvic radiotherapy technique in patients with prostate cancer. *Int J Radiat Oncol Biol Phys* 48:649-656

Nutting CM, Morden J, Harrington KJ et al., 2011. Parotid-sparing intensity modulated versus conventional radiotherapy in head and neck cancer (PARSPORT): a phase 3 multicentre randomised controlled trial. *Lancet Oncol* 12(2):127-36

Oehler Ch, Lang S, Dimmerling P et al., 2014. PTV margin definition in hypofractionated IGRT of localized prostate cancer using cone beam CT and orthogonal image pairs with fiducial markers. *Radiat Oncol* 9:229

Osei EK, Jiang R, Barnett R et al., 2009. Evaluation of daily online set-up errors and organ displacement uncertainty during conformal radiation treatment of the prostate. *Brit J Radiology* 82:49-61

Ost P, De Meerleer G, De Gersem W et al., 2011. Analysis of prostate bed motion using daily cone-beam computed tomography during postprostatectomy radiotherapy. *Int J Radiat Oncol Biol Phys* 79(1):188-194

Peeters ST, Heemsbergen WD, Koper PC et al., 2006. Dose-response in radiotherapy for localized prostate cancer: Results of the Dutch multicenter randomized phase III trial comparing 68 Gy of radiotherapy with 78 Gy. *J Clin Oncol* 24:1990-1996

Pehlivan B, Pichenot Ch, Castaing M et al., 2009. Interfractional set-up errors evaluation by daily electronic portal imaging of IMRT in head and neck cancer patients. *Acta Oncol* 48:440-445

Perks J, Turnbull H, Liu T et al. 2011. Vector analysis of prostate patient setup with image-guided radiation therapy via kV cone beam computed tomography. *Int J Radiat Oncol Biol Phys* 79(3):915-919

Pirzkall A, Carol M, Lohr F et al., 2000. Comparison of intensity-modulated radiotherapy with conventional conformal radiotheraphy for complex-shaped tumors. *Int J Radiat Oncol Biol Phys* 48:1371-1380

Polat B, Wilbert J, Baier K et al., 2007. Nonrigidd patient setup errors in the head-and-neck region. *Strahlenther Onkol* 9:506-511

Pollack A, Hanlon AL, Horwitz EM et al., 2006. Dosimetry and preliminary acute toxicity in the first 100 men treated for prostate cancer on a randomized hypofractionation dose escalation trial. *Int J Radiat Oncol Biol Phys* 64:518-26

Poulsen PR, Muren LP, Høyer M, 2007. Residual set-up errors and margins in on-line image-guided prostate localization in radiotherapy. *Radiother Oncol* 85:201-206

Pow EH, Kwong DL, McMillan AS et al., 2006. Xerostomia and quality of life after intensity modulated radiotherapy vs. conventional radiotherapy for early stage nasopharyngeal carcinoma. Initial report on a randomized controlled clinical trial. *Int J Radiat Oncol Biol Phys* 66:981-91

Remeijer P, Geerlof E, Ploeger L et al., 2000. 3-D portal image analysis in clinical practice: an evaluation of 2-D and 3-D analysis techniques as applied to 30 prostate cancer patients. *Int J Radiat Oncol Biol Phys* 46(5):1281-1290

Schallenkamp JM, Herman MG, Kruse JJ et al., 2005. Prostate position relative to pelvic bony anatomy based on intraprostatic gold markers and electronic portal imaging. *Int J Radiat Oncol Biol Phys* 63(3):800-811

Schulze D, Liang J, Yan D et al., 2009. Comparison of various online IGRT strategies: The benefits of online treatment plan re-optimization. *Radiotherapy and Oncology* 90:367-376

Strbac B and Jokic VS, 2013. Evaluation of set-up errors in head and neck radiotherapy using electronic portal imaging. *Physica Medica* 29:531-536

Stroom JC, de Boer HC, Huizenga H, Visser AG, 1999. Inclusion of geometrical uncertainties in radiotherapy treatment planning by means of coverage probability. *Int J Radiat Oncol Biol Phys* 43:905-919

Suzuki M, Nishimura Y, Nakamatsu K et al., 2006. Analysis of interfractional set-up errors and intrafractional organ motions during IMRT for head and neck tumors to define an appropriate planning target volume (PTV)- and planning organs at risk volume (PRV)-margins. *Radiother Oncol* 78:283-290

Van Herk M, Remeijer P, Rasch C et al., 2000. The probability of correct target dosage: Dose-population histograms for deriving treatment margins in radiotherapy. *Int J Radiat Oncol Biol Phys* 47:1121-1135

Van Herk M, 2004. Errors and Margins in Radiotherapy. *Seminars in Radiation Oncology* 14:52-64

Van Herk M, 2007. Different Styles of Image-Guided Radiotherapy. *Seminars in Radiation Oncology* 17:258-267

Verellen D, De Ridder M., Storme G., 2008. A (short) history of image-guided therapy. *Elsevier Ireland Ltd. Radiotheraphy and Oncology* 86:4-13

Wang J, Bai S, Chen N et al., 2009. The clinical feasibility and effect of online cone beam computer tomography-guided intensity-modulated radiotherapy for nasopharyngeal cancer. *Radiother Oncol* 90:221-227

White E and Kane G, 2007. Radiation Medicine Practice in the Image-Guided Radiation Therapy Era: New Roles and New Opportunities. *Semin Radiat Oncol* 17:298-305

Zeidan OA, Langen KM, Meeks SL et al., 2007. Evalutation of image-guidance protocols in the treatment of head and neck cancers. *Int J Radiat Oncol Biol Phys* 67:670-677

Zumsteg Z, DeMarco J, Lee StP et al. 2012. Image Guidance During Head-and-Neck Cancer Radiation Therapy: Analysis of Alignment Trends With In-Room Cone-Beam Computed Tomography Scans. *Int J Radiat Oncol Biol Phys* 83,No.2:712-719

10. Acknowledgements

Mein größter Dank geht an Frau Dr. rer. nat. Yvonne Dzierma für die außerordentlich gute Betreuung und engagierte Unterstützung, ihre ständige Gesprächsbereitschaft und Motivation. Vielen Dank für die geduldige Beantwortung all meiner Fragen und die viele Zeit die du für mich aufgebracht hast. Eine bessere Betreuung für meine Dissertation hätte ich mir wirklich nicht wünschen können.

Weiterhin möchte ich mich bei meinem Doktorvater, Prof. Dr. med. Marcus Niewald, für die Vergabe dieses Themas im Rahmen einer Doktorarbeit bedanken. Vielen Dank, dass Sie das Zustandekommen der Arbeit ermöglicht haben und immer für mich ansprechbar waren.

Ein weiterer Dank gilt Herrn Dr. rer. nat. Frank Nüsken, der mir mit seinem Fachwissen zur Seite stand und immer bereit war mit konstruktiver Kritik, Anregungen und Ideen zur Gestaltung der Dissertation beizutragen. Vielen Dank auch für die Unterstützung bei der Vorbereitung für das Doktorandenkolloquium.

Des Weiteren möchte ich mich bei Herrn Prof. Dr. med. Christian Rübe und allen Mitarbeitern und Mitarbeiterinnen der Klinik für Strahlentherapie und Radioonkologie der Universitätsklinik des Saarlandes für die Hilfe und Beratung danken. Ich habe mich in Ihrer Klinik stets willkommen gefühlt und empfand die Arbeitsatmosphäre als sehr angenehm.

Ein besonderer Dank geht an meinen Freund, Christoph Schumacher, der mir stets Mut zugesprochen und mich in meiner Arbeit bestärkt hat und an meine Eltern, Hans und Vicky Beyhs, die in jeglicher Hinsicht die Grundsteine für meinen Weg gelegt haben. Vielen Dank für eure liebevolle Unterstützung und Motivation. Ohne euch an meiner Seite wäre all dies nicht möglich gewesen.

Weiterhin möchte ich mich bei meinen Großeltern bedanken. Meinem Großvater, Gonzalo Docal, der mit beigebracht hat immer mein Bestes zu geben und für den Ausbildung und Wissenschaft eines der größten Güter war. Und meiner Großmutter, Sarita Docal, einer der gutherzigsten und optimistischsten Menschen die ich kennenlernen durfte. Sie haben mein Leben auf große Weise inspiriert.

Zu guter Letzt möchte ich mich bei allen Menschen bedanken die in der Wissenschaft und Forschung tätig sind. Durch ihre harte Arbeit und unermüdliches Vorantreiben der wissenschaftlichen Entwicklungen ist die Medizin heute in der Lage unglaubliche Dinge zu vollbringen. Seit meiner eigenen Erfahrung mit Brustkrebs vor zwei Jahren weis ich dies umso mehr zu schätzen. Meine Krankheit hat mir verdeutlicht wie wichtig diese Arbeit ist und wie dankbar ich sein kann, dass es so viele Menschen weltweit gibt, die Ihr Leben der Forschung widmen. Ich hoffe ich konnte mit meiner Dissertation einen kleinen Beitrag für die weitere Entwicklung der Strahlentherapie leisten.

11. Curriculum vitae

Monica Elisa Beyhs

Mainzer Strasse 61

66121 Saarbrücken

Telefon: 0176 – 63170967

Email: monica.beyhs@gmx.de

Geboren: 10.03.1983 in Düsseldorf

Nationalität: Deutsch, USA

Familienstand: ledig

Arbeit

11/2010 – heute	Assistenzärztin in der Klinik für Hals-Nasen-Ohren-Heilkunde, Kopf- und Halschirurgie, Caritas Klinik St. Theresia , Saarbrücken
05/2010 – 11/2010	Assistenzärztin in der Klinik für Allgemein-, Viszeral-, Thorax- und Tumorchirurgie, Caritas Klinik St. Theresia, Saarbrücken

Ausbildung

Studium

11/2009	Zweiter Abschnitt der Ärztlichen Prüfung, Universität des Saarlandes
08/2008	Beginn des Praktischen Jahres
10/2005 – 07/2006	Studium der Humanmedizin an der Universidad de La Laguna, Teneriffa, Spanien (ERASMUS Program)
09/2005	Erster Abschnitt der Ärztlichen Prüfung, Universität des Saarlandes
10/2002 – 11/2009	Studium der Humanmedizin an der Universität des Saarlandes, Homburg

Praktische Erfahrung im Studium

04/2009 – 08/2009	Tätigkeit im Rahmen des Praktischen Jahres an der Winterbergklinik in Saarbrücken im Fachbereich Innere Medizin
12/2008 – 04/2009	Tätigkeit im Rahmen des Praktischen Jahres an der Universitätsklinik Köln im Fachbereich HNO
08/2008 – 12/2008	Tätigkeit im Rahmen des Praktischen Jahres am Hospital Puerta del Mar in Cádiz, Spanien (Universitätsklinik der Universidad de Cádiz) im Fachbereich Allgemeinchirurgie
04/2008	Famulatur in der Pädiatrie des Holtz Childrens Hospital der Universität von Miami, Miller School of Medicine, in Miami, Florida, USA
07/2007	Famulatur in der Hals-, Nasen-, Ohrenklinik der Universitätsklinik Homburg
2007 – 2008	Studentischer Tutor des Blockpraktikums für Pädiatrie an der Universitätsklinik Homburg
03/2007	Famulatur in der Allgemein Chirurgie der Universitätsklinik Virgen de la Victoria, in Málaga, Spanien
09/2006	Famulatur in der Gynäkologischen Klinik des Hospital Universitario de Canarias, La Laguna, Spanien

Schule

03/2002	Allgemeine Hochschulreife, Gymnasium auf der Karthause, Koblenz - Leistungskurse: Biologie, Englisch, Deutsch
1992 – 2002	Gymnasium auf der Karthause, Koblenz
09/1998 – 07/1999	Amity Regional High School, Woodbridge, Connecticut, USA
1988 – 1992	Grundschule Buchholz